74 Lessons from the Mathematics of Two-Dimensional Euclidean Quantum Gravity

二维欧几里得量子引力数学的 74 条经验

Timothy Budd

蒂莫西·巴德

Contents

目录

T. Budd (✉)

T. 巴德 (✉)

Radboud University, Nijmegen, The Netherlands

荷兰奈梅亨拉德堡德大学

e-mail: t.budd@science.ru.nl

电子邮箱:t.budd@science.ru.nl

Abstract

摘要

The search for a mathematical foundation for the path integral of Euclidean quantum gravity calls for the construction of random geometry on the spacetime manifold. Following developments in physics on the two-dimensional theory, random geometry on the 2-sphere has in recent years received much attention in the mathematical literature, which has led to a fully rigorous implementation of the path integral formulation of two-dimensional Euclidean quantum gravity. In this chapter, we review several important mathematical developments that may serve as guiding principles for approaching Euclidean quantum gravity in dimensions higher than two. Our starting point is the discrete geometry encoded by random planar maps, which realizes a lattice discretization of the path integral. We recap the enumeration of planar maps via their generating functions and show how bijections with trees explain the surprising simplicity of some of these. Then we explain how to handle infinite planar maps and to analyze their exploration via the peeling process. The aforementioned trees provide the basis for the construction of the universal continuum limit of the random discrete geometries, known as the Brownian sphere, which represents the random geometry underlying two-dimensional Euclidean quantum gravity in the absence of matter.

寻找欧几里得量子引力路径积分的数学基础，需要在时空流形上构造随机几何。继二维理论的物理学进展之后，二维球面上的随机几何近年来在数学文献中受到广泛关注，已经实现了二维欧几里得量子引力路径积分表述的完全严格构造。本章我们综述若干重要的数学进展，它们可作为研究二维以上欧几里得量子引力的指导原则。我们的出发点是随机平面地图编码的离散几何，它实现了路径积分的格点离散化。我们概括了通过生成函数对平面地图计数的方法，并说明与树的双射如何解释其中部分结果出人意料的简洁性。随后我们阐述如何处理无限平面地图，并通过剥离过程分析它们的探索过程。上述树为构造随机离散几何的通用连续极限 (即布朗球面) 提供了基础，布朗球面代表了无物质情形下二维欧几里得量子引力对应的随机几何。

Keywords

关键词

2D quantum gravity · Random geometry · Random planar maps · Tree bijections · Scaling limits · Brownian sphere · Peeling process

二维量子引力 · 随机几何 · 随机平面地图 · 树双射 · 标度极限 · 布朗球面 · 剥离过程

Introduction

介绍

Euclidean Quantum Gravity

欧几里得量子引力

The path integral approach to Euclidean quantum gravity [1, 2] aims at assigning a mathematical meaning to a functional integral of the form

欧几里得量子引力的路径积分方法 [1, 2] 旨在为如下形式的泛函积分赋予数学意义

$$\mathcal{Z} = \int \mathcal{D}\left[g_{ab}\right] e^{-S\left[g_{ab}\right]}, \tag{1}$$

where the integration is over all isometry classes $[g_{ab}]$ of Riemannian metrics g_{ab} on a d -dimensional spacetime manifold M with an appropriate action $S[g_{ab}]$, like the (Euclidean) Einstein-Hilbert action

其中积分遍历 d 维时空流形 M 上黎曼度量 g_{ab} 的所有等距类 $[g_{ab}]$ ，并搭配合适的作用量 $S[g_{ab}]$ ，例如 (欧几里得) 爱因斯坦-希尔伯特作用量

$$S\left[g_{ab}\right] = \frac{1}{16\pi G_{\mathrm{N}}} \int_{M} \mathrm{d}^{d} x \sqrt{g}\,(-R + 2\Lambda)\,. \tag{2}$$

It has the key advantage over the Feynman path integral of Lorentzian quantum gravity that, at least formally, the integrand is real and positive, allowing for an interpretation of $\mathcal{Z}$ as a partition function of a statistical system in which $e^{-S\left[g_{ab}\right]}$ takes on the role of the Boltzmann weight assigned to the geometry $[g_{ab}]$. Putting aside the matter of relating the two path integrals via a ”Wick rotation,” it turns the problem of Euclidean quantum gravity into a question of probability theory: does there exist a suitable probability measure

相比洛伦兹量子引力的费曼路径积分，它的核心优势在于: 至少在形式上被积函数是实正的，因此可以将 $\mathcal{Z}$ 解释为统计系统的配分函数，其中 $e^{-S\left[g_{ab}\right]}$ 对应分配给几何构型 $[g_{ab}]$ 的玻尔兹曼权重。暂且不论通过「威克转动」关联两种路径积分的问题，欧几里得量子引力由此被转化为概率论中的一个问题: 是否存在合适的概率测度

$$\frac{1}{Z}\mathcal{D}\left[g_{ab}\right] e^{-S[g_{ab}]} \tag{3}$$

on the space of geometries on M ?

定义在 M 上的几何空间?

Needless to say, there are significant challenges on the way to answering this question. As with other (Euclidean) quantum field theory, any approximation scheme of the integral (1) will encounter both ultraviolet and infrared divergencies that have to be suitably regularized. The absence of a background geometry, peculiar to gravity, makes categorizing the field degrees of freedom by scale (and thus deciding which are infrared or ultraviolet) already a nontrivial affair, because a notion of scale necessarily involves the dynamical metric itself. In addition, since gravity is perturbatively non-renormalizable, one should be prepared to deal with metric degrees of freedom at short-length scales (i.e., in the ultraviolet) that are strongly interacting. Based on this, one may question whether the space of Riemannian metrics provides an arena general enough to host the sought-after probability measure, since many classical notions of Riemannian geometry (like curvature and geodesics) may be lost when the metric becomes too irregular, for instance, if the metric tensor is non-differentiable or even distributional. It may thus be necessary to find an appropriate generalization of the Riemannian metric that can support such a measure. Finally, in constructing the measure, one should overcome the issue that the Einstein-Hilbert action (for $d \geq 3$) is unbounded from below, suggesting that certain highly curved geometries will receive much higher Boltzmann weight than the classical Einstein solutions (known as conformal factor problem [3,4]).

毫无疑问，回答这个问题的道路上存在诸多重大挑战。和其他 (欧几里得) 量子场论一样，对积分 (1) 的任何近似方案都会遇到紫外和红外发散，必须对其做适当正则化处理。引力特有的问题是不存在背景几何，因此按标度对场自由度分类 (进而判断是红外还是紫外自由度) 本身就是一件非平凡的工作，因为标度的概念必然依赖动力学度量本身。此外，引力在微扰下是不可重整的，因此我们需要做好应对短距离 (即紫外区域) 强相互作用度量自由度的准备。由此，我们可以合理质疑: 黎曼度量空间是否足够宽泛，能够承载我们寻找的概率测度？因为当度量变得极不规则时 (例如度量张量不可微、甚至退化为分布时)，黎曼几何的许多经典概念 (如曲率和测地线) 都会失效。因此，有必要对黎曼度量做适当推广，使其能够支撑这样的测度。最后，在构造测度的过程中，我们需要克服爱因斯坦-希尔伯特作用量 (针对 $d \geq 3$) 无下界的问题: 这意味着某些高度弯曲的几何会得到比经典爱因斯坦解高得多的玻尔兹曼权重，该问题也被称为共形因子问题 [3,4]。

A mathematically precise construction of the partition function has not been achieved yet for any manifold of dimension $d \geq 3$, but significant progress is reported elsewhere in the handbook. Notably, renormalization group methods [5-7] (see [8] for a thorough account) have found indications that Euclidean quantum gravity is asymptotically safe [9], meaning that is renormalizable with an interacting fixed point in the ultraviolet. Lattice discretization approaches like Euclidean dynamical triangulations [10-13] and causal dynamical triangulations [14, 15] provide a complementary perspective based on numerical methods.

截至目前，还没有对任何 $d \geq 3$ 维流形完成配分函数的数学严格构造，但手册的其他部分已经记录了重大进展。值得注意的是，重整化群方法 [5-7](详尽综述见 [8]) 已有迹象表明欧几里得量子引力是渐近安全的 [9]，即它在紫外存在相互作用不动点，因此是可重整的。格点离散化方法，例如欧几里得动力学三角剖分 [10-13] 和因果动力学三角剖分 [14,15]，基于数值方法为我们提供了互补的视角。

In this chapter, however, we focus on Euclidean quantum gravity on the two-dimensional sphere which admits a fully rigorous probabilistic interpretation. It has been long known in the physics literature that the partition function in two dimensions is susceptible to analytic computation from various starting points, including the lattice approaches via dynamical triangulations [16-20] and matrix models [21-23] as well as conformal field theory approaches via Liouville field theory [24-27]. The focus of this chapter, however, is on the developments in the mathematical literature in the last two decades that have put these computations on a rigorous footing and have culminated in an unambiguous construction of the probability measure (3) representing two-dimensional Euclidean quantum gravity.

但本章我们聚焦于二维球面上的欧几里得量子引力，该场景可以给出完全严格的概率诠释。物理学文献中很早就已知，二维情形的配分函数可以从多个不同出发点做解析计算，包括动力学三角剖分格点方法 [16-20]、矩阵模型 [21-23]，以及刘维尔场论框架下的共形场论方法 [24-27]。但本章的重点是近二十年来数学领域的研究进展: 这些工作将上述计算建立在严格基础上，并最终成功构造出代表二维欧几里得量子引力的概率测度 (3)，不存在任何歧义。

Of course, it is a greatly simplified toy model compared to quantum gravity on more realistic four-dimensional manifolds, but one that is far from trivial and already requires us to depart from certain classical intuition coming from Riemannian geometry. It thus forms an important test bed for our mathematical methods, and several lessons can be learned (at least on what not to take for granted when searching for higher-dimensional analogues).

当然，和更贴近现实的四维流形上的量子引力相比，它是一个大大简化的玩具模型，但它远非平凡，已经要求我们摒弃黎曼几何带来的部分经典直觉。因此它是检验我们数学方法的重要试验场，我们也能从中学到很多经验 (至少能知道在寻找高维推广时，哪些不能理所当然地默认成立)。

Two-Dimensional Quantum Gravity

二维量子引力

One aspect which sets gravity in two dimensions apart from its higher-dimensional counterparts is that Einstein's field equations in vacuum are trivial: every Riemannian metric is a solution when $\Lambda = 0$, and none is when $\Lambda \neq 0$. This is tied to the fact that the curvature integral in the Einstein-Hilbert action (2) for $d = 2$ is a topological invariant due to the Gauss-Bonnet formula, so fixing the manifold $M = S^2$ to be the 2-sphere the only dependence on the metric is through its total volume $\int_{S^2} \sqrt{g}$. The partition function (1) can therefore formally be recast as an ordinary integration over the volume V of the canonical partition function $\mathcal{Z}_V$,

二维引力区别于高维引力的一个特点是，真空中的爱因斯坦场方程是平凡的: 当 $\Lambda = 0$ 时，任意黎曼度量都是方程的解，而当 $\Lambda \neq 0$ 时不存在解。这一点关联着一个事实: 由于高斯-博内公式，$d = 2$ 的爱因斯坦-希尔伯特作用量 (2) 中的曲率积分是拓扑不变量，因此将流形 $M = S^2$ 固定为二维球面时，作用量对度量的依赖仅体现在总体积 $\int_{S^2} \sqrt{g}$ 上。配分函数 (1) 因此可以在形式上改写为对体积 V 的普通积分，积分对象是正则配分函数 $\mathcal{Z}_V$,

$$\mathcal{Z}_V = \int \mathcal{D}[g_{ab}]\, \delta\left(V - \int_{S^2} \sqrt{g}\right), \quad \mathcal{Z} = \int_0^\infty \mathrm{d}V e^{-\frac{\Lambda}{16\pi G_N} V} \mathcal{Z}_V. \tag{4}$$

Since every geometry of volume V receives the same Boltzmann weight, the probability measure of two-dimensional quantum gravity (at fixed volume) should amount to a suitable notion of sampling a metric on S^2 uniformly at random.

由于体积 V 的每种几何都拥有相同的玻尔兹曼权重，二维量子引力 (固定体积下) 的概率测度等价于在 S^2 上均匀随机抽样度量的恰当定义。

It is not at all obvious how to interpret this in the infinite-dimensional space of Riemannian geometries on S^2 , but two-dimensional Euclidean dynamical triangulations (EDT) provides a natural lattice discretization [16-20]. Instead of considering the full set of Riemannian geometries on S^2 , one restricts to the piecewise flat geometries that can be assembled from a fixed number of equilateral Euclidean triangles of identical size. This introduces both an ultraviolet cutoff, by having a finite lattice spacing, and an infrared cutoff, by limiting the maximal diameter of the geometry. Since the set of geometries is now finite, one can easily select a uniform random metric by assigning equal probability to each. Then the hope is that this probability measure admits a well-defined continuum limit upon shrinking the triangles while increasing their number. We will review this limit, known as the Brownian sphere, in detail in the mathematical framework of random planar maps, where informally, the building blocks are arbitrary regular (but mostly even-sided) polygons with unit side length.

如何在 S^2 上无穷维的黎曼几何空间中诠释这一点完全不显然, 但二维欧几里得动力三角剖分 (EDT) 提供了自然的晶格离散化方案 [16-20]。该方法不直接考虑 S^2 上的全体黎曼几何，而是将研究范围限制为由固定数量、大小一致的等边欧几里得三角形拼接而成的分段平坦几何。这种引入同时带来了有限晶格间距带来的紫外截断，以及限制几何最大直径带来的红外截断。由于几何集合此时是有限的，我们可以很容易地为每个几何赋予相等概率，得到均匀随机度量。人们期望，在缩小三角形尺寸并增加三角形数量的过程中，该概率测度存在定义良好的连续极限。我们将在随机平面地图的数学框架下详细回顾这个被称为布朗球面的极限，不严格地说，在随机平面地图中，结构单元是任意边长为单位长度的正多边形 (且大多数边数为偶数)。

Based on the extensive mathematical literature, we can summarize some important lessons as follows:

基于大量已有数学研究，我们可以将一些重要结论总结如下:

- The universality observed in enumeration formulas for planar maps can be understood combinatorially via the existence of bijections between maps and trees (section ”Bijection with Trees”).
    - 平面地图计数公式中观测到的普适性，可以通过地图与树之间存在双射从组合角度理解 (参见章节“与树的双射”)。
- The infrared cutoff in the probability measure can be consistently removed by considering the limit of random infinite planar maps in an appropriate topology, known as the local topology (section ”Local Limits”). Often the random infinite geometry is easier to analyze than one of fixed finite size, for instance, when studying explorations (section ”The Peeling Process”).
    - 概率测度中的红外截断可以通过取恰当拓扑 (即局部拓扑) 下随机无穷平面地图的极限一致地移除 (参见章节“局部极限”)。随机无穷几何通常比固定有限大小的几何更容易分析，例如在研究探测过程时就是如此 (参见章节“剥离过程”)。

- The ultraviolet cutoff can be removed via a continuum limit in which the lattice spacing scales appropriately with the size of the random planar map (section "Continuum Limit: Brownian Geometry"). The convergence takes place with respect to the Gromov-Hausdorff topology on the space of (compact) metric spaces (sets equipped with distance functions), which is significantly larger than the space of Riemannian geometries. The limit, known as the Brownian sphere, is a random metric space with the topology of S^2 and well-defined notion of geodesics, providing a precise realization of the probability measure in (3). However, it is not Riemannian as becomes apparent when examining its geodesics more closely (section "Properties of the Brownian Sphere").

- 紫外截断可以通过连续极限移除: 在该极限下，晶格间距随随机平面地图的尺寸按恰当比例缩放 (参见章节“连续极限: 布朗几何”)。收敛是针对 (紧致) 度量空间 (装备距离函数的集合) 空间上的格罗莫夫-豪斯多夫拓扑成立的，该空间远大于黎曼几何空间。这个被称为布朗球面的极限是一个随机度量空间，拥有 S^2 拓扑和定义良好的测地线概念，是 (3) 中概率测度的精准实现。但更细致地考察它的测地线就会发现，它不是黎曼空间 (参见章节“布朗球面的性质”)。

- Removing both cutoffs naturally leads to a random metric space, known as the Brownian plane (section "Local Limits"), with exact scaling symmetry, in the sense that multiplying all distances by a positive constant does not change its distribution. Such a scale-invariant random geometry should be interpreted as realizing a fixed point of the renormalization group associated with Euclidean quantum gravity.

- 同时移除两种截断后自然得到一个被称为布朗平面的随机度量空间 (参见章节“局部极限”)，它具备精确标度对称性: 即所有距离乘以正常数不会改变它的分布。这种标度不变的随机几何应当被诠释为欧几里得量子引力相关重整化群不动点的实现。

Planar Maps and Their Enumeration

平面地图及其计数

Before delving into random geometries and their properties, we will discuss in this section how discrete surfaces are conveniently encoded in terms of maps and how one can approach their enumeration.

在深入研究随机几何及其性质之前，我们将在本节讨论离散曲面如何方便地用地图编码，以及如何研究它们的计数问题。

Maps as Discrete Surfaces

作为离散曲面的地图

In the previous section, we informally introduced discrete surfaces as two-dimensional Riemannian geometries that can be obtained from gluing together regular Euclidean polygons. But since we are interested in precise enumeration, it is important to choose the combinatorial representation in an unambiguous fashion.

在上一节中，我们已经非正式地介绍了离散曲面: 它们是可以通过拼接正则欧几里得多边形得到的二维黎曼几何。但由于我们关注精确计数，因此必须以无歧义的方式选择组合表示。

A simple way to do so is to start with a finite set of regular polygons of unit side length and label the sides by integers $1, 2, \dots, 2n$ in an arbitrary fashion. Given a matching of $\{1, \dots, 2n\}$, i.e., a partition of $\{1, \dots, 2n\}$ into pairs, one may construct a closed surface by gluing the $2n$ sides accordingly (see Fig. 1). More precisely, we assume that the polygons have an orientation and that their sides, also referred to as half-edges, are oriented in counterclockwise direction. We can then make the gluing operation unambiguous by requiring that pairs of half-edges are identified with opposite orientation. If the resulting geometry is connected, this gluing of polygons is called a map.

实现这一点的一个简单方法是: 从有限个单位边长的正则多边形出发，以任意方式用整数标记所有边 $1, 2, \dots, 2n$。给定 $\{1, \dots, 2n\}$ 的一个匹配，也就是将 $\{1, \dots, 2n\}$ 划分为若干对，我们就可以按照匹配规则拼接 $2n$ 条边，得到一个闭合曲面 (参见图 1)。更准确地说，我们假设所有多边形都带有定向，它们的边 (也称为半边) 沿逆时针方向定向。为了让拼接操作无歧义，我们要求配对的半边以相反定向粘合在一起。如果最终得到的几何是连通的，这种多边形的拼接就称为一个地图。

Observe that the $2n$ half-edges of a map are identified into a graph with n edges (hence half-edges) that is embedded in a topological surface, which is necessarily orientable and determined by its genus. This brings us to an alternative definition of a map as a graph together with a proper embedding in a closed oriented surface, where by proper embedding, we mean that the edges do not intersect themselves or other edges, except where they meet at vertices, and that the edges together delimit a collection of topological disks, called the faces of the map (which are nothing but the interiors of the polygons above). One then views two maps as equivalent if they can be related via an orientation-preserving homeomorphism of the surface. We should remark that graphs (and thus maps) are allowed to have more than one edge between a pair of vertices and to have edges starting and ending at the same vertex.

不难看出，一个地图的 $2n$ 个半边会被粘合为一个图，它包含 n 条边，因此才会有「半边」的称呼，这个图嵌入在一个拓扑曲面上，该曲面一定是可定向的，由其亏格唯一确定。这就给出了地图的另一个等价定义: 地图是一个图附带它在闭合定向曲面上的真嵌入；真嵌入指的是边不会和自身或其他边相交，仅允许在顶点处相交，且所有边共同围出若干拓扑圆盘，这些圆盘就是地图的面 (也就是上文所说的多边形内部)。如果两个地图可以通过曲面的保定向同胚互相转换，就称它们等价。需要说明的是，图 (以及相应的地图) 允许一对顶点之间存在多条边，也允许起点和终点是同一个顶点的边。

The sets of vertices, edges, and faces of a map $\mathfrak{m}$ are denoted $\mathrm{V}(\mathfrak{m})$, $\mathrm{E}(\mathfrak{m})$, and $F(\mathfrak{m})$ respectively. According to Euler's formula, the numbers of vertices, edges and faces are related by

一个地图中顶点、边、面的集合 $\mathfrak{m}$ 分别记为 $\mathrm{V}(\mathfrak{m})$, $\mathrm{E}(\mathfrak{m})$ 和 $F(\mathfrak{m})$。根据欧拉公式，顶点数、边数和面数满足关系

$$|V(\mathfrak{m})| - |E(\mathfrak{m})| + |F(\mathfrak{m})| = 2 - 2g, \tag{5}$$

where g is the genus of the corresponding surface. In the case $g = 0$, we are dealing with a planar map, i.e., a polygonal gluing into a topological sphere or, equivalently, a planar graph properly embedded in the

sphere. We take the degree of a vertex or face to be the number of edges incident to it (where we count an edge twice if both endpoints are at the same vertex or both sides adjacent to the same face). Special families of maps that we will encounter are triangulations (In the literature, these triangulations are sometimes called type I, because loops and multiple edges between vertices are allowed. Loopless triangulations, which forbid loops but allow multiple edges, are type II. Simple triangulations forbid both and are type III.), quadrangulations, and even maps, whose faces all have degree three, degree four, or even degree respectively. Even planar maps are also known as bipartite planar maps, because the vertices of such a map can be colored with two colors such that the endpoints of each edge have different color. This should be contrasted with the case of even maps of genus $g \geq 1$, which are not necessarily bipartite.

其中 g 是对应曲面的亏格。当 $g = 0$ 时，我们得到的是平面地图，也就是拼接多边形得到拓扑球面，等价于真嵌入在球面中的平面图。顶点或面的度数定义为与它关联的边数 (如果一条边的两个端点都在同一个顶点，或者一条边的两侧都属于同一个面，这条边记两次)。我们会遇到几类特殊的地图: 三角化、四角化，以及偶地图，它们分别对应所有面的度数都是三、所有面的度数都是四，以及所有面的度数都是偶数的情况。平面偶地图也被称为二部平面地图，因为这类地图的顶点可以用两种颜色染色，使得每条边的两个端点颜色不同，需要注意的是亏格为 $g \geq 1$ 的偶地图不一定是二部图。(文献中，这类三角化有时被称为 I 型三角化，因为允许顶点之间存在环和重边；无环三角化禁止环但允许重边，是 II 型；简单三角化同时禁止环和重边，是 III 型。)

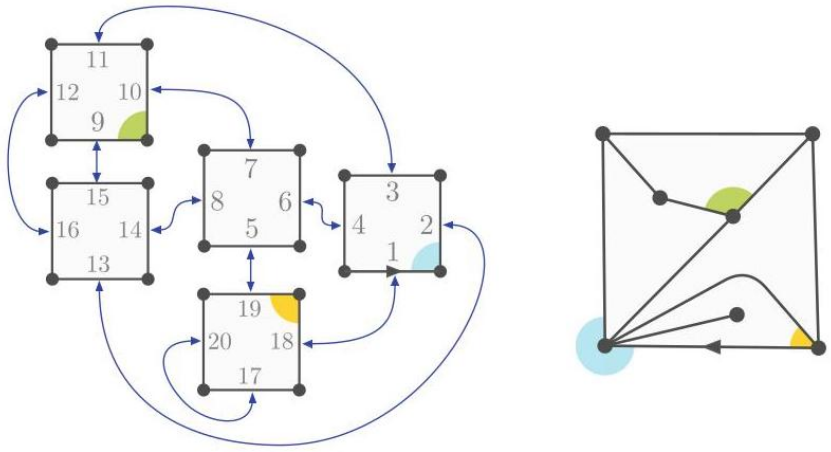

Fig. 1 A planar map as a gluing of polygons and as an embedded graph. This example shows a (rooted) quadrangulation with 5 faces, 10 edges, and 7 vertices. Colors have been added to guide the eye

图 1 分别表示为多边形拼接和嵌入图的平面地图。本例是一个有 5 个面、10 条边、7 个顶点的 (有根) 四角化，添加颜色是为了便于观察

It should be observed that the polygonal gluing provides a highly redundant description of a map, since the half-edges carry an arbitrary labeling, whereas a description in terms of unlabeled embedded graphs is often too abstract to work with. This is especially true when the map in question possesses internal symmetries, i.e., when there exist orientation-preserving homeomorphisms of the sphere that nontrivially permute the edges and vertices of the map, called automorphisms. In such a case, the number of labeled maps corresponding to the same unlabeled map $\mathfrak{m}$ is dependent on the size of the automorphism group $\mathrm{Aut}(\mathfrak{m})$ and is given by $(2n)!/|\mathrm{Aut}(\mathfrak{m})|$. A practical middle ground is to consider unlabeled but rooted maps, meaning that each map comes with a distinguished oriented edge (i.e., a distinguished half-edge). Sending a labeled map

to the (unlabeled) rooted map obtained by distinguishing its half-edge with label 1 is precisely $(2n-1)$!-to-1, so the enumeration of both types is more easily related to each other.

需要注意的是，多边形粘合给出的地图描述是高度冗余的，因为半棱带有任意标号；而无标号嵌入图的描述又往往过于抽象，不便于计算处理。当讨论中的地图存在内对称性 (即存在球面保定向同胚能够非平凡置换地图的棱和顶点，这类变换被称为自同构) 时，这一点尤为明显。这种情况下，对应同一个无标号地图 $\mathfrak{m}$ 的有标号地图数量取决于自同构群 $\mathrm{Aut}(\mathfrak{m})$ 的大小，可由 $(2n)!/|\mathrm{Aut}(\mathfrak{m})|$ 给出。一个实用的折中方案是考虑无标号但有根的地图，即每个地图带有一条特殊的定向棱 (也就是一个特殊半棱)。把一个有标号地图对应到将标号 1 的半棱指定为特殊半棱得到的 (无标号) 有根地图，这恰好是 $(2n-1)$ 对一的映射，因此两类地图的计数可以更方便地相互推导。

Random Planar Map Models

随机平面地图模型

We are now ready to formulate in a precise combinatorial way the partition function of two-dimensional Euclidean dynamical triangulations (EDT) as a lattice discretization of the partition function (4). It can be defined as a summation over all unlabeled, labeled, or rooted planar triangulations as

我们现在可以用精确的组合方式，将二维欧几里得动力学三角剖分 (EDT) 的配分函数表述为式 (4) 配分函数的格点离散化。它可以定义为对所有无标号、有标号或有根平面三角剖分的求和，形式为

$$Z_{\mathrm{EDT}}(q_3) = \sum_{\substack{\text{unlabeled planar}\\ \text{triangulations m}}} \frac{q_3^{|\mathrm{F(m)}|}}{|\mathrm{Aut}(\mathrm{m})|} = \sum_{\substack{\text{labeled planar}\\ \text{triangulations m}}} \frac{q_3^{|\mathrm{F(m)}|}}{(2\,|\mathrm{E}(\mathrm{m})|)!} \tag{6}$$

$$= \sum_{\substack{\text{rooted planar}\\ \text{triangulations }\mathfrak{m}}} \frac{q_3^{|\mathrm{F}(\mathfrak{m})|}}{2\,|\mathrm{E}(\mathfrak{m})|} = \sum_{k=1}^{\infty} \frac{q_3^{2k}}{6k} T_k,$$

(7)

where q_3 can be interpreted as the exponential of the lattice cosmological constant and T_k is the number of rooted planar triangulations with $2k$ triangles. In particular $3q_3 Z'_{\mathrm{EDT}}(q_3) = \sum_{k=1}^{\infty} q_3^{2k} T_k$ is nothing but the generating function of these numbers T_k , so its stands to reason that the enumeration of maps is at the heart of the model. If $q_3 > 0$ is small enough that the sum converges, the Boltzmann weights define a probability distribution on triangulations known as the Boltzmann triangulation. Furthermore, T_k essentially is the corresponding canonical partition function of triangulations of fixed size $2k$, which therefore describes a random triangulation known as the uniform (rooted) triangulation of size $2k$, meaning that each rooted triangulation with $2k$ triangles occurs with equal probability $1/T_k$.

其中 q_3 可解释为格点宇宙学常数的指数，T_k 是含 $2k$ 个三角形的有根平面三角剖分的数量。特别地，$3q_3 Z'_{\mathrm{EDT}}(q_3) = \sum_{k=1}^{\infty} q_3^{2k} T_k$ 正是这些数量 T_k 的生成函数，因此地图计数是该模型的核心。若 $q_3 > 0$ 足够小使得求和收敛，玻尔兹曼权重就会在三角剖分上定义出一个概率分布，称为玻尔兹曼三角剖分。此外，T_k 本质上就是固定大小 $2k$ 三角剖分对应的正则配分函数，它因此描述了一种随机三角剖分，称为大小为 $2k$ 的均匀 (有根) 三角剖分，即每个含 $2k$ 个三角形的有根三角剖分都以相等概率 $1/T_k$ 出现。

One may generalize this model to maps with faces of arbitrary degree by introducing a sequence of (non-negative) weights $\mathbf{q} = (q_1, q_2, q_3, \ldots)$ and assigning those to the faces according to their degree as well as a weight $t > 0$ to each vertex. Denoting the space of all rooted planar maps by $\mathcal{M}$, we are thus considering the partition function

我们可以将该模型推广到含任意次面的地图: 引入一组非负权重 $\mathbf{q} = (q_1, q_2, q_3, \ldots)$，按面的次数将权重分配给各个面，并给每个顶点赋予权重 $t > 0$。记所有有根平面地图的空间为 $\mathcal{M}$，我们于是考虑如下配分函数

$$Z(t, \mathbf{q}) = \sum_{\mathfrak{m} \in \mathcal{M}} t^{|\mathrm{V}(\mathfrak{m})|} \prod_{f \in \mathrm{F}(\mathfrak{m})} q_{\deg f}. \tag{8}$$

Since the sum is over rooted planar maps, this partition function generalizes $3q_3 Z'_{\mathrm{EDT}}(q_3)$ rather than the partition function $Z_{\mathrm{EDT}}(q_3)$ of unlabeled triangulations. If $Z(t, \mathbf{q}) < \infty$, we can normalize the summand by $1/Z(t, \mathbf{q})$ and take it to define a probability distribution on $\mathcal{M}$, which is called the $(t, \mathbf{q})$ -Boltzmann planar map. The parameter t actually is redundant here, because by Euler' s formula (5), we have

由于求和是对有根平面地图进行的，该配分函数推广的是 $3q_3 Z'_{\mathrm{EDT}}(q_3)$，而非无标号三角剖分的配分函数 $Z_{\mathrm{EDT}}(q_3)$。若满足 $Z(t, \mathbf{q}) < \infty$，我们可以用 $1/Z(t, \mathbf{q})$ 对求和项归一化，由此在 $\mathcal{M}$ 上定义一个概率分布，称为 $(t, \mathbf{q})$ 玻尔兹曼平面地图。参数 t 在此处实际上是冗余的，因为根据欧拉公式 (5) 我们有

$$Z(t, \mathbf{q}) = t^2 \sum_{\mathfrak{m} \in \mathcal{M}} \prod_{f \in \mathrm{F}(\mathfrak{m})} t^{-1 + \frac{1}{2}\deg f} q_{\deg f} = t^2 Z(1, \tilde{\mathbf{q}}), \ \tilde{q}_k := t^{-1+\frac{1}{2}k} q_k,$$

(9)

meaning that the $(t, \mathbf{q})$ -Boltzmann planar map is the same as the $\tilde{\mathbf{q}}$ -Boltzmann planar map (with $t = 1$). For combinatorial reasons, it can be useful to keep the parameter t, while we will often set $t = 1$ later without loss of generality.

这说明 $(t, \mathbf{q})$ 玻尔兹曼平面地图与 $\tilde{\mathbf{q}}$ 玻尔兹曼平面地图 (满足 $t = 1$) 是等价的。出于组合考量，保留参数 t 会更方便，而我们后续通常会在不失一般性的前提下令 $t = 1$。

We could have chosen to assign weights to the vertices depending on their degrees instead of the faces, but the resulting models are related by duality. Here the dual of a genus- g map $\mathfrak{m}$ is the map $\mathfrak{m}^\dagger$ obtained by interchanging the roles of vertices and faces of $\mathfrak{m}$ while keeping the same incidence relations. More operationally, one places a vertex of $\mathfrak{m}^\dagger$ in each face of $\mathfrak{m}$, and one connects these by drawing an edge of $\mathfrak{m}^\dagger$ intersecting each edge of $\mathfrak{m}$. The root of $\mathfrak{m}^\dagger$ is taken to be the oriented edge starting at the root face and

crossing the root of $\mathfrak{m}$. Since this is a bijection from $\mathcal{M}$ to itself and the vertex degrees of $\mathfrak{m}^\dagger$ agree with the face degrees of $\mathfrak{m}$, the dual of a $\mathbf{q}$ -Boltzmann planar map is distributed according to the model with vertex weights. A hybrid version, in which both vertices and faces receive weights, poses significant additional challenges, and only limited progress has been made toward solving such models (see [28-31]).

我们原本可以选择根据顶点的度数而非面来给顶点分配权重，但得到的模型可通过对偶性关联。亏格为 g 的地图 $\mathfrak{m}$ 的对偶地图 $\mathfrak{m}^\dagger$ ，是交换 $\mathfrak{m}$ 中顶点与面的角色、同时保持相同关联关系得到的地图。更便于操作地说，我们在 $\mathfrak{m}$ 的每个面中放置一个 $\mathfrak{m}^\dagger$ 的顶点，然后画一条 $\mathfrak{m}^\dagger$ 的边连接这些顶点，这条边会与 $\mathfrak{m}$ 的每条边相交。$\mathfrak{m}^\dagger$ 的根取为从根面出发、穿过 $\mathfrak{m}$ 根的有向边。由于这是 $\mathcal{M}$ 到自身的双射，且 $\mathfrak{m}^\dagger$ 的顶点度数与 $\mathfrak{m}$ 的面度数一致，因此 $\mathbf{q}$ -玻尔兹曼平面地图的对偶服从带顶点权重的模型分布。若同时给顶点和面分配权重，这种混合版本会带来额外的重大挑战，目前求解这类模型仅取得了有限进展 (参见文献 [28-31])。

We start by recalling the classic approach to map enumeration initiated by Tutte in the 1960s [32-34] and which is at the heart of the developments in the EDT (see [20] for an overview and [35,36] for more recent accounts).

我们首先回顾图特在 1960 年代开创的经典地图计数方法 [32-34]，该方法是欧几里得动态三角化 (EDT) 领域诸多发展的核心 (综述参见 [20]，最新论述参见 [35,36])。

Disk Function

圆盘函数

The central idea is that, while it is difficult to write an equation for the partition function itself, it is straightforward to obtain one for the generating function of maps with a boundary of controlled length. Here by boundary or root face (denoted f_{r}), we simply mean the face that lies on the left of the root edge, and its degree is referred to as the perimeter of the map. One thus considers the disk generating function

核心思想是: 虽然直接为配分函数写出方程十分困难，但我们可以很容易地得到边界长度固定的平面地图的生成函数。此处的边界又称根面 (记为 f_{r})，我们仅指根边左侧的面，其度数被称为地图的周长。据此我们定义圆盘生成函数

$$W^{(\ell)}(t,\mathbf{q}) := \sum_{\substack{\text{rooted planar maps } \mathfrak{m} \\ \deg(f_{\mathrm{r}})=\ell}} t^{|\mathrm{V}(\mathfrak{m})|} w_{\mathbf{q}}(\mathfrak{m}),\ w_{\mathbf{q}}(\mathfrak{m}) := \prod_{f\in \mathrm{F}(\mathfrak{m})\setminus\{f_{\mathrm{r}}\}} q_{\deg f},$$

(10)

where by convention, we set $W^{(0)}(t,\mathbf{q}) = t$, counting the map consisting of a single vertex and no edges. In the following, we will drop the explicit dependence on $\mathbf{q}$ for notational simplicity and simply write $W^{(\ell)}$.

按照约定，我们设定 $W^{(0)}(t,\mathbf{q}) = t$ ，对应计数仅含单个顶点、不含边的地图。下文为简化符号，会省略 $\mathbf{q}$ 的显式依赖，直接记为 $W^{(\ell)}$ 。

For any $\ell \geq 1$ one can decompose a rooted map by removing the root edge, which either leads to a map with one face less or to a pair of maps (see Fig. 2). At the level of generating functions, this decomposition

leads to the famous Tutte equation or loop equation [34]

对任意 $\ell \geq 1$，我们都可以通过移除根边分解根地图: 要么得到一个少一张面的地图，要么得到一对地图 (参见图 2)。在生成函数层面，该分解给出著名的图特方程，又称环路方程 [34]

$$W^{(\ell)} = \sum_{k=1}^{\infty} q_k W^{(\ell+k-2)} + \sum_{p=0}^{\ell-2} W^{(p)} W^{(\ell-p-2)}. \ (\ell \geq 1)$$

(11)

By introducing a generating variable x for the boundary length ℓ ,

我们引入生成变量 x 对应边界长度 ℓ ,

$$W(x) := \sum_{\ell=0}^{\infty} W^{(\ell)} x^{-\ell-1}, \ V'(x) := x - \sum_{k=1}^{\infty} q_k x^{k-1}, \tag{12}$$

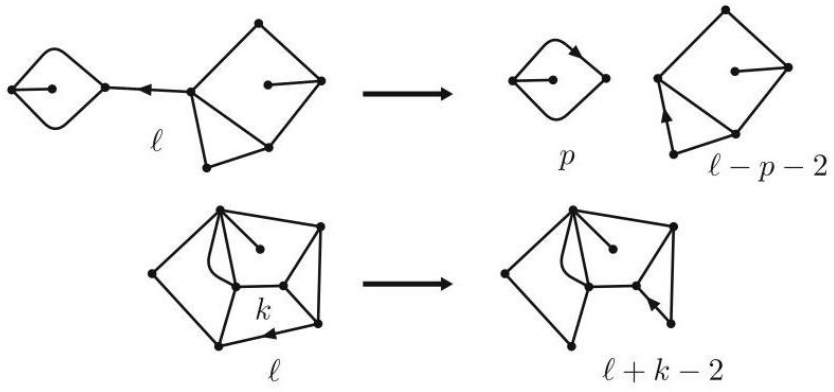

Fig. 2 Dropping the root edge of a map of perimeter ℓ leads either to a pair of maps of perimeters p and $\ell - p - 2$ for some $0 \leq p \leq \ell - 2$ or to a single map of perimeter $\ell + k - 2$ for $k \geq 1$

图 2 移除周长为 ℓ 的地图的根边后，要么得到一对周长分别为 p 和 $\ell - p - 2$ 的地图 (满足某个 $0 \leq p \leq \ell - 2$)，要么得到一张周长为 $\ell + k - 2$ 的地图 (对应 $k \geq 1$)

this equation can be seen to be equivalent to $W(x)^2 - V'(x) W(x)$ being analytic at $x = 0$. More precisely, we have the identity

可以看出该方程等价于 $W(x)^2 - V'(x) W(x)$ 在 $x = 0$ 处解析。更准确地说，我们有如下恒等式

$$V'(x) W(x) - W(x)^2 = Q(x) := t - \sum_{p=0}^{\infty} x^p \sum_{k=p+2}^{\infty} q_k W^{(k-p-2)}, \tag{13}$$

which is solved by

其解为

$$W(x) = \frac{1}{2}\left(V'(x) - \sqrt{V'(x)^2 - 4Q(x)}\right). \tag{14}$$

Here the sign in front of the square root is determined by the requirement that $xW(x) \to t$ as $x \to \infty$.

此处根号前的符号由条件 $xW(x) \to t$ 当 $x \to \infty$ 确定。

Let us for the moment assume that only finitely many weights are nonzero, such that $V'(x)$ and $Q(x)$ are both polynomials. The results, however, can be shown to hold more generally, as we will see in section "Bijection with Trees," where we will be more careful about convergence issues. In the polynomial case, one can make the one-cut assumption (or use Brown's Theorem [37]) that the polynomial $V'(x)^2 - 4Q(x)$ factorizes as

我们暂时假设只有有限个权重非零，因此 $V'(x)$ 和 $Q(x)$ 均为多项式。但我们会在“与树的双射”一节中更严谨地讨论收敛性问题，届时会证明该结论可推广至更一般的情况。对于多项式情形，我们可以使用单割假设 (或布朗定理 [37])，即多项式 $V'(x)^2 - 4Q(x)$ 可分解为

$$V'(x)^2 - 4Q(x) = M(x)^2 (x - c_+)(x - c_-), \ (c_+ > c_-) \tag{15}$$

where the sign of $M(X)$ is chosen such that $V'(x)/(xM(x)) \to 1$ as $x \to \infty$. Hence,

其中 $M(X)$ 的符号按条件 $V'(x)/(xM(x)) \to 1$ 当 $x \to \infty$ 选取。因此可得:

$$W(x) = \frac{1}{2}\left(V'(x) - M(x)\sqrt{(x - c_+)(x - c_-)}\right). \ (x \in \mathbb{C} \setminus [c_-, c_+]) \tag{16}$$

The polynomial $M(x)$ and the endpoints $c_\pm = c_\pm(t, \mathbf{q})$ of the branch cut are then completely determined in terms of the weights t and $\mathbf{q}$ by expanding the right-hand side around $x = \infty$ and imposing the condition $xW(x) \to t$ as $x \to \infty$.

多项式 $M(x)$ 与支割端点 $c_\pm = c_\pm(t, \mathbf{q})$ 可完全由权重 t 、$\mathbf{q}$ 确定: 只需将右侧在 $x = \infty$ 附近展开，并施加条件 $xW(x) \to t$ 当 $x \to \infty$ 即可。

This can be made more explicit by performing the Zhukovsky transformation [35]

我们可以通过茹科夫斯基变换 [35] 将其写得更显式

$$x(z) = \frac{c_+ + c_-}{2} + \frac{c_+ - c_-}{4}\left(z + \frac{1}{z}\right), \tag{17}$$

which is designed such that $W(x(z))$ becomes a Laurent polynomial in z (i.e., a polynomial in z and $1/z$),

其设计目的是让 $W(x(z))$ 成为 z 上的洛朗多项式 (即 z 和 $1/z$ 上的多项式),

$$W(x(z)) = \frac{1}{2}V'(x(z)) - M(x(z))\frac{c_+ - c_-}{8}\left(z - \frac{1}{z}\right) \equiv \frac{1}{2}V'(x(z)) + y(z). \tag{18}$$

The pair of functions $x(z), y(z)$ is known as the spectral curve of the model and plays an important role in topological recursion [35, 38, 39], which relates generating functions of maps with multiple boundaries or higher genus to the disk function. Since we will stick to the planar case, we will not delve into this topic.

函数对 $x(z), y(z)$ 被称为该模型的谱曲线，在拓扑递归中发挥重要作用 [35, 38, 39]，拓扑递归将含多个边界或更高亏格的地图的生成函数与圆盘函数关联起来。由于本文我们仅讨论平面情形，因此不对该主题展开深入探讨。

Note that under the transformation $z \to 1/z$ the first term in (18) is symmetric, $V'(x(1/z)) = V'(x(z))$, while the second is antisymmetric, $y(z) = -y(1/z)$. Since $W(x(z)) = t\frac{4}{c_+ - c_-}z^{-1} + O\left(z^{-2}\right)$, it follows that for any $p \geq 0$, we have

注意到在变换 $z \to 1/z$ 下，式 (18) 中的第一项是对称的，即 $V'(x(1/z)) = V'(x(z))$，而第二项是反对称的，即 $y(z) = -y(1/z)$。由于 $W(x(z)) = t\frac{4}{c_+ - c_-}z^{-1} + O\left(z^{-2}\right)$，因此对任意 $p \geq 0$，我们有

$$0 = \frac{1}{2}[z^p]V'(x(z)) + [z^p]y(z) = \frac{1}{2}[z^{-p}]V'(x(z)) - [z^{-p}]y(z), \tag{19}$$

where the notation $\left[z^k\right]f(z)$ for a Laurent polynomial f refers to the coefficient of z^k in f. Hence

其中劳伦多项式 f 的记号 $\left[z^k\right]f(z)$ 指的是 f 中 z^k 的系数。因此

$$[z^{-p}]W(x(z)) = [z^p]V'(x(z)) \overset{(12)}{=} \frac{c_+ - c_-}{4}\mathbf{1}_{\{p=1\}} - \sum_{k=1}^{\infty} q_k [z^p]x(z)^{k-1}. \tag{20}$$

The equations $\left[z^0\right]W(x(z)) = 0$ and $\left[z^{-1}\right]W(x(z)) = 4t/(c_+ - c_-)$ then uniquely determine $c_\pm$ in terms of $\mathbf{q}$ and t.

方程 $\left[z^0\right]W(x(z)) = 0$ 和 $\left[z^{-1}\right]W(x(z)) = 4t/(c_+ - c_-)$ 由此可以通过 $\mathbf{q}$ 和 t 唯一确定 $c_\pm$。

The partition function (8) can be retrieved from $W^{(2)}$ by the observation that zipping open the root edge of a rooted map results bijectively in a rooted map with boundary of length 2 and at least two faces. Hence

配分函数 (8) 可从 $W^{(2)}$ 得到，因为我们注意到: 拉开有根地图的根边，会得到一个双射对应，对应一张边界长度为 2 且至少包含两个面的有根地图。因此

$$Z(t, \mathbf{q}) = W^{(2)} - t^2 \overset{(11)}{=} \sum_{k=1}^{\infty} q_k W^{(k)}. \tag{21}$$

Pointed Maps

带点地图

Expression (16) for the disk function already displays a degree of universality, in that the general structure is independent of the weights $\mathbf{q}$ and t. This universality becomes more explicit when one considers planar maps with a distinguished face of specified degree [19, 20, 38, 40], whose generating functions depend only

on $c_\pm$. Let us concentrate on the special case of planar maps with a distinguished vertex, which are also called pointed planar maps. The generating function $W_\bullet^{(\ell)}(t,\mathbf{q})$ is defined just like $W^{(\ell)}(t,\mathbf{q})$ in (10), except the sum runs over pointed planar maps and the distinguished vertex does not receive weight t . It should be clear that pointed and unpointed disk functions are related by a t -derivative,

圆盘函数的表达式 (16) 已经展现出一定的普适性，其整体结构不依赖于权重 $\mathbf{q}$ 和 t 。当我们研究带有指定度数的特殊面的平面地图时，这种普适性会更加明显，这类平面地图的生成函数仅依赖于 [19, 20, 38, 40] 、$c_\pm$ 。下面我们聚焦于特殊情形: 带有特殊顶点的平面地图，这类地图也被称为带点平面地图。生成函数 $W_\bullet^{(\ell)}(t,\mathbf{q})$ 的定义与 (10) 式中的 $W^{(\ell)}(t,\mathbf{q})$ 定义一致，唯一区别是求和遍历所有带点平面地图，且特殊顶点不带有权重 t 。显然，带点与不带点圆盘函数的关系可由对 t 求导得到,

$$W_\bullet^{(\ell)} = \frac{\partial}{\partial t} W^{(\ell)},\ W_\bullet(x) = \sum_{\ell=0}^{\infty} W_\bullet^{(\ell)} x^{-\ell-1} = \frac{\partial}{\partial t} W(x). \tag{22}$$

Inserting (18) and applying the chain rule while observing that $V'(x)$ does not depend on the weight t , one finds the relation [35]

代入 (18) 式并应用链式法则，同时注意到 $V'(x)$ 不依赖于权重 t ，我们可得如下关系 [35]

$$W_\bullet(x(z)) = \frac{\partial y(z)}{\partial t} - \frac{y'(z)}{x'(z)} \frac{\partial x(z)}{\partial t}. \tag{23}$$

Now one should observe that the right-hand side of

现在可以观察到

$$z x'(z) W_\bullet(x(z)) = z x'(z) \frac{\partial y(z)}{\partial t} - z y'(z) \frac{\partial x(z)}{\partial t} \tag{24}$$

is a Laurent polynomial that is symmetric under $z \to 1/z$, while the left-hand side approaches 1 when $z \to \infty$, because $x W_\bullet(x) \to 1$ as $x \to \infty$. Hence, the full Laurent polynomial must be identically equal to 1. Inverting the Zhukovsky transformation then leads to the universal formula

的右侧是在 $z \to 1/z$ 下对称的洛朗多项式，当 $z \to \infty$ 时左侧趋近于 1，这是因为当 $x \to \infty$ 时的 $x W_\bullet(x) \to 1$ 。因此，整个洛朗多项式恒等于 1。对茹科夫斯基变换求逆后即可得到普适公式

$$W_\bullet(x) = \frac{1}{\sqrt{(x-c_+)(x-c_-)}}. \tag{25}$$

Bipartite Maps

二部地图

If only $q_2, q_4, \ldots$ are nonzero, we are dealing with bipartite planar maps, and the branch cut $[c_-, c_+]$ becomes symmetric around 0 . For future reasons, we introduce the notation

若只有 $q_2, q_4, \ldots$ 非零，则我们讨论的是二部平面地图，且分支割线 $[c_-, c_+]$ 关于 0 对称。为后续研究方便，我们引入记号

$$R(t, \mathbf{q}) = \frac{1}{4}c_+^2 = \frac{1}{4}c_-^2 = t + O\left(t^2\right), \tag{26}$$

such that

使得

$$x(z) = \sqrt{R}\left(z + \frac{1}{z}\right), \; W_\bullet(x) = \frac{1}{\sqrt{x^2 - 4R}}. \tag{27}$$

From the last formula, we deduce by series expansion around $x = \infty$ that

根据上式，我们通过在 $x = \infty$ 附近做级数展开推导出

$$W_\bullet^{(2\ell)} = \binom{2\ell}{\ell} R^\ell. \tag{28}$$

Note in particular that $W_\bullet^{(2)} = 2R$. By removing the contribution $2t$ of the maps consisting of a single edge and zipping closed the boundary of the remaining maps, we obtain the generating function

特别注意 $W_\bullet^{(2)} = 2R$ 。通过移除由单条边构成的地图的贡献 $2t$ ，并将剩余地图的边界收缩闭合，我们得到配分函数

$$\frac{\partial}{\partial t} Z = 2R - 2t \tag{29}$$

for pointed bipartite planar maps. Equation (20) with $p = 1$ and $\left[z^{-1}\right] W(x(z)) = t/\sqrt{R}$ results in the explicit recursive equation

对应带点二部平面地图。将方程 (20) 代入 $p = 1$ 和 $\left[z^{-1}\right] W(x(z)) = t/\sqrt{R}$ 后，可得显式递推方程

$$R = t + \sum_{k=1}^{\infty} q_{2k} \binom{2k-1}{k} R^k. \tag{30}$$

The simple form of this equation and the universal form of the pointed disk function $W_\bullet(z)$ have appeared rather miraculously. In the following sections, we will give two explanations for this simplicity, a bijective approach involving combinatorial trees and a probabilistic approach involving a peeling exploration. As a bonus, both approaches provide insights into the geometry of the $\mathbf{q}$ -Boltzmann maps.

该方程的简洁形式与带点圆盘函数 $W_\bullet(z)$ 的普适形式来得相当巧妙。在下文中，我们将给出两种解释这种简洁性的方法: 一种是涉及组合树的双射方法，另一种是涉及剥落探索的概率方法。此外，两种方法都能为我们揭示 $\mathbf{q}$ -玻尔兹曼地图的几何性质。

Bijection with Trees

与树的双射

The solution method presented to determine the generating function of planar maps required some ingenuity (that can be traced back to Tutte): the generating function $Z(t, \mathbf{q})$ could not be identified as a solution of an equation, but introducing an additional generating variable x for the root face degree, such an equation could be found, which miraculously could be solved rather explicitly. Compared to planar maps, trees are much simpler objects because their generating functions do naturally satisfy an equation (without introducing extra variables) and therefore feature prominently in the combinatorial literature (see [41] for an overview). A natural strategy to enumerate non-treelike objects, or to explain a mysterious simplicity in the enumeration, is to seek bijective relations with trees. This route has played a central role in the mathematical developments of planar maps, and a good number of examples of such tree bijection are known (see [42-47] for a non-exhaustive list). We will focus on the Bouttier-DiFrancesco-Guitter (BDFG) bijection [45] that is well suited for the enumeration of planar maps with control on the face degrees. We restrict our attention to bipartite planar maps and refer the reader to [45] for the general case.

本文介绍的求解平面图生成函数的方法需要一些巧妙构思 (可追溯至塔特): 生成函数 $Z(t, \mathbf{q})$ 无法直接被识别为某个方程的解，但引入根面度的额外生成变量 x 后，就能得到这样一个方程，而且它居然可以相当显式地求解。和平面图相比，树是简单得多的对象，因为它们的生成函数自然满足方程 (无需引入额外变量)，因此在组合学文献中占据重要地位 (综述参见 [41])。对非树状结构对象计数，或是解释计数中出现的神秘简洁性，一个自然的策略就是寻找其与树的双射关系。这条路线在平面图的数学发展中发挥了核心作用，目前已知大量这类树双射的例子 (非完整列表参见 [42-47])。我们将重点介绍布蒂耶-迪弗朗切斯科-吉特 (BDFG) 双射 [45]，该双射非常适合对控制面度条件下的平面图计数。我们这里仅讨论二部平面图，一般情况读者可参考 [45]。

The Bouttier-DiFrancesco-Guitter Bijection

布蒂耶-迪弗朗切斯科-吉特双射

In the last section, we have seen that particularly pointed maps admit simple generating functions, so let us consider a rooted bipartite planar map $\mathfrak{m}$ with a distinguished vertex, which we call the origin. Naturally one may assign a label ℓ_v to each vertex $v \in \mathrm{V}(\mathfrak{m})$ by taking ℓ_v to be the graph distance along the edges of $\mathfrak{m}$ from v to the origin (Fig. 3a). Because $\mathfrak{m}$ is bipartite, the labels at the endpoints of each edge differ exactly by 1. For reasons that will become clear soon, let us restrict to the situation where the labels along the root edge of $\mathfrak{m}$ increase from its start to end. This is the case for exactly half of the maps, so by (29) these should be enumerated by $R - t$, for which we will deduce a bijective explanation.

在上一节中我们看到，特殊带点地图拥有简单的生成函数，因此我们考察一个带有区别顶点 (我们称之为原点) 的根二部平面图 $\mathfrak{m}$ 。我们自然可以给每个顶点 $v \in \mathrm{V}(\mathfrak{m})$ 分配一个标签 ℓ_v ，其中 ℓ_v 是 $\mathfrak{m}$ 中沿边从 v 到原点的图距离 (图 3a)。由于 $\mathfrak{m}$ 是二部图，每条边两端点的标签恰好相差 1。出于很快就会明晰的原因，我们限定讨论 $\mathfrak{m}$ 的根边上标签从起点到终点递增的情况。恰好有一半的地图满足该条件，因此根据式 (29)，这类地图的计数由 $R - t$ 给出，我们将推出它的双射解释。

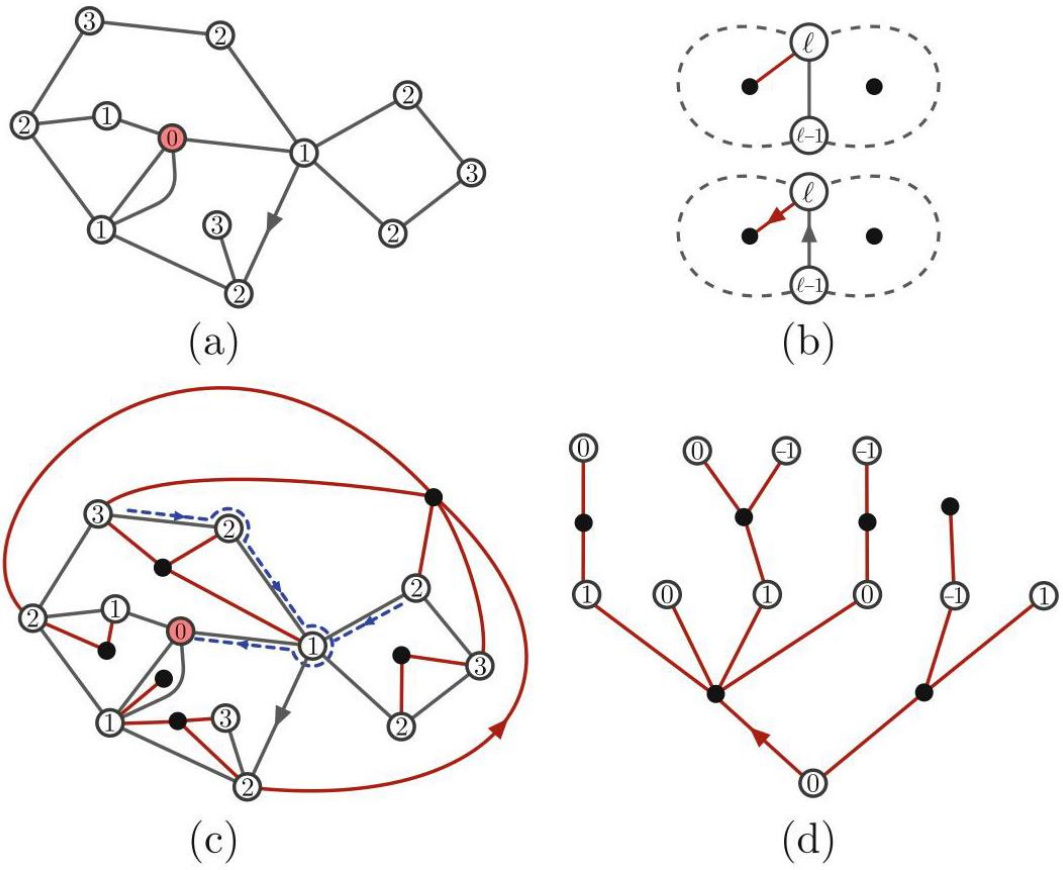

Fig. 3 The Bouttier-DiFrancesco-Guitter bijection. (a) A rooted even planar map $\mathfrak{m}$ with a distinguished vertex (shaded in red) together with its canonical labeling by the graph distance. (b) The prescription for drawing new (red) edges and a new root. (c) The result of applying the prescription to $\mathfrak{m}$. The (blue) dashed lines indicate two leftmost geodesics. (d) After deleting the edges of $\mathfrak{m}$ and the origin and shifting the labels such that the start of the root edge receives label 0, one obtains the mobile t

图 3 布蒂耶-迪弗朗切斯科-吉特双射。(a) 带有一个区别顶点 (红色阴影) 的根偶平面图 $\mathfrak{m}$ ， 以及按图距离得到的规范标签。(b) 绘制新 (红色) 边和新根的规则。(c) 对 $\mathfrak{m}$ 应用规则得到的结果，蓝色虚线表示两条最左测地线。(d) 删除 $\mathfrak{m}$ 的边和原点，移动标签使根边起点获得标签 0 后，得到的动树 t

The Bouttier-DiFrancesco-Guitter (BDFG) bijection provides an encoding of these maps in terms of so-called mobiles. A mobile is a tree t, i.e., a rooted planar map with only one face, with black vertices and integer-labeled white vertices satisfying the following properties (see Fig. 3d for an example):

布蒂耶-迪弗朗切斯科-吉特 (BDFG) 双射提供了这类地图用所谓动树的编码。动树是一棵树 t，即仅含一个面的根平面图，包含黑色顶点和带整数标签的白色顶点，满足下述性质 (示例见图 3d):

(i) The two endpoints of each edge have different color.

(i) 每条边的两个端点颜色不同。

(ii) The root edge starts at a white vertex with label 0 .

(ii) 根边起始于标签为 0 的白色顶点。

(iii) Around each black vertex, if a white neighbour has label ℓ then the next white neighbour in clockwise order around the black vertex must have label at least $\ell - 1$.

(iii) 对任意黑色顶点，若其一个白色邻点的标签为 ℓ ，则顺时针方向下该黑色顶点的下一个白色邻点的标签至少为 $\ell - 1$ 。

From Planar Maps to Trees

从平面地图到树

The procedure to associate a mobile $\mathfrak{t}$ to $\mathfrak{m}$ is as follows:

将流动树 $\mathfrak{t}$ 关联到 $\mathfrak{m}$ 的步骤如下:

1. Let the vertices of $\mathfrak{m}$ be white and draw a new black vertex in each face of $\mathfrak{m}$ (Fig. 3c).

1. 将 $\mathfrak{m}$ 的顶点设为白色，在 $\mathfrak{m}$ 的每个面中绘制一个新的黑色顶点 (图 3c)。

2. For each edge e of $\mathfrak{m}$, let v be the endpoint of e with the largest label. Draw a new edge starting at v and ending on the black vertex within the face to the left of e when facing v (Fig. 3b). If e is the root of $\mathfrak{m}$, we take the new edge to be the new root (oriented away from v).

2. 对于 $\mathfrak{m}$ 的每条边 e ，设 v 是 e 中标号最大的端点。绘制一条新边，起点为 v ，终点为朝向 v 时 e 左侧面内的黑色顶点 (图 3b)。若 e 是 $\mathfrak{m}$ 的根，则将这条新边设为新根 (方向背离 v)。

3. Remove all original edges of $\mathfrak{m}$ as well as the origin vertex (Fig. 3d).

3. 移除 $\mathfrak{m}$ 所有原有边和原点顶点 (图 3d)。

4. Shift all labels uniformly such that the root vertex receives label 0.

4. 统一平移所有标号，使根顶点的标号为 0。

Why does this procedure result in a mobile? The main feature of the construction is that $\mathfrak{t}$ cannot have any cycles. The explanation is that for any edge e of $\mathfrak{m}$, one can find a curve, called the leftmost geodesic, starting at (say, the midpoint of) e and ending at the origin that does not intersect t. This immediately implies the impossibility of cycles in t , because every cycle in t would enclose the origin on one side and at least one edge on the other side, contradicting the existence of a leftmost geodesic path from that edge to the origin.

为什么这个过程得到的是流动树？该构造的核心特点是 $\mathfrak{t}$ 不存在任何环。解释如下: 对于 $\mathfrak{m}$ 的任意边 e，总能找到一条称为最左测地线的曲线，从 e (例如其中点) 出发，终止于原点，且不与 $\mathfrak{t}$ 相交。这直接说明 t 中不可能存在环, 因为 t 的任意环都会将原点围在一侧, 至少将一条边围在另一侧, 与这条边到原点存在最左测地线矛盾。

The leftmost geodesic is constructed as follows (see the dashed curve in Fig. 3c for an example): denote the endpoints of e by v_ℓ and $v_{\ell-1}$ with labels ℓ and $\ell-1$, respectively. The curve starts by traversing e toward $v_{\ell-1}$. If $\ell = 1, v_{\ell-1}$ is the origin, and we are done. Otherwise, the curve circles around $v_{\ell-1}$ in clockwise direction until it encounters an edge with endpoint at distance $\ell - 2$, that we denote $v_{\ell-2}$. Such an edge always exists due to the definition of the graph distance, and by construction of t, one encounters no edge of t along the way. Traversing the edge to $v_{\ell-2}$ and iterating, one obtains a curve ending at the origin v_0, since that is the unique vertex with minimal label. The path $v_\ell, v_{\ell-1}, \dots, v_0$ in $\mathfrak{m}$ is called the leftmost geodesic, because it is a path of minimal length from v_ℓ to the origin and at each vertex it chooses the leftmost option among such minimal paths.

最左测地线构造如下 (示例参见图 3c 中的虚线): 记 e 的两个端点为 v_ℓ 和 $v_{\ell-1}$，对应标号分别为 ℓ 和 $\ell-$ 减 1。曲线从起点出发沿 e 向 $v_{\ell-1}$ 行进。若 $\ell = 1, v_{\ell-1}$ 是原点，则构造完成。否则，曲线绕 $v_{\ell-1}$ 顺时针旋转，直到遇到一个端点距离为 $\ell - 2$ 的边，记该边为 $v_{\ell-2}$。根据图距离的定义，这样的边一定存在，并且由 t 的构造可知，旋转过程中不会遇到 t 的任何边。沿边行进到 $v_{\ell-2}$ 后重复上述步骤，最终就能得到一条终止于原点 v_0 的曲线，因为原点是唯一标号最小的顶点。$\mathfrak{m}$ 中的路径 $v_\ell, v_{\ell-1}, \dots, v_0$ 被称为最左测地线，因为它是从 v_ℓ 到原点的最短长度路径，且在每个顶点处都从所有最短路径中选择了最靠左的选项。

In the absence of cycles, the number of connected components of $\mathfrak{t}$ is given by $|V(t)| - |E(t)|$. But by construction, $|V(t)| = |V(m)| + |F(m)| - 1$ and $|E(t)| = |E(m)|$, which together with Euler's formula (5) implies that t has a single connected component and is thus a tree. That the labels satisfy the properties of a mobile is straightforwardly checked from the construction.

在无环的前提下，$\mathfrak{t}$ 的连通分量数量由 $|V(t)| - |E(t)|$ 给出。但根据构造，结合 $|V(t)| = |V(m)| + |F(m)| - 1$ 和 $|E(t)| = |E(m)|$ 与欧拉公式 (5)，可推导出 t 只有一个连通分量，因此是一棵树。标号满足流动树的性质也可通过构造直接验证。

From Trees to Planar Maps

从树到平面图

Starting from a mobile $\mathfrak{t}$, one constructs a map $\mathfrak{m}$ in a reverse fashion. The angular region around a vertex v that is delimited by two neighbouring edges incident to v is called a corner of v. The contour of a face f is the cyclic sequence of corners one encounters while walking around the perimeter of f while keeping the edges on the right-hand side. The contour of (the unique face of) a tree thus visits all its corners in clockwise direction. The procedure is then as follows:

从活动图 $\mathfrak{t}$ 出发，我们可以通过逆过程构造出平面图 $\mathfrak{m}$ 。顶点 v 的两条相邻关联边围出的顶点周围角区域称为 v 的一个角。面 f 的轮廓是沿面周长行走、始终保持边在右手侧时经过的角的循环序列。因此树 (唯一面) 的轮廓会按顺时针方向访问它的所有角。构造步骤如下:

1. Add a new white vertex (the origin) with label $\ell_{\min}-1$ in the face of $\mathfrak{t}$, where $\ell_{\min}$ is the minimal label of $\mathfrak{t}$.

1. 在 $\mathfrak{t}$ 的面中添加一个带标签 $\ell_{\min}-1$ 的新白色顶点 (原点)，其中 $\ell_{\min}$ 是 $\mathfrak{t}$ 的最小标签。

2. For each corner c of a white vertex with label ℓ in $\mathfrak{t}$, we draw a new edge from c to the next corner of a white vertex in the contour that has label $\ell-1$ in case $\ell>\ell_{\min}$ or to the origin in case $\ell=\ell_{\min}$. If c is the corner of the root vertex that sits left of the root edge, then the new edge is taken to be the new root (oriented away from c).

2. 对于 $\mathfrak{t}$ 中标签为 ℓ 的白色顶点的每个角 c ，我们从 c 向轮廓中满足 $\ell>\ell_{\min}$ 条件下标签为 $\ell-1$ 的下一个白色顶点角，或满足 $\ell=\ell_{\min}$ 条件下的原点绘制一条新边。若 c 是根边左侧的根顶点角，则这条新边即为新根 (方向背离 c)。

3. Remove all edges of $\mathfrak{t}$.

3. 删除 $\mathfrak{t}$ 的所有边。

One can show [45] that the construction is well-defined for any mobile, in the sense that the edges in the second step can be drawn unambiguously in a non-intersecting fashion and that this is precisely the inverse of the construction in section "From Planar Maps to Trees." Note that the labels of $\mathfrak{t}$ need to be shifted by $1-\ell_{\min}$ to arrive at the graph distances to the origin.

可以证明 [45]，该构造对任意活动图都是良定义的: 第二步中的边可以无歧义、无交叉地画出，且该构造恰好是"从平面图到树"一节中构造的逆。注意需要将 $\mathfrak{t}$ 的标签平移 $1-\ell_{\min}$ ，才能得到到原点的图距离。

Let us make an observation about the leftmost geodesics that will become important later [48]. We have precisely one such geodesic $v_\ell, v_{\ell-1}, \dots, v_{\ell_{\min}-1}$ of length $\ell-\ell_{\min}+1$ for each corner c of a white vertex with label ℓ in $\mathfrak{t}$, and the path can be easily deduced from the sequence of labels in the contour of $\mathfrak{t}$: for $\ell_{\min}\le i<\ell$ the vertex v_i is simply the first vertex with label i encountered when following the contour starting from c . In particular, two geodesics from corner c at vertex v and coner c' at vertex v' will typically merge before reaching the origin (see Fig. 3c). The merge happens at a vertex with label $\max(k,k')-1$ where k is the minimal label along the contour between c (inclusive) and c' (exclusive) and k' is the minimal labels in the contour between c' (inclusive) and c (exclusive). Although one cannot easily deduce the graph distance $d_{\mathrm{gr}}(v,v')$, we do find an upper bound by concatenating the geodesics up to their merger,

我们对最左测地线做一个观察，这一点在后续非常重要 [48]。对于 $\mathfrak{t}$ 中标签为 ℓ 的白色顶点的每个角 c，恰好存在一条长度为 $\ell - \ell_{\min} + 1$ 的最左测地线 $v_\ell, v_{\ell-1}, \dots, v_{\ell_{\min}-1}$，该路径可以很容易地从 $\mathfrak{t}$ 轮廓的标签序列得到: 对于 $\ell_{\min} \le i < \ell$，顶点 v_i 就是从 c 出发沿轮廓行走遇到的第一个标签为 i 的顶点。特别地，来自顶点 v 的角 c 和顶点 v' 的角 c' 的两条测地线通常会在到达原点前合并 (见图 3c)，合并发生在标签为 $\max(k, k') - 1$ 的顶点处，其中 k 是 c (含) 到 c' (不含) 之间轮廓的最小标签，k' 是 c' (含) 到 c (不含) 之间轮廓的最小标签。尽管我们无法直接推导出图距离 $d_{\mathrm{gr}}(v, v')$，但可以通过将两条测地线连接到合并点得到它的一个上界，

$$d_{\mathrm{gr}}(v, v') \le \ell_v + \ell_{v'} - 2\max(k, k') + 2. \tag{31}$$

Enumeration Based on the Trees

基于树的枚举

In the BDFG bijection, each face of $\mathfrak{m}$ of degree $2k$ corresponds to a black vertex in t of degree k and each vertex, except for the distinguished one, to a white vertex of $\mathfrak{t}$. As a consequence, the generating function $R(t, \mathbf{q}) - t$ from (29) for (half of) the pointed bipartite planar maps is also the generating function of mobiles with at least one edge and a weight t per white vertex and a weight q_{2k} per black vertex of degree k. These mobiles admit a convenient recursive decomposition. Let us denote the root vertex by v_0. If the degree of the black vertex at the end of the root edge is k, then it has $k-1$ white children $v_1, \dots, v_{k-1}$. Each vertex v_i, together with its offspring, excluding the branch of the root edge in case of v_0, determines a mobile, once the labels have been shifted such that the root vertex v_i receives label 0. Noting that these mobiles may take the form of a single white vertex with no children, this leads immediately to the equation

在 BDFG 双射中，$\mathfrak{m}$ 的每个次数为 $2k$ 的面对应 t 中一个次数为 k 的黑顶点，除特殊顶点外，其余每个顶点对应 $\mathfrak{t}$ 的一个白顶点。因此，式 (29) 中针对带根二分平面图 (半数情况) 的生成函数 $R(t, \mathbf{q}) - t$，同时也是至少含一条边、每个白顶点带权重 t、每个次数为 k 的黑顶点带权重 q_{2k} 的移动生成函数。这类移动存在简洁的递归分解。记根顶点为 v_0。若根边末端黑顶点的次数为 k，则它有 $k-1$ 个白子节点 $v_1, \dots, v_{k-1}$。每个顶点 v_i 连同其后代，当顶点为 v_0 时排除根边所在分支，将根顶点 v_i 平移标记为 0 后，就确定了一个移动。注意到这类移动可以是单个没有子节点的白顶点，由此我们直接得到方程

$$R - t = \sum_{k=1}^{\infty} q_{2k} \sum_{\substack{\text{labelson} \\ v_1,\dots,v_{k-1}}} \begin{array}{ccccc} & R & R & R & \\ \boxed{?} & \boxed{?} & \boxed{?} & \boxed{?} & \\ c & p & p & & \end{array} = \sum_{k=1}^{\infty} q_{2k} \binom{2k-1}{k} R^k, \tag{32}$$

because there are precisely $\binom{2k-1}{k}$ choices for the labels $\ell_1, \cdots, \ell_{k-1}$ on $v_1, \dots, v_{k-1}$ satisfying the requirements $\ell_1 \ge -1, \ell_k \le 1$, and $\ell_{i+1} \ge \ell_i - 1$ for $i = 1, \dots, k-1$. We thus reproduce Eq. (30). Since the summand gives the contribution of maps with root face of degree $2k$, we also reproduce

因为满足要求 $\ell_1 \geq -1, \ell_k \leq 1$ 的 $v_1, \ldots, v_{k-1}$ 上恰好有 $\binom{2k-1}{k}$ 种标签 $\ell_1, \cdots, \ell_{k-1}$ 的选择，$i = 1, \ldots, k-1$ 对应 $\ell_{i+1} \geq \ell_i - 1$ 种选择。我们由此得到了式 (30)。由于求和项给出根面次数为 $2k$ 的地图的贡献，我们也得到了

$$W_\bullet^{(2k)} = 2\binom{2k-1}{k} R^k = \binom{2k}{k} R^k, \tag{33}$$

where the factor of 2 compensates for the fact that only half of the edges adjacent to the root face have increasing label and can thus serve as root edge.

其中因子 2 修正了如下事实: 只有半数与根面相邻的边满足标签递增，因此可以作为根边。

Admissibility and Criticality

可容许性与临界性

So far, we have ignored issues of convergence in the computations of partition functions, which is okay if one chooses to work only at the level of formal generating series. However, soon we will be questioning the statistical properties of random maps, so we better make sure that the probability measures are sane. Luckily, the tree bijections allow one to easily deduce criteria on the weight sequence $\mathbf{q}$. Restricting to non-pathological cases where at least one of $q_4, q_6, \ldots$ is nonzero, we say $\mathbf{q}$ is admissible when the generating function of rooted, pointed planar maps (with weight $t = 1$ per vertex) is finite, $R(\mathbf{q}) = R(t = 1, \mathbf{q}) < \infty$. This implies the same for (unpointed) rooted planar maps, $Z(\mathbf{q}) < \infty$, and those with boundary, $W^{(2\ell)}(\mathbf{q}) < \infty$, for all $\ell \geq 1$. With some extra work, one can show that the converse is true as well [49, 50] , namely, that $Z(\mathbf{q}) < \infty$ or $W^{(2\ell)}(\mathbf{q}) < \infty$ for some $\ell \geq 1$ implies $R(\mathbf{q}) < \infty$, so any of these criteria can be used as definition of admissibility.

截至目前，我们在配分函数的计算中一直忽略收敛问题，这在仅处理形式生成级数层面的工作时是可行的。但我们很快就要研究随机地图的统计性质，因此最好确保概率测度是合理的。幸运的是，树双射可以方便推导出权重序列 $\mathbf{q}$ 的判别准则。限制在至少有一个 $q_4, q_6, \ldots$ 非零的非病态情形下，当根化带点平面地图 (每个顶点带权重 $t = 1$) 的生成函数有限时，我们称 $\mathbf{q}$ 是可容许的，$R(\mathbf{q}) = R(t = 1, \mathbf{q}) < \infty$ 。这对 (不带点) 根化平面地图 $Z(\mathbf{q}) < \infty$ 以及带边界的平面地图 $W^{(2\ell)}(\mathbf{q}) < \infty$ 而言同样成立，对所有 $\ell \geq 1$ 都成立。经过额外推导可以证明，逆命题也成立 [49, 50] ，即对某个 $\ell \geq 1$ ，$Z(\mathbf{q}) < \infty$ 或 $W^{(2\ell)}(\mathbf{q}) < \infty$ 有限可以推出 $R(\mathbf{q}) < \infty$ ，因此这些判别准则中的任意一个都可以用作可容许性的定义。

From Eq. (32) it follows that a necessary condition for $\mathbf{q}$ to be admissible is that the equation

由式 (32) 可得，$\mathbf{q}$ 可容许的一个必要条件是方程

$$g_{\mathbf{q}}(r) = 1 \text{ , where } g_{\mathbf{q}}(r) = r - \sum_{k=1}^{\infty} q_{2k} \binom{2k-1}{k} r^k \tag{34}$$

has at least one solution, since $g_{\mathbf{q}}(R) = 1$ when $\mathbf{q}$ is admissible. It turns out that this is also sufficient and that $R(\mathbf{q})$ is given by the smallest positive fixed point [51]. The reasoning is instructive, so we will summarize it here.

至少存在一个解，因为当 $\mathbf{q}$ 可容许时满足 $g_{\mathbf{q}}(R) = 1$ 。事实证明这个条件也是充分的，且 $R(\mathbf{q})$ 由最小正不动点给出 [51]。推导过程富有启发性，因此我们在此做简要总结。

If $g_{\mathbf{q}}(r_1) = 1$, we have the identity

若 $g_{\mathbf{q}}(r_1) = 1$ ，我们有恒等式

$$r_1^{-1} + \sum_{k=1}^{\infty} q_{2k} \binom{2k-1}{k} r_1^{k-1} = 1. \tag{35}$$

Since each term is positive, we may interpret them as probabilities and explicitly construct a random mobile as follows. We start with a single white node, which we designate to be active. Then at each step, we visit each active white node, and with probability r_1^{-1} , we deactivate the node, or with probability $\binom{2k-1}{k} r_1^{k-1}$, we insert a black descendant which in turn has $k-1$ new active white descendants. The crux is to determine whether this random process produces a finite or an infinite tree. By adding up the probabilities of all finite mobiles thus produced, one finds that the mobile will be finite with probability

由于所有项均为正，我们可以将其解释为概率，并按如下方式显式构造随机活动图。我们从单个被标记为激活的白色节点开始，之后每一步访问所有激活的白色节点: 以概率 r_1^{-1} 停用该节点，或以概率 $\binom{2k-1}{k} r_1^{k-1}$ 插入一个黑色子节点，该黑色子节点又带有 $k-1$ 个新的激活白色子节点。关键在于确定这个随机过程生成有限树还是无限树。对所有由此生成的有限活动图的概率求和后，可得活动图为有限的概率为

$$\frac{1}{r_1} \sum_{\text{mobiles t}} \prod_{\text{black vertices } v} \binom{2\deg v - 1}{\deg v} q_{2\deg v}. \tag{36}$$

On the other hand, the number of active white nodes at each step in our construction has precisely the law of a Bienayme-Galton-Watson (BGW) process. It is well known that the probability of extinction of such a process is 1 if and only if the mean offspring per individual is less or equal to 1 . In our case, the mean offspring is $\sum_{k=1}^{\infty} k q_{2k} \binom{2k-1}{k} r_1^{k-1} = 1 - g'_{\mathbf{q}}(r_1)$. Since $g_{\mathbf{q}}(0) = 0$ and r_1 is the first solution to $g_{\mathbf{q}}(r) = 1$, we must have $g'_{\mathbf{q}}(r_1) \in [0, 1)$. So the mean offspring is at most 1, implying that the probability (36) equals 1 and therefore $R(\mathbf{q}) = r_1$. This verifies our claim.

另一方面，我们构造中每一步的活跃白节点数恰好满足比安梅-高尔顿-沃森 (BGW) 过程的分布规律。众所周知，该过程的灭绝概率为 1 当且仅当每个个体的平均后代数量小于等于 1。在我们的情形中，平均后代数量为 $\sum_{k=1}^{\infty} k q_{2k} \binom{2k-1}{k} r_1^{k-1} = 1 - g'_{\mathbf{q}}(r_1)$ 。由于 $g_{\mathbf{q}}(0) = 0$ 且 r_1 是 $g_{\mathbf{q}}(r) = 1$ 的第一个解，我们必有 $g'_{\mathbf{q}}(r_1) \in [0, 1)$ 。因此平均后代数量至多为 1，说明概率 (36) 等于 1，因此 $R(\mathbf{q}) = r_1$ 。这就验证了我们的结论。

This last observation naturally leads to a distinction between admissible sequences $\mathbf{q}$ that are subcritical, if $g_{\mathbf{q}}'(R) > 0$, and those that are critical, if $g_{\mathbf{q}}'(R) = 0$ (Fig.4). To understand the difference, we can have a look at the generating function $R(t, \mathbf{q})$ that includes a weight $t \in [0,1]$ per vertex, which satisfies

这一结论自然将可容许序列 $\mathbf{q}$ 分为两类: 若满足 $g_{\mathbf{q}}'(R) > 0$ 则为次临界，若满足 $g_{\mathbf{q}}'(R) = 0$ 则为临界 (图 4)。为理解二者的区别，我们来看生成函数 $R(t, \mathbf{q})$ ，它对每个顶点赋予权重 $t \in [0,1]$ ，满足

$$g_{\mathbf{q}}(R(t, \mathbf{q})) = t. \tag{37}$$

The probability that a (unpointed but rooted) $\mathbf{q}$ -Boltzmann map has precisely n vertices is

(未标记但有根的) $\mathbf{q}$ -玻尔兹曼映射恰好有 n 个顶点的概率为

$$\mathbb{P}_{\mathbf{q}}(n \text{ vertices }) = \frac{1}{nZ}\left[t^{n-1}\right] R(t, \mathbf{q}) = \frac{1}{nZ}\left[t^{n-1}\right] g_{\mathbf{q}}^{-1}(t). \tag{38}$$

For large n this probability is thus determined by singularity analysis of $g_{\mathbf{q}}^{-1}$.

因此当 n 很大时，该概率由 $g_{\mathbf{q}}^{-1}$ 的奇异分析决定。

Let’ s first focus on the case where $g_{\mathbf{q}}$ has radius of convergence larger than $R(\mathbf{q})$, in which case $\mathbf{q}$ is called regular. This happens, for instance, when only a finite number of weights q_{2k} are nonzero. In the subcritical case $g_{\mathbf{q}}'(R) > 0$, we have that $g_{\mathbf{q}}^{-1}(t)$ has radius of convergence larger than 1 . Therefore, the number of vertices has an exponential tail: there exists a $c > 0$ such that for all $n \geq 0$,

我们首先关注 $g_{\mathbf{q}}$ 的收敛半径大于 $R(\mathbf{q})$ 的情况，此时称 $\mathbf{q}$ 为正则的。例如，当只有有限个权重 q_{2k} 非零时就会出现这种情况。在次临界情形 $g_{\mathbf{q}}'(R) > 0$ 中，我们得到 $g_{\mathbf{q}}^{-1}(t)$ 的收敛半径大于 1。因此顶点数具有指数尾: 存在 $c > 0$ 使得对所有 $n \geq 0$,

$$\mathbb{P}_{\mathbf{q}}(n \text{ vertices }) \leq e^{-cn}. \text{ (regular subcritical)} \tag{39}$$

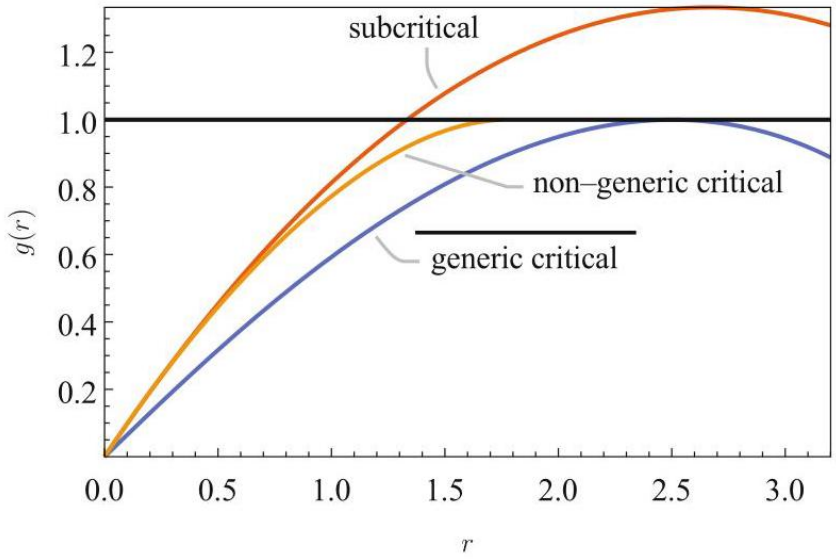

Fig. 4 Examples of the curves $g_{\mathbf{q}}(r)$ for subcritical, regular critical, and non-generic critical weight sequences $\mathbf{q}$

图 4 次临界、正则临界和非正则临界权重序列 $\mathbf{q}$ 对应的曲线 $g_{\mathbf{q}}(r)$ 示例

In the critical case $g'_{\mathbf{q}}(R)=0$, we necessarily have $g''_{\mathbf{q}}(R)<0$, and therefore $g_{\mathbf{q}}^{-1}(t)=R-\sqrt{\frac{1-t}{\frac{1}{2}|g''_{\mathbf{q}}(R)|}}+o\left(\sqrt{1-t}\right)$. The same expansion applies to the more general case of generic critical $\mathbf{q}$, in which $g_{\mathbf{q}}$ is allowed to have a radius of convergence as small as $R(\mathbf{q})$, but for which $g''_{\mathbf{q}}(R)$ is still finite. Singularity analysis then implies that

在临界情形 $g'_{\mathbf{q}}(R)=0$ 下，我们必然得到 $g''_{\mathbf{q}}(R)<0$，因此有 $g_{\mathbf{q}}^{-1}(t)=R-\sqrt{\frac{1-t}{\frac{1}{2}|g''_{\mathbf{q}}(R)|}}+o\left(\sqrt{1-t}\right)$。该展开式同样适用于更一般的一般临界 $\mathbf{q}$ 情形，在该情形下 $g_{\mathbf{q}}$ 的收敛半径可以小至 $R(\mathbf{q})$，但 $g''_{\mathbf{q}}(R)$ 仍然有限。随后奇异性分析表明

$$\mathbb{P}_{\mathbf{q}}(n \text{ vertices}) \overset{n\to\infty}{\sim} cn^{\gamma_s-2},\ \gamma_s=-\frac{1}{2}.\ \text{(generic critical)} \tag{40}$$

(Here and in the following, we will use the notation $f(n) \overset{n\to\infty}{\sim} g(n)$ if $f(n)$ is asymptotic to $g(n)$ as $n\to\infty$, i.e., when $\lim_{n\to\infty} f(n)/g(n)=1$.). The string susceptibility exponent γ_s is thus a universal critical exponent for generic critical Boltzmann maps.

(此处及下文中，若当 $n\to\infty$ 时 $f(n)$ 渐近于 $g(n)$，即当 $\lim_{n\to\infty} f(n)/g(n)=1$ 时，我们将使用记号 $f(n) \overset{n\to\infty}{\sim} g(n)$。) 因此弦散射指数 γ_s 是一般临界玻尔兹曼映射的普适临界指数。

One may escape this universality only when $g_{\mathbf{q}}$ has radius of convergence exactly equal to $R(\mathbf{q})$ and $g''_{\mathbf{q}}(R)=-\infty$. In particular, $\mathbf{q}$ is called non-generic critical of type a if [52-55]

仅当 $g_{\mathbf{q}}$ 的收敛半径恰好等于 $R(\mathbf{q})$ 且满足 $g''_{\mathbf{q}}(R)=-\infty$ 时，才能脱离该普适性。特别地，若满足 [52-55]，则称 $\mathbf{q}$ 为 a 类非一般临界

$$g_{\mathbf{q}}(r)=1-C(R-r)^{a-\frac{1}{2}}+o\left((R-r)^{a-\frac{1}{2}}\right). \tag{41}$$

Observe that we need to take $a\in(3/2,5/2)$ to ensure $g'_{\mathbf{q}}(R)=0$ and $g''_{\mathbf{q}}(R)=-\infty$. In this case $g_{\mathbf{q}}^{-1}(t)=R-\left(\frac{1}{C}(1-t)\right)^{2/(2a-1)}+o\left((1-t)^{2/(2a-1)}\right)$, and therefore one finds

注意我们需要取 $a\in(3/2,5/2)$ 来保证 $g'_{\mathbf{q}}(R)=0$ 和 $g''_{\mathbf{q}}(R)=-\infty$ 成立。在该情形下有 $g_{\mathbf{q}}^{-1}(t)=R-\left(\frac{1}{C}(1-t)\right)^{2/(2a-1)}+o\left((1-t)^{2/(2a-1)}\right)$，因此可得

$$\mathbb{P}_{\mathbf{q}}(n \text{ vertices}) \sim cn^{\gamma_s-2},\ \gamma_s=-\frac{2}{2a-1}.\ \text{(non-generic critical)} \tag{42}$$

An example [53, 56] of such a non-generic critical weight sequence $\mathbf{q}$ of type $a\in(3/2,5/2)$ is

这类 $a \in (3/2, 5/2)$ 型非一般临界权重序列 $\mathbf{q}$ 的一个例子 [53, 56] 为

$$q_{2k} = 2\cos(a\pi)\frac{\Gamma\left(\frac{1}{2}+a\right)\Gamma\left(\frac{1}{2}+k-a\right)}{\Gamma\left(\frac{1}{2}\right)\Gamma\left(\frac{1}{2}+k\right)}(4a-2)^{-k}\mathbf{1}_{\{k\geq 2\}}, \tag{43}$$

for which

对该例子有

$$R(\mathbf{q}) = a - 1/2,\ g_{\mathbf{q}}(r) = 1-(1-r/R)^{a-\frac{1}{2}}. \tag{44}$$

In full generality, it holds that an admissible sequence $\mathbf{q}$ is critical if and only if the number of vertices of a $\mathbf{q}$ -Boltzmann planar map has infinite variance. Critical random maps are therefore much more likely to be very large than subcritical ones, making them the natural choice to investigate scaling limits. Perhaps more importantly, we will see later in section "Peeling Infinite Boltzmann Planar Maps" that critical random maps naturally occur within infinite maps.

一般而言，可容许序列 $\mathbf{q}$ 是临界的当且仅当 $\mathbf{q}$ -玻尔兹曼平面映射的顶点数方差无穷。因此临界随机映射比次临界随机映射更可能取很大的规模，这使得临界随机映射成为研究标度极限的自然选择。或许更重要的是，我们将在后文“剥离无限玻尔兹曼平面映射”一节中看到，临界随机映射自然出现在无限映射中。

Geodesic Distance Statistics

测地线距离统计

Besides providing a combinatorial interpretation to the simple enumeration formulas for pointed maps, the tree bijection provides a natural way to study geodesic distances. To illustrate this, let us focus on the simplest example of quadrangula-tions, i.e., $q_k = q_4\delta_{k,4}$, referring the interested reader to [57] for the general case. From the previous discussion, it easily follows that random quadrangulations are subcritical when $q_4 < 1/12$ and generic critical for $q_4 = 1/12$.

除了给带点地图的简单计数公式提供组合解释外，树双射还为研究测地线距离提供了自然方法。为说明这一点，我们聚焦于四角化最简单的例子，即 $q_k = q_4\delta_{k,4}$ ，感兴趣的读者可参阅文献 [57] 了解一般情况。从之前的讨论不难推出: 当 $q_4 < 1/12$ 时，随机四角化是次临界的；当 $q_4 = 1/12$ 时，随机四角化是一般临界的。

In the corresponding mobiles, the black vertices all have degree two, meaning that we may as well merge the pair of edges adjacent to each black vertex to obtain a tree with white vertices only (Fig. 5). The labels between neighboring white vertices are then seen to differ by at most 1, such that (32) becomes

在对应的移动图中，所有黑点的度均为 2，这意味着我们可以合并每个黑点相邻的边对，得到一棵仅含白点的树 (图 5)。此时可以看到相邻白点的标签差至多为 1，因此式 (32) 变为

$$R - t = 3q_4 R^2. \tag{45}$$

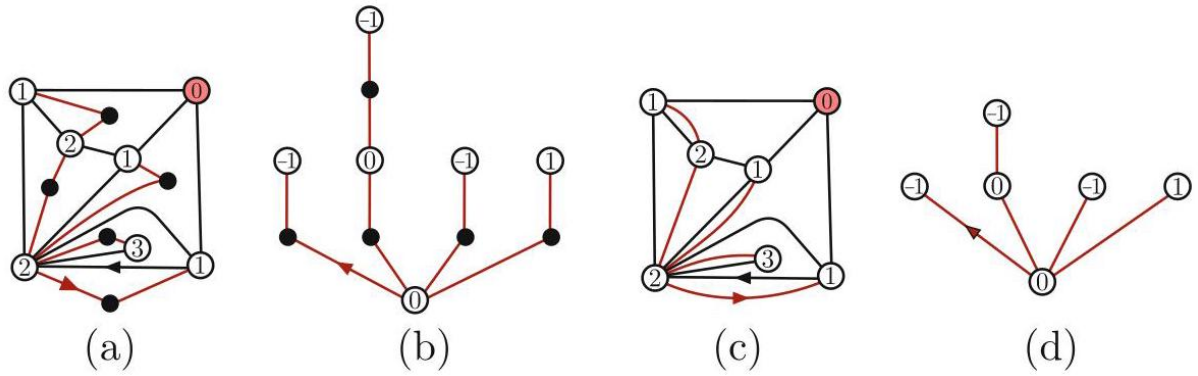

Fig. 5 (a) The BDFG bijection applied to the quadrangulation of Fig. 1 results in the mobile (b) with all black vertices of degree 2. Merging the edges incident to black vertices results in the Cori-Vaugelin-Schaeffer bijection between rooted pointed quadrangulations (c) and labeled plane trees (d)

图 5 (a) 将 BDFG 双射应用于图 1 的四角化，得到所有黑点度均为 2 的移动图 (b)；合并黑点关联的边后，得到根带点四角化 (c) 与标号平面树 (d) 之间的 Cori-Vaugelin-Schaeffer 双射

This bijection between pointed quadrangulations and labeled trees is precisely the Cori-Vaugelin-Schaeffer bijection [42, 44]. One can approach the enumeration of quadrangulations with control on geodesic distances [57] by introducing the generating function R_d of quadrangulations in which the labels increase along the root edge and such that the start of the root edge has label at most d . Then $R_0 = Z$, because for $d = 0$, the origin must be located at the start of the root edge, and $\lim_{d\to\infty} R_d = R$, while

带点四角化和标号树之间的这个双射正是 Cori-Vaugelin-Schaeffer 双射 [42,44]。我们可以通过引入生成函数来对控制测地线距离的四角化进行计数 [57]，R_d 是满足沿根边标签递增且根边起点标签不超过 d 的四角化的生成函数。此时有 $R_0 = Z$ ，这是因为当 $d = 0$ 时，原点必须位于根边的起点，故 $\lim_{d\to\infty} R_d = R$ ，而

$$G_d = R_d - R_{d-1} \tag{46}$$

is the generating function of pointed quadrangulations in which the start and end of the root edge are at distance exactly d and $d+1$ from the origin, respectively. The reason to work with R_d instead of directly with G_d is that R_d satisfies a recursion equation that generalizes (45),

是根边起点和终点到原点的距离恰好分别为 d 和 $d+1$ 的带点四角化的生成函数。我们使用 R_d 而非直接使用 G_d 的原因是 R_d 满足一个推广式 (45) 的递推方程，

$$R_d - t = q_4 R_d \left(R_{d-1} + R_d + R_{d+1}\right). \tag{47}$$

We can understand this equation by interpreting R_d as the generating function of trees with positive integer labels that differ by at most 1 between neighbors and such that the root vertex receives label $d+1$. Observing that the endpoint of the root edge has label $d, d+1$, or $d+2$ leads to the above formula.

我们可以通过将 R_d 解释为满足相邻顶点标签差至多为 1，且根顶点标签为 $d+1$ 的正整数标号树的生成函数，来理解该方程。注意到根边端点的标签为 $d, d+1$ 或 $d+2$，即可推导出上述公式。

Equation (47) can be solved explicitly [57], yielding

方程 (47) 可以显式求解 [57]，结果为

$$R_d = R\frac{\left(1-x^{d+1}\right)\left(1-x^{d+4}\right)}{\left(1-x^{d+2}\right)\left(1-x^{d+3}\right)},\ x+\frac{1}{x}+4=\frac{1}{q_4 R},\ |x|<1. \tag{48}$$

This exact expression allows us already to deduce some statistics concerning geodesic distances in large random quadrangulations. For instance, we can consider the situation where we condition a pointed critical quadrangulation $\mathfrak{m}$ to have its distance $d_\bullet(\mathfrak{m})$ between the root vertex and the origin to be exactly equal to d and then ask about the distribution of the size of $\mathfrak{m}$. It satisfies

这个精确表达式已经可以让我们推导出大型随机四角化中测地线距离的相关统计。例如，我们可以考虑这样的情形: 给带点临界四角化 $\mathfrak{m}$ 条件化，要求根顶点和原点之间的距离 $d_\bullet(\mathfrak{m})$ 恰好等于 d，再研究 $\mathfrak{m}$ 的大小分布，它满足

$$\mathbb{E}\left[e^{-\lambda|\mathrm{F}(\mathfrak{m})|} d_\bullet(\mathfrak{m})=d\right]=\frac{G_d\left(q_4=\frac{1}{12}e^{-\lambda}\right)}{G_d\left(q_4=\frac{1}{12}\right)}.$$

Inserting (46) and (48), one may check that to achieve a nontrivial limit, one should scale λ proportionally to d^{-4} as $d\to\infty$.

代入 (46) 和 (48) 可以验证，要得到非平凡极限，当 $d\to\infty$ 时，应当让 λ 与 d^{-4} 成比例缩放。

Put differently, if we let $\lambda=\Lambda\varepsilon^2$ for $\Lambda>0$ fixed and consider $|F(\mathfrak{m})|\,\varepsilon^2$ to be a rescaled area of $\mathfrak{m}$, then $R\left(\frac{1}{12}e^{-\Lambda\varepsilon^2}\right)=2-2\sqrt{\Lambda}\varepsilon+O\left(\varepsilon^2\right)$, and $x\left(\frac{1}{12}e^{-\Lambda\varepsilon^2}\right)=1-\sqrt{6}\sqrt[4]{\Lambda}\sqrt{\varepsilon}+O(\varepsilon)$. Keeping $d\sqrt{3\varepsilon/2}=D$ fixed while sending $d\to\infty$ leads to a nontrivial limit $x^d=e^{-2\sqrt[4]{\Lambda}D}+O\left(\sqrt{\varepsilon}\right)$. Hence

换句话说，如果我们固定 $\lambda=\Lambda\varepsilon^2$ 中的 $\Lambda>0$，将 $|F(\mathfrak{m})|\,\varepsilon^2$ 视为 $\mathfrak{m}$ 的重标度面积，则可得 $R\left(\frac{1}{12}e^{-\Lambda\varepsilon^2}\right)=2-2\sqrt{\Lambda}\varepsilon+O\left(\varepsilon^2\right)$ 和 $x\left(\frac{1}{12}e^{-\Lambda\varepsilon^2}\right)=1-\sqrt{6}\sqrt[4]{\Lambda}\sqrt{\varepsilon}+O(\varepsilon)$。保持 $d\sqrt{3\varepsilon/2}=D$ 不变，令 $d\to\infty$ 趋于极限，可得到非平凡极限 $x^d=e^{-2\sqrt[4]{\Lambda}D}+O\left(\sqrt{\varepsilon}\right)$。因此

$$\lim_{\varepsilon\searrow 0}\mathbb{E}\left[e^{-\Lambda|\mathrm{F}(\mathfrak{m})|\varepsilon^2}\,\middle|\, d_\bullet(\mathfrak{m})=\lfloor\sqrt{2/3}D/\sqrt{\varepsilon}\rfloor\right]=\Lambda^{3/4}D^3\frac{\cosh\sqrt[4]{\Lambda}D}{\sinh^3\sqrt[4]{\Lambda}D}. \tag{49}$$

The right-hand side is known as the geodesic two-point function of two-dimensional quantum gravity with cosmological constant Λ, which was identified first by Ambjorn and Watabiki in [58]. In particular,

右侧即为带有宇宙学常数 Λ 的二维量子引力的测地两点函数，最早由 Ambjorn 与 Watabiki 在文献 [58] 中给出。特别地，

$$\lim_{\varepsilon \searrow 0} \mathbb{E}\left[|\mathrm{F}(\mathfrak{m})| \,\middle|\, d_\bullet(\mathfrak{m}) = \left\lfloor \sqrt{2/3} D / \sqrt{\varepsilon} \right\rfloor \right] = \frac{D^4}{15},$$

which signals that typical geodesic distances in a quadrangulation with n faces are of order $n^{1/4}$.

这表明，带有 n 个面的四角化中，典型测地线距离的阶为 $n^{1/4}$。

Continuum Limit: Brownian Geometry

连续极限: 布朗几何

The previous calculation has shown that the distribution of the geodesic distance between a single pair of random points (in this case the root and origin vertex) is under analytic control and that one can study its scaling limit. It is natural to ask whether this can be generalized to the distances between all pairs of points simultaneously for random maps of increasing size. This is a question about scaling limits of metric spaces.

之前的计算已经表明，单个随机点对 (本情形中为根顶点与原点顶点) 的测地线距离分布是可以解析控制的，我们可以研究其标度极限。自然会有一个问题: 对于尺寸不断增大的随机地图，这个结论能否推广到所有点对之间的距离同时成立？这是一个关于度量空间标度极限的问题。

From Maps to Metric Spaces

从地图到度量空间

Recall that a metric space is a pair (V, d) consisting of a set V and a distance function $d : V \times V \to \mathbb{R}$ satisfying $d(x,x) = 0$ for $x \in V, d(x,y) = d(y,x) > 0$ when $x \neq y$ and the triangle inequality $d(x,z) \leq d(x,y) + d(y,z)$ for all $x, y, z \in V$. We denote the space of all compact metric spaces, viewed up to isometry, by $\mathbb{M}$. Note that this is a huge space: it contains all finite metric spaces, all metric spaces induced by compact Riemannian manifolds of arbitrary dimension and topology, but also much wilder spaces.

回顾一下，度量空间是一个对 (V, d)，由集合 V 和距离函数 $d : V \times V \to \mathbb{R}$ 构成，满足对任意 $x \in V, d(x,y) = d(y,x) > 0$，当 $x \neq y$ 时成立 $d(x,x) = 0$，且对所有 $x, y, z \in V$ 成立三角不等式 $d(x,z) \leq d(x,y) + d(y,z)$。我们将所有在等距同构意义下等价的紧度量空间构成的空间记为 $\mathbb{M}$。请注意这个空间规模极大: 它包含所有有限度量空间，所有任意维度、任意拓扑的紧黎曼流形诱导的度量空间，甚至还有许多性质更差的空间。

There are multiple ways one can associate a metric space to a map $\mathfrak{m}$, but a practical choice in light of the previous bijection is to consider the finite metric space $\left(\mathrm{V}(\mathfrak{m}), d_{\mathrm{gr}}\right) \in \mathbb{M}$, i.e., the set of vertices equipped with the graph distance. Alternatives are the dual graph distance on the set of faces, which we will encounter in section "Geometry," or the Riemannian metric space induced by the gluing of regular polygons (as studied

for example in [59]). For maps with not too large face degrees, in particular generic critical Boltzmann maps, one expects this choice to have little influence on scaling limits. For non-generic critical maps, the situation is different, as we will see in section "The Peeling Process".

目前有多种方法可以将度量空间关联到地图 $\mathfrak{m}$，但结合此前的双射来看，实用的选择是考虑有限度量空间 $\left(\mathrm{V}(\mathfrak{m}), d_{\mathrm{gr}}\right) \in \mathbb{M}$，即顶点集合配备图距离得到的空间。其他可选方案包括面集合上的对偶图距离 (我们会在"几何"一节介绍)，或是拼接正多边形诱导的黎曼度量空间 (例如文献 [59] 中研究的情形)。对于面度数不太大的地图，尤其是一般的临界玻尔兹曼地图，人们认为这种选择对标度极限几乎没有影响。如我们会在"剥离过程"一节看到的，对于非一般的临界地图，情况则有所不同。

If we take $\mathfrak{m}$ to be a uniform quadrangulation with n faces, then our previous discussion suggests that the metric space $\left(\mathfrak{m}, n^{-1/4} d_{\mathrm{gr}}\right)$, in which the graph distance is normalized by the typical distance $n^{1/4}$ between random vertices, somehow approaches a continuous random metric space. More generally we could consider a q-Boltzmann planar map and condition on the number n of faces.

如果我们取 $\mathfrak{m}$ 为有 n 个面的均匀四角化，那么我们此前的讨论表明，将图距离按随机顶点间的典型距离 $n^{1/4}$ 归一化后得到的度量空间 $\left(\mathfrak{m}, n^{-1/4} d_{\mathrm{gr}}\right)$ 会趋近于一个连续随机度量空间。更一般地，我们也可以考虑 q-玻尔兹曼平面地图，并固定面数 n 作条件化。

The Gromov-Hausdorff Topology

格罗莫夫-豪斯多夫拓扑

What does it mean for a sequence of random metric spaces in $\mathbb{M}$ to have a limit? In order to make sense of this, we need to be able to quantify similarity between metric spaces. This is achieved by the Gromov-Hausdorff distance d_{GH} on $\mathbb{M}$. We will not provide a full definition but provide an equivalent characterization in terms of correspondences [60, Sec. 7.3.3]. A correspondence between sets V_1 and V_2 is a subset $R \subset V_1 \times V_2$ such that each element of V_1 and each element of V_2 occurs at least once in a pair in R. We should thus think of a correspondence as a many-to-many mapping between V_1 and V_2. If V_1 and V_2 are metric spaces, with distances d_1 and d_2 respectively, then the distortion

$\mathbb{M}$ 中的随机度量空间序列存在极限是什么意思？要理解这个问题，我们需要能够量化度量空间之间的相似性，这可以通过 $\mathbb{M}$ 上的格罗莫夫-豪斯多夫距离 d_{GH} 实现。我们不给出完整定义，而是基于对应关系给出等价刻画 [60, 第 7.3.3 节]。集合 V_1 与 V_2 之间的对应关系是满足以下条件的子集 $R \subset V_1 \times V_2$：V_1 的每个元素、V_2 的每个元素都至少出现在 R 的一个配对中。因此我们可以把对应关系理解为 V_1 和 V_2 之间的多对多映射。如果 V_1 和 V_2 是度量空间，距离分别为 d_1 和 d_2，那么畸变

$$\operatorname{dis}(R) = \sup_{(x_1,x_2),(y_1,y_2)\in R} \left| d_1(x_1,y_1) - d_2(x_2,y_2) \right| \tag{50}$$

of a correspondence R quantifies how far this mapping is from being an isometry. The Gromov-Hausdorff distance d_{GH} between metric spaces (V_1, d_1) and (V_2, d_2) is then (half) the minimal distortion possible,

对应关系 R 的畸变量化了该映射距离等距映射的差距。度量空间 (V_1, d_1) 和 (V_2, d_2) 之间的格罗莫夫-豪斯多夫距离 d_{GH} 就是最小可能畸变的一半，

$$d_{\mathrm{GH}}\left(\left(V_1, d_1\right),\left(V_2, d_2\right)\right)=\frac{1}{2} \inf_{\text{correspondences } R} \operatorname{dis}(R). \tag{51}$$

Remarkably the Gromov-Hausdorff distance turns the space $\mathbb{M}$ of all compact metric spaces into a metric space itself, with several pleasant properties like being complete (every Cauchy sequence has a limit) and separable (it contains a countable dense subset). A random metric space is nothing but a probability measure on $\mathbb{M}$. The Gromov-Hausdorff distance or, more precisely, the topology it induces on $\mathbb{M}$ allows one to decide whether a sequence of random metric spaces converges in distribution to a limiting random metric space.

值得注意的是，格罗莫夫-豪斯多夫距离本身将所有紧度量空间构成的空间 $\mathbb{M}$ 变成了一个度量空间，它具备若干良好性质，比如完备性 (每个柯西序列都存在极限) 和可分性 (包含一个可数稠密子集)。随机度量空间本质上就是定义在 $\mathbb{M}$ 上的概率测度。格罗莫夫-豪斯多夫距离，更准确地说，它在 $\mathbb{M}$ 上诱导的拓扑，让我们可以判断随机度量空间序列是否依分布收敛到极限随机度量空间。

Now we are in a position to formulate precise scaling limit results. If $\mathbf{q}$ is generic critical and $\mathfrak{m}_n$ is a $\mathbf{q}$ -Boltzmann planar map conditioned to have n vertices (or n faces or n edges), then there exists a constant $C>0$ such that we have the convergence in distribution in the Gromov-Hausdorff topology

现在我们可以给出精确的标度极限结论了。如果 $\mathbf{q}$ 是通有临界的，$\mathfrak{m}_n$ 是条件为具有 n 个顶点 (或 n 个面、或 n 条边) 的 $\mathbf{q}$ -玻尔兹曼平面地图，则存在常数 $C>0$ 使得我们可以得到格罗莫夫-豪斯多夫拓扑下的依分布收敛

$$\left(\mathfrak{m}_n, C n^{-1/4} d_{\mathrm{gr}}\right) \xrightarrow[n \to \infty]{(\mathrm{d})} \mathbf{B} \tag{52}$$

toward a random metric space $\mathbf{B}$ that is called the Brownian map or Brownian sphere (see Fig. 6). This famous result was first proved by Le Gall [61], in the case of regular critical q-Boltzmann maps (as well as uniform triangulations) when conditioned on the number of faces, and simultaneously using different methods by Miermont [62], in the case of quadrangulations. The extension to the generic critical case and conditioning on any of the vertices, edges, and faces is due to Marzouk [63]. Many other families of maps have been shown to share the same limit, like uniform maps [64], uniform simple triangulations and quadrangulations [65], non-bipartite Boltzmann maps [66], uniform cubic planar graphs [67], and more. In the case of uniform triangulations, it is also known that the convergence is robust under local deformations of the metric [68].

收敛到名为布朗地图或布朗球的随机度量空间 $\mathbf{B}$ (见图 6)。这一著名结论最初由 Le Gall[61] 证明，针对的是条件给定面数的正则临界 q-玻尔兹曼地图 (包括均匀三角剖分)，Miermont[62] 同时用不同方法证明了四角剖分的情况。将结论推广到通有临界情形、并且可以条件给定顶点数、边数或面数的工作由 Marzouk[63] 完成。目前已经知道许多其他地图族也拥有相同的极限，例如均匀地图 [64]、均匀单三角剖分与单四角剖分 [65]、非二部玻尔兹曼地图 [66]、均匀三次平面图 [67] 等等。对于均匀三角剖分，目前也已知该收敛在度量的局部形变下具有稳定性 [68]。

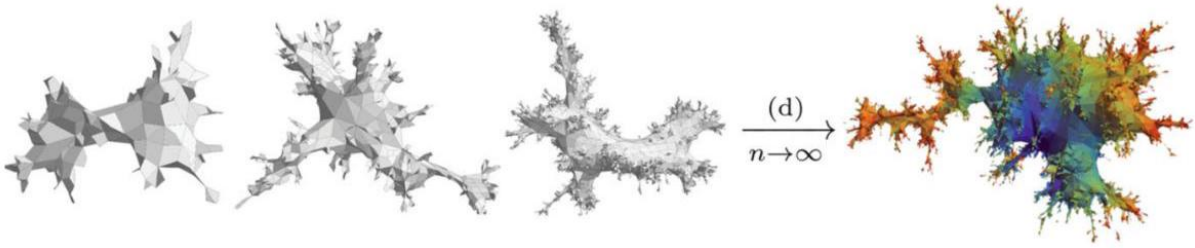

Fig. 6 Visualizations of simulated uniform quadrangulations with increasing number n of faces as well as the Brownian sphere (on the right). The images are an attempt at faithfully embedding the metric spaces in 3D Euclidean space

图 6 随着面数 n 增加，模拟得到的均匀四角剖分以及最右侧的布朗球的可视化。这些图尝试将度量空间忠实嵌入到三维欧几里得空间中

Discussing the full proof of (52) is beyond the scope of this chapter, but we can highlight the important ingredients. Importantly, we need to understand the Brownian sphere, and it should not come as a surprise that its construction heavily relies on random trees.

讨论 (52) 的完整证明超出了本章的范围，但我们可以重点介绍其中的核心要素。重点是，我们需要理解布朗球，它的构造极大依赖随机树，这一点并不出人意料。

Continuum Random Tree

连续随机树

Recall that a pointed rooted quadrangulation with n faces, with the extra condition that the distance from the origin increases along the root edge, is uniquely encoded by a labeled rooted plane tree with n edges. The labels are allowed to differ by at most 1 along the edges. This means that each rooted plane tree admits precisely 3^n different labelings. In particular, if the quadrangulation is chosen uniformly at random, then the associated tree, after forgetting its labels, is a uniform random plane tree with n edges. Seen as metric spaces, when equipped with the graph distance, such trees admit a well-known scaling limit themselves: the continuum random tree (CRT) introduced by Aldous [69]. One can view this statement as a limit in the Gromov-Hausdorff sense, analogously to (52), but with a normalization $n^{-1/2}$ instead of $n^{-1/4}$.

回顾一下: 带有 n 个面，且满足根边方向上从起点出发距离严格递增的有根带点四角剖分，可由一棵带有 n 条边的有根标号平面树唯一编码。边上顶点标号的差至多为 1，这意味着每棵有根平面树恰好有 3^n 种不同的标号方式。特别地，如果均匀随机选取四角剖分，那么忘掉标号后对应的树就是一棵带有 n 条边的均匀随机平面树。作为度量空间，这类树装备图距离后本身就存在广为人知的标度极限: 由 Aldous 提出的连续随机树 (CRT)[69]。可以将这个结论看作 Gromov-Hausdorff 意义下的极限，和 (52) 类似，只不过归一化项是 $n^{-1/2}$ 而非 $n^{-1/4}$ 。

However, in the case of plane trees, there is a stronger topology that is also easier to work with, namely, convergence at the level of contour functions. Recall the definition of the contour of a plane tree t from section "From Trees to Planar Maps." Let $C_t(i)$ for $i = 0, 1, \dots, 2n$ be the graph distance from the i th corner in the

contour to the root vertex. By linear interpolation, this gives rise to the contour function $C_{\mathfrak{t}} : [0, 2n] \to \mathbb{R}_{\geq 0}$. In the case of a uniform plane tree, $C_{\mathfrak{t}}$ has the law of a random walk with increments ± 1 started at $C_{\mathfrak{t}}(0) = 0$ and conditioned to stay non-negative before returning to zero after $2n$ steps, $C_t(2n) = 0$. It should therefore not come as a surprise that with Brownian scaling, we obtain the convergence in distribution (with respect to the uniform norm topology on real functions on the interval $[0, 1]$)

但对于平面树，存在更强也更易于处理的拓扑，即等高线函数层面的收敛。回顾“从树到平面地图”一节中平面树 t 等高线的定义，设 $C_t(i)$ 对应 $i = 0, 1, \dots, 2n$，表示等高线中第 i 个角到根顶点的图距离。通过线性插值可以得到等高线函数 $C_{\mathfrak{t}} : [0, 2n] \to \mathbb{R}_{\geq 0}$。对于均匀平面树，$C_{\mathfrak{t}}$ 服从随机游走律: 步长增量为 ± 1，从 $C_{\mathfrak{t}}(0) = 0$ 出发，要求在 $2n$ 步后回到 0 前始终非负，即 $C_t(2n) = 0$。因此不难发现，经过布朗标度后我们可以得到分布收敛 (关于区间 $[0, 1]$) 上实函数的一致范数拓扑)

$$\left(t \mapsto \frac{C_{\mathfrak{t}}(2nt)}{c\sqrt{2n}} \right) \xrightarrow[n\to\infty]{(\mathrm{d})} \mathbf{e} \tag{53}$$

where $\mathbf{e} : [0, 1] \to \mathbb{R}_{\geq 0}$ is a Brownian excursion [70], i.e., a standard Brownian motion started at $\mathbf{e}(0) = 0$ and conditioned to stay non-negative until returning to zero after unit time, $\mathbf{e}(1) = 0$.

其中 $\mathbf{e} : [0, 1] \to \mathbb{R}_{\geq 0}$ 是布朗游弋 [70]，即从 $\mathbf{e}(0) = 0$ 出发、要求单位时间后回到 0 前始终非负的标准布朗运动，$\mathbf{e}(1) = 0$。

Any continuous excursion $X : [0, 1] \to \mathbb{R}_{\geq 0}$ naturally gives rise to a continuous metric space called a real tree. This is achieved by considering the metric

任意连续游弋 $X : [0, 1] \to \mathbb{R}_{\geq 0}$ 都可以自然生成一个称为实树的连续度量空间，这一构造通过下述度量实现:

$$d_X(s, t) = X(s) + X(t) - 2 \inf_{u \in [s,t]} X(u), \ 0 \leq s \leq t \leq 1 \tag{54}$$

on $[0, 1]$, which identifies two points s, t at the same height whenever X does not drop below that height between s and t (see Fig. 7c), i.e., $X(s) = X(t)$ and $X(u) \geq X(s)$ for all $u \in [s, t]$. (More precisely, this determines a pseudo-metric on $[0, 1]$. If we consider the equivalence relation $s \sim t$ when $d_X(s, t) = 0$, then d_X descends to a proper metric on the quotient $[0, 1]/\sim$.) In the case of a Brownian excursion $X = \mathbf{e}$, this random metric space defines the continuum random tree. Moreover, the convergence (53) of contour functions implies that the random tree $\mathfrak{t}$ converges in distribution, upon rescaling its graph distance by $1/\sqrt{2n}$, to the CRT in the Gromov-Hausdorff topology [71].

在 $[0, 1]$ 上，只要 X 在 s 与 t 之间不低于该高度，就会将同一高度的两个点 s, t 等同起来 (见图 7c)，即对所有 $u \in [s, t]$ 都有 $X(s) = X(t)$ 和 $X(u) \geq X(s)$。(更准确地说，这在 $[0, 1]$ 上定义了一个伪度量。如果我们考虑等价关系: 当 $s \sim t$ 时 $d_X(s, t) = 0$ 成立，那么 d_X 就可以诱导出商空间 $[0, 1]/\sim$ 上的真度量。) 对于布朗游弋 $X = \mathbf{e}$，这个随机度量空间就定义了连续统随机树。此外，轮廓函数的收敛性 (53) 意味着，将随机树 $\mathfrak{t}$ 的图距离按 $1/\sqrt{2n}$ 重标度后，其分布在 Gromov-Hausdorff 拓扑下收敛到 CRT[71]。

The convergence (53) can be obtained much more generally for random plane trees, including the random mobiles associated with generic critical q-Boltzmann maps [51, Sec. 4]. Indeed, one may interpret the CRT

as a universal scaling limit of random treelike geometries, which is known in the physics literature as the branched polymer universality class [17,72-74].

收敛性 (53) 可以在更一般的随机平面树中得到，包括与一般临界 q-玻尔兹曼映射关联的随机活动标架 [51, 第 4 节]。事实上，我们可以将 CRT 看作随机树形几何的普适标度极限，这在物理学文献中被称为分支聚合物普适类 [17,72-74]。

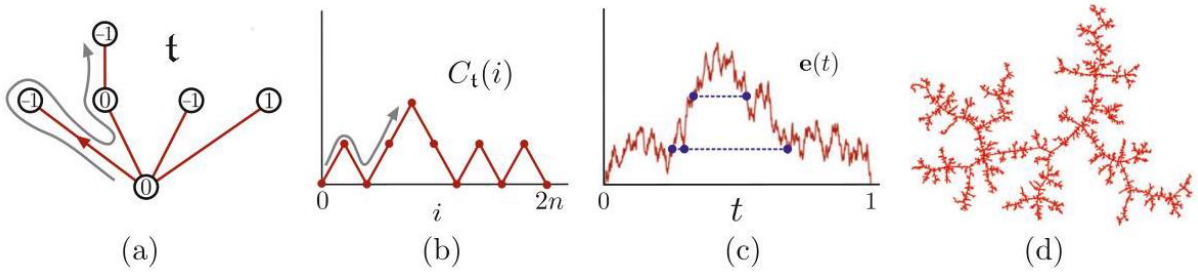

Fig. 7 (a) The plane tree t from Fig. 5. (b) Its contour function $C_t(i)$. (c) The Brownian excursion $\mathbf{e}(t)$ and examples of a pair and a triple of points that is identified by $d_{\mathbf{e}}$. (d) An illustration of the CRT

图 7 (a) 来自图 5 的平面树 t。(b) 它的轮廓函数 $C_t(i)$。(c) 布朗游弋 $\mathbf{e}(t)$ 以及被 $d_{\mathbf{e}}$ 等同的一对点和三个点的示例。(d) CRT 的图示

Definition of the Brownian Sphere

布朗球面的定义

Geodesic distances in the quadrangulations, at least toward the origin, are encoded in the labels of the trees. Once the tree is known, they satisfy a very simple law: the increments along the edges are independent and uniform in $\{-1,0,1\}$. In particular, if one examines the labels along a single path of vertices starting at the root and ending at a leaf of the tree, then the labels describe a random walk with steps in $\{-1,0,1\}$. Since the length of a typical path is of order $\sqrt{n}$, the range of the random walk, and thus of the graph distances in the quadrangulation, is of order $\sqrt[4]{n}$, in accordance with the observations in section "Geodesic Distance Statistics." If we summarize the labels of the corners visited in the contour of $\mathfrak{t}$ by the label function $\ell_{\mathfrak{t}} : [0,2n] \to \mathbb{R}$, then one should thus expect the rescaled label function $t \mapsto \ell_{\mathfrak{t}}(2nt)/\sqrt[4]{n}$ to admit a limit as $n \to \infty$.

四角化中的测地线距离 (至少相对于原点而言) 由树的标签编码。确定树结构后，这些距离服从非常简单的规律: 沿边的标签增量在 $\{-1,0,1\}$ 中独立均匀分布。特别地，若考察从根出发到树叶子的一条单顶点路径上的标签，这些标签就对应步长在 $\{-1,0,1\}$ 中的随机游走。由于典型路径的长度为 $\sqrt{n}$ 量级，因此随机游走的极差 (也就是四角化中图距离的极差) 为 $\sqrt[4]{n}$ 量级，这与“测地线距离统计”一节中的观测结果一致。如果我们用标签函数 $\ell_{\mathfrak{t}} : [0,2n] \to \mathbb{R}$ 总结 $\mathfrak{t}$ 轮廓中访问到的角点的标签，那么可以预期，当 $n \to \infty$ 时，重标度后的标签函数 $t \mapsto \ell_{\mathfrak{t}}(2nt)/\sqrt[4]{n}$ 会存在极限。

This limit corresponds to the (head of the) Brownian snake [75], which informally amounts to a Brownian motion indexed by the branches of a CRT (Fig. 8). More precisely, given a Brownian excursion $\mathbf{e}$ that describes the contour of a CRT, we let $Z : [0,1] \to \mathbb{R}$ be the random continuous function with $Z(0) = Z(1) = 0$, zero mean $\mathbb{E}[Z(t)] = 0$, and Gaussian distribution determined by

该极限对应 (首) 布朗蛇 [75]，通俗来说就是以连续随机树 (CRT) 的分支为索引的布朗运动 (图 8)。更准确地说，给定描述 CRT 轮廓的布朗徘徊 $\mathbf{e}$，我们设 $Z : [0,1] \to \mathbb{R}$ 是满足 $Z(0) = Z(1) = 0$、零均值 $\mathbb{E}[Z(t)] = 0$ 且服从高斯分布的随机连续函数，其分布由下式确定

$$\mathbb{E}\left[(Z(s) - Z(t))^2\right] = d_{\mathbf{e}}(s,t). \tag{55}$$

(Compare this with standard Brownian motion $B : \mathbb{R} \to \mathbb{R}$ on the line satisfying $\mathbb{E}\left[(B(s) - B(t))^2\right] = |s-t|$, which is the natural metric on $\mathbb{R}$.). If $Z(t)$ attains its minimum at $t_0 = \arg\min_{[0,1]} Z \in [0,1]$, then we wish to interpret t_0 as the origin (the analogue of the distinguished vertex in the map) and $Z(t) - Z(t_0)$ as the distance $D(t,t_0)$ from the t to the origin. In order to define a metric space, we should specify distances $D(s,t)$ between all pairs of points $s,t \in [0,1]$. It is not immediately clear how to do this, but the inequality (31) derived back in section "From Trees to Planar Maps" suggests a natural upper bound on $D(s,t)$. Namely, one should be able to follow the geodesics from s and t to the origin until they merge. If $t_0 \notin [s,t]$, then the point of merging is $u = \arg\min_{[s,t]} Z \in [0,1]$, and if $t_0 \in (s,t)$, then $u = \arg\min_{[0,t]\cup[s,1]} Z \in [0,1]$. The continuous analogue of (31) is then

(可将其与直线上满足 $\mathbb{E}\left[(B(s) - B(t))^2\right] = |s-t|$ 的标准布朗运动 $B : \mathbb{R} \to \mathbb{R}$ 对比，$\mathbb{E}\left[(B(s) - B(t))^2\right] = |s-t|$ 是 $\mathbb{R}$ 上的自然度量)。若 $Z(t)$ 在 $t_0 = \arg\min_{[0,1]} Z \in [0,1]$ 处取得最小值，我们可将 t_0 解释为原点 (对应地图中特殊顶点的类似物)，将 $Z(t) - Z(t_0)$ 解释为 t 到原点的距离 $D(t,t_0)$。要定义一个度量空间，我们需要明确所有点对 $s,t \in [0,1]$ 之间的距离 $D(s,t)$。这件事并非一目了然，但“从树到平面图”一节推导出的不等式 (31) 为 $D(s,t)$ 给出了一个自然的上界。具体来说，我们可以沿 s 和 t 到原点的测地线行进，直到它们交汇。若 $t_0 \notin [s,t]$，则交汇点为 $u = \arg\min_{[s,t]} Z \in [0,1]$；若 $t_0 \in (s,t)$，则 $u = \arg\min_{[0,t]\cup[s,1]} Z \in [0,1]$。因此 (31) 的连续类似物为

$$D(s,t) \le D^\circ(s,t) := Z(s) + Z(t) - 2Z(u). \tag{56}$$

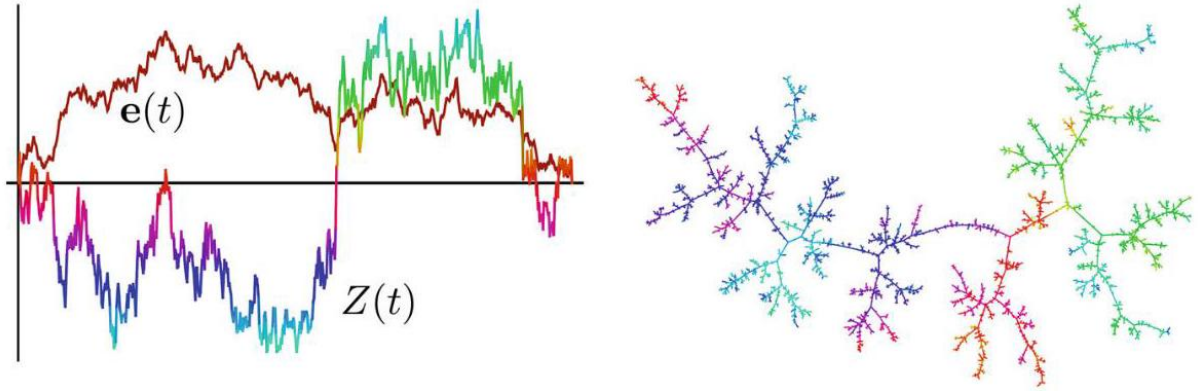

Fig. 8 A simulation of the Brownian snake $(\mathbf{e}, Z)$ illustrated as functions on $[0,1]$ (left) and as coloring of an embedding of $\mathbf{t}$ in the plane (right). The colors in both figures match

图 8 布朗蛇 $(\mathbf{e}, Z)$ 的模拟，左图展示为 $[0,1]$ 上的函数，右图展示为 $\mathbf{t}$ 平面嵌入的着色。两图颜色相互对应

However, $d_{\mathbf{e}}(t,t') = 0$ does not imply $D^\circ(s,t) = D^\circ(s,t')$, essentially because some points will have multiple shortest geodesics to the origin, so $D^\circ(s,t)$ does not determine a metric on $[0,1]/\sim$. But it can be shown [48, 76] that there is a unique (largest) metric $D(s,t)$ satisfying the inequality and that it is obtained by stringing together many pieces of geodesics to the origin,

但 $d_{\mathbf{e}}(t,t') = 0$ 并不蕴含 $D^\circ(s,t) = D^\circ(s,t')$，这本质上是因为部分点到原点存在多条最短测地线，因此 $D^\circ(s,t)$ 无法确定 $[0,1]/\sim$ 上的度量。但可以证明 [48, 76] : 存在唯一的 (最大) 度量 $D(s,t)$ 满足上述不等式，该度量通过拼接多条通往原点的测地线片段得到，

$$D(s,t) := \inf\{D^\circ(s,u_1) + D^\circ(v_1,u_2) + \cdots + D^\circ(v_k,t) : u_i \sim v_i \text{ for } 1 \le i \le k\}. \tag{57}$$

This random metric on $[0,1]$, with pairs of points s,t identified whenever $D(s,t) = 0$, is called the Brownian map [76] or Brownian sphere $\mathbf{B} = ([0,1]/\sim, D)$.

当 $D(s,t) =$ 为 0 时将对应点对 s,t 做等价认同后，$[0,1]$ 上的这个随机度量就被称为布朗地图 [76] 或布朗球面 $\mathbf{B} = ([0,1]/\sim, D)$。

Properties of the Brownian Sphere

布朗球面的性质

Even though it is a pretty wild metric space (judging by Fig.6), the Brownian sphere is still a topological manifold. Indeed, the metric $D(s,t)$ induces a topology on $[0,1]/\sim$ that was shown in [77] to be that of the 2-sphere. The anomalous scaling of geodesic distances with respect to areas, which we already observed in section "Geodesic Distance Statistics," is reflected in the Brownian sphere having a Hausdorff dimension equal to 4 almost surely [48].

尽管布朗球面是一个性质相当复杂的度量空间 (从图 6 即可看出)，它仍然是一个拓扑流形。事实上，度量 $D(s,t)$ 会在 $[0,1]/\sim$ 上诱导出一个拓扑，文献 [77] 已证明该拓扑就是二维球面的拓扑。我们已经在“测地距离统计”一节中提到过，测地距离相对于面积存在反常标度，这一点体现在布朗球面的豪斯多夫维数几乎处处为 4[48]。

Besides the metric structure, the Brownian sphere possesses a natural volume measure coming from the Lebesgue measure on the interval $[0,1]$, which in particular provides a means of sampling uniform points in the surface. The root (corresponding to the endpoints of the interval $[0,1]$) and the origin (corresponding to $\arg\min_{[0,1]} Z$) are such uniform points themselves. The volume measure is precisely the scaling limit of the discrete measure that assigns equal volume to each vertex (or face) of the map, normalized to have total

volume equal to one. Proving this [78, 79] requires a refinement of the convergence to the Gromov-Hausdorff-Prokhorov topology that also takes into account the structure provided by the measure. Recently it has been demonstrated [80] that the volume measure does not provide extra information, but is completely determined by the metric.

除度量结构外，布朗球面还拥有一个自然的体积测度，它源自区间 $[0,1]$ 上的勒贝格测度，这个测度尤其可用于在曲面中对均匀点进行采样。根点 (对应区间 $[0,1]$ 的端点) 和原点 (对应 $\arg\min_{[0,1]} Z$) 本身就是这类均匀点。该体积测度正是离散测度的连续极限: 离散映射给每个顶点 (或面) 分配相等体积，再归一化总体积为 1，其极限就是这个体积测度。要证明这一点 [78, 79]，需要对格罗莫夫-豪斯多夫-普罗霍罗夫拓扑下的收敛性进行细化，同时也要考虑测度提供的结构。最近的研究 [80] 表明，体积测度并不携带额外信息，它完全由度量决定。

To get a feeling for the fractal geometric of the Brownian sphere, it is instructive to examine its geodesics (see, e.g., [62,81-85]). The Brownian sphere $\mathbf{B}$ is a geodesic space, in the sense that for any two points $x, y \in \mathbf{B}$ at distance $r = D(x,y)$, there is a continuous geodesic $\Gamma : [0,r] \to \mathbf{B}$ with $\Gamma(0) = x$ and $\Gamma(r) = y$ such that $D(\Gamma(s), \Gamma(t)) = t - s$ for $0 \le s \le t \le r$. If x and y are sampled uniformly (from the volume measure), this geodesic is unique [82]. This is similar to the situation in a Riemannian manifold, but the similarity stops when considering the structure of multiple geodesics. We have already argued, based on the analysis of leftmost geodesics in section "From Trees to Planar Maps," that the geodesics from x and y to a third uniform point z , say the origin, almost surely merge before reaching z (Fig. 9). This suggests that essentially there is just one way to approach a typical point z via a geodesic route, contrary to Riemannian geometry where one can approach a point from any angle via a geodesic. Of course, there will be atypical points $z \in \mathbf{B}$ that have more than one geodesic ending at z : for instance, the interior points of geodesics have at least two, and the merger points of geodesics at least three. In fact, it has been shown [84, 85] that the set of points of $\mathbf{B}$ where $m = 1, 2, 3$ or 4 geodesics meet has Hausdorff dimension $5 - m$. No such points exist where $m = 6$ geodesics meet [84], while it is an open question whether there are points with $m = 5$ geodesics [84,85]. Perhaps even more strikingly, the geodesic frame [83] of $\mathbf{B}$, which is the union of all geodesics minus their endpoints between pairs of points in $\mathbf{B}$, has Hausdorff dimension one [84], equal to the dimension of a single geodesic.

想要直观感受布朗球面的分形几何性质，研究其测地线是很好的方法 (参见例如文献 [62,81-85])。布朗球面 $\mathbf{B}$ 是一个测地空间，具体来说，对任意距离为 $r = D(x,y)$ 的两个点 $x, y \in \mathbf{B}$ ，都存在连续测地线 $\Gamma : [0,r] \to \mathbf{B}$ ，满足端点为 $\Gamma(0) = x$ 和 $\Gamma(r) = y$ ，且对任意 $0 \le s \le t \le r$ 都有 $D(\Gamma(s), \Gamma(t)) = t - s$ 成立。若 x 和 y 服从 (体积测度下的) 均匀分布，则两点间的测地线几乎必然唯一 [82]。这一性质与黎曼流形的情形相似，但多测地线的结构就完全不同了。我们已经在“从树到平面地图”一节中，基于对最左测地线的分析提出，从 x 和 y 到第三个均匀点 (例如原点) z 的测地线，几乎必然在抵达 z 之前就汇合了 (图 9)。这说明，通过测地线接近典型点 z 的路径本质上只有一条，这和黎曼几何完全相反——在黎曼几何中，可以从任意角度通过测地线接近一个点。当然，也存在非典型点 $z \in \mathbf{B}$ ，这些点可以有不止一条测地线终止于 z : 例如，测地线的内点至少有两条，测地线的汇合点至少有三条。事实上已经证明 [84, 85] ，在 $\mathbf{B}$ 中，有 $m = 1, 2, 3$ 或 4 条测地线相交的点集，其豪斯多夫维数为 $5 - m$ 。不存在有 $m = 6$ 条测地线相交的点 [84]，而是否存在有 $m = 5$ 条测地线相交的点仍是一个开放问题 [84,85]。或许更令人惊讶的是，$\mathbf{B}$ 的测地线架 [83]——即 $\mathbf{B}$ 中所有点对之间测地线去掉端点后的并集——的豪斯多夫维数为 1[84]，和单条测地线的维数相等。

The Brownian Sphere from Liouville Quantum Gravity

来自刘维尔量子引力的布朗球面

The Brownian sphere, introduced to capture the scaling limit of random planar maps, gives a mathematically precise interpretation of what we would like to call pure quantum gravity on the 2-sphere. There is another way of constructing the same random metric space, starting from random Riemannian geometry on the 2- sphere, going under the name of Liouville quantum gravity, which has seen a flurry of activity in recent years in probability theory. Summarizing these developments, and their connections to Liouville Conformal Field Theory and the Mating of Trees approach, goes far beyond the scope of this chapter, so we direct the reader to several key papers [86-96] and review articles [97-99]. Here we restrict to superficially describing the process to arrive at a metric space that is known to agree with the Brownian sphere.

布朗球面是为刻画随机平面地图的标度极限引入的，它对我们所说的二维球面上的纯量子引力给出了数学上严格的解释。构造这同一个随机度量空间还有另一种方法，它从二维球面上的随机黎曼几何出发，名为刘维尔量子引力，近年来概率论领域围绕它开展了大量研究。总结这些发展，以及它们和刘维尔共形场论、树配对方法的关联，远远超出了本章的范围，因此我们建议读者阅读几篇关键论文 [86-96] 和综述文章 [97-99]。本文仅浅层次描述这一构造过程，最终得到的度量空间已被证实与布朗球面一致。

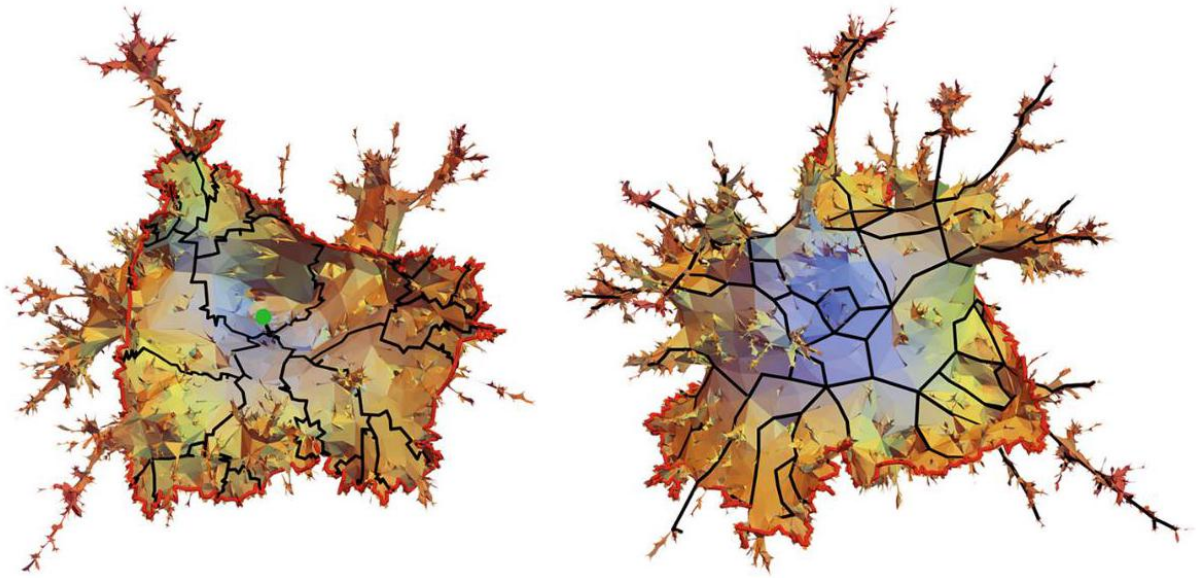

Fig. 9 On the left, a simulation of the hull of a geodesic ball of radius r around the origin (green dot) in the Brownian sphere, where the boundary at distance r is shown in red. A variety of geodesics (of length r) from boundary points to the origin is depicted in black, illustrating the merging of geodesics. On the right, an illustration of the geodesic frame on the same surface, obtained by considering the union of geodesics between many pairs of (well-separated) random points

图 9 左图为布朗球面中原点 (绿点) 周围半径 r 的测地球包的模拟结果，距离原点 r 处的边界以红色标出。多条长度为 r 的、从边界点指向原点的测地线以黑色画出，展示了测地线的合并现象。右图为同一曲面上测地框架的示意图，该框架由多对 (分隔良好的) 随机点之间的测地线的并集构造得到

The general idea, going back to Polyakov [24] in the context of non-critical bosonic string theory, is to uniformize Riemannian metrics g_{ab} on the 2-sphere as conformal rescalings of a fixed background metric $\hat{g}_{ab}$,

这一核心思路可以追溯到非临界玻色弦理论背景下的 Polyakov[24]，该方法将二维球面上的黎曼度量 g_{ab} 一致化为固定背景度量 $\hat{g}_{ab}$ 的共形重标度，

$$g_{ab}(x) = e^{\gamma\phi(x)}\hat{g}_{ab}(x), \tag{58}$$

and study the conformal field theory of the Liouville field ϕ for gravity, possibly coupled to conformal matter fields. Liouville quantum gravity with Liouville coupling $\gamma \in (0,2)$ corresponds to the rigorous path integral quantization of the Liouville field ϕ with action

进而研究用于引力的刘维尔场 ϕ 的共形场论，它可以与共形物质场耦合。带有刘维尔耦合 $\gamma \in (0,2)$ 的刘维尔量子引力对应刘维尔场 ϕ 带作用量的严格路径积分量子化

$$S_{\mathrm{L}}[\phi] = \frac{1}{4\pi}\int_{S^2} \mathrm{d}^2x\sqrt{\hat{g}}\left(\hat{g}^{ab}\partial_a\phi\partial_b\phi + Q\widehat{R}\phi + 4\pi\widehat{\mu}e^{\gamma\phi}\right), \tag{59}$$

where $\widehat{\mu} > 0$ is a cosmological constant, $\widehat{R}$ the scalar curvature of $\hat{g}_{ab}$, and

其中 $\widehat{\mu} > 0$ 是宇宙学常数，$\widehat{R}$ 是 $\hat{g}_{ab}$ 的标量曲率，且

$$Q = \frac{2}{\gamma} + \frac{\gamma}{2} \tag{60}$$

The value of γ is determined by the central charge $c \in (-\infty, 1)$ of the coupled matter system and is related to $Q \in (2,\infty)$ via

γ 的值由耦合物质系统的中心荷 $c \in (-\infty,1)$ 决定，并通过下式与 $Q \in (2,\infty)$ 关联

$$c = 25 - 6Q^2. \tag{61}$$

Pure gravity thus corresponds to $c = 0, Q = 5/\sqrt{6}$, and $\gamma = \sqrt{8/3}$. For a rigorous construction of the path integral as a measure on an appropriate function space of fields $\phi : S^2 \to \mathbb{R}$ using so-called Gaussian Multiplicative Chaos, we refer the reader to [92, 100 − 102] . This is achieved by considering the measure as a deformation of the Gaussian Free Field (GFF) on the 2-sphere with metric $\hat{g}_{ab}$, which is the random massless scalar field with action corresponding to the quadratic part of (59).

因此纯引力对应 $c=0, Q=5/\sqrt{6}$，且 $\gamma=\sqrt{8/3}$。关于如何利用所谓高斯乘性混沌，将路径积分严格构造为适当场函数空间 $\phi: S^2 \to \mathbb{R}$ 上的测度，我们建议读者参考 [92, 100 − 102]。该构造是通过将上述测度视为二维球面上带度量 $\hat{g}_{ab}$ 的高斯自由场 (GFF) 的变形完成的，高斯自由场是满足作用量对应 (59) 二次项的无质量随机标量场。

In connection with the (unit-volume) Brownian sphere, we are interested in the unit-volume Liouville field, which can be shown [92, 103] to be related to the GFF by a manageable deterministic position-dependent shift. For simplicity, we consider the Riemann sphere $\mathbb{C}\cup\{\infty\} \cong S^2$ with the flat Euclidean background metric $\hat{g}_{ab} = \delta_{ab}$ on $\mathbb{C} \cong \mathbb{R}^2$. Since the GFF and ϕ are logarithmically correlated, $\mathbb{E}[\phi(x)\phi(y)] \sim \log 1/|x-y|$ as $x \to y$, the random field cannot be pointwise defined, and regularization is necessary to make sense of the exponential $e^{\gamma\phi(x)}$. This can be achieved by averaging ϕ over a neighborhood of small radius $\varepsilon > 0$, for instance, by taking $\phi_\varepsilon(x)$ to be a version of ϕ mollified by the heat kernel,

结合 (单位体积) 布朗球面，我们研究单位体积刘维尔场，已有文献 [92, 103] 证明该场可通过一个易处理的位置依赖确定性变换与高斯自由场建立联系。为简化讨论，我们考虑黎曼球面 $\mathbb{C}\cup\{\infty\} \cong S^2$，其带有平坦欧几里得背景度量 $\hat{g}_{ab} = \delta_{ab}$ 定义在 $\mathbb{C} \cong \mathbb{R}^2$ 上。由于高斯自由场和 ϕ 是对数相关的，$\mathbb{E}[\phi(x)\phi(y)] \sim \log 1/|x-y|$ 如 $x \to y$ 所示，该随机场无法逐点定义，必须通过正则化才能让指数 $e^{\gamma\phi(x)}$ 有意义。这可以通过对小半径 $\varepsilon > 0$ 邻域内的 ϕ 取平均实现，例如，将 $\phi_\varepsilon(x)$ 取为经热核磨光后的 ϕ，

$$\phi_\varepsilon(x) = \int_{\mathbb{C}} \mathrm{d}^2 y \frac{1}{\pi\varepsilon^2} e^{-\frac{|x-y|^2}{\varepsilon^2}} \phi(y). \tag{62}$$

Then $\phi_\varepsilon(x)$ is a nice continuous random function that one can exponentiate to give a random Riemannian metric

此时 $\phi_\varepsilon(x)$ 是性质良好的连续随机函数，对其取指数即可得到随机黎曼度量

$$g^\varepsilon_{ab} = e^{\gamma\overline{\phi}_\varepsilon(x)}\delta_{ab},\ \overline{\phi}_\varepsilon(x) := \phi_\varepsilon(x) - \frac{1}{\gamma}\log\left(\int_{S^2} e^{\gamma\phi_\varepsilon(x)}\mathrm{d}^2x\right). \tag{63}$$

of unit volume, $\int_{S^2}\sqrt{g^\varepsilon}\mathrm{d}^2x = 1$. The unit-volume Liouville quantum measure μ_ϕ on $S^2 \cong \mathbb{C}\cup\{\infty\}$ is then defined as the limiting measure [86,100-102],

满足单位体积条件，$\int_{S^2}\sqrt{g^\varepsilon}\mathrm{d}^2x = 1$。$S^2 \cong \mathbb{C}\cup\{\infty\}$ 上的单位体积刘维尔量子测度 μ_ϕ 由此定义为极限测度 [86,100-102],

$$\mu_\phi = \lim_{\varepsilon\to 0} e^{\gamma\overline{\phi}_\varepsilon(x)}\mathrm{d}^2x. \tag{64}$$

It is independent of the chosen background metric $\hat{g}_{ab}$ and transforms covariantly under conformal transformations of S^2 [86]. In the pure-gravity case $\gamma = \sqrt{8/3}$ this random measure should correspond to the measure on the Brownian sphere, which we discussed in section "Properties of the Brownian Sphere."

该测度与所选背景度量 $\hat{g}_{ab}$ 无关,且在 S^2 共形变换下满足协变变换性质 [86]。在纯引力情形 $\gamma = \sqrt{8/3}$ 下，该随机测度应当对应我们在“布朗球面的性质”一节讨论过的布朗球面上的测度。

The usual metric space structure one would associate to a Riemannian metric like g^ε_{ab} would be based on the shortest length $\int_0^1 \mathrm{d}t\sqrt{g^\varepsilon_{ab}\dot\Gamma^a\dot\Gamma^b} = \int_0^1 \mathrm{d}t\,|\dot\Gamma|\, e^{\frac{\gamma}{2}\overline{\phi}_\varepsilon}(\Gamma(t))$ of paths $\Gamma : [0,1] \to S^2$ between two points, resulting in the geodesic distance

对于类似 g^ε_{ab} 的黎曼度量，通常的度量空间结构由两点间路径 $\Gamma : [0,1] \to S^2$ 的最短长度 $\int_0^1 \mathrm{d}t\sqrt{g^\varepsilon_{ab}\dot\Gamma^a\dot\Gamma^b} = \int_0^1 \mathrm{d}t\,|\dot\Gamma|\, e^{\frac{\gamma}{2}\overline{\phi}_\varepsilon}(\Gamma(t))$ 定义，由此得到测地线距离

$$d_{g^\varepsilon}(x,y) = \inf\left\{\int_0^1 \mathrm{d}t\,|\dot\Gamma|\, e^{\frac{\gamma}{2}\overline{\phi}_\varepsilon(\Gamma(t))} : \text{ paths } \Gamma \text{ from } \Gamma(0)=x \text{ to } \Gamma(1)=y\right\}. \tag{65}$$

However, this cannot be the right answer! Shifting the field ϕ in a small neighborhood by a constant c leads to a local increase of volume, as measured by μ_ϕ, by a factor $e^{\gamma c}$, while local geodesic distances $d_{g^\varepsilon}(x,y)$ scale by a factor $\sqrt{e^{\gamma c}}$. This is at odds with the anomalous scaling of these quantities in the Brownian sphere, in which they should differ by a power of 4, i.e., the Hausdorff dimension of the metric space.

然而，这不可能是正确答案！将场 ϕ 在一个小邻域内平移一个常数 c 会导致由 μ_ϕ 度量的局域体积增加因子 $e^{\gamma c}$，而局域测地距离 $d_{g^\varepsilon}(x,y)$ 的缩放因子为 $\sqrt{e^{\gamma c}}$。这与布朗球中这些量的反常标度矛盾，在布朗球中二者应当相差 4 的幂次，即该度量空间的豪斯多夫维数。

More generally, each value of the coupling constant $\gamma \in (0,2)$ is expected to correspond to a universality class of two-dimensional quantum gravity coupled to conformal matter and have an associated Hausdorff dimension $d_\gamma > 2$ with $d_{\sqrt{8/3}} = 4$. So the appropriate definition, going under the name of Liouville first passage percolation [95, 96, 104, 105] , is to set

更一般地，人们认为耦合常数 $\gamma \in (0,2)$ 的每个取值对应一类二维量子引力共形物质耦合的普适类，且对应关联豪斯多夫维数 $d_\gamma > 2$，满足 $d_{\sqrt{8/3}} =$ 等于 4。因此，被称为刘维尔首次通过渗流 [95, 96, 104, 105] 的合适定义为设定

$$\xi = \frac{\gamma}{d_\gamma} \tag{66}$$

and consider instead the metric

转而考虑度量

$$D^\varepsilon_\phi(x,y) = \inf\left\{\int_0^1 \mathrm{d}t\,|\dot\Gamma|\, e^{\xi\overline{\phi}_\varepsilon(\Gamma(t))} : \text{ paths } \Gamma \text{ from } \Gamma(0)=x \text{ to } \Gamma(1)=y\right\}. \tag{67}$$

It has been demonstrated [95, 96, 105] that $D^\varepsilon_\phi(\cdot,\cdot)/a_\varepsilon$ with an appropriate normalization $a_\varepsilon \approx \varepsilon^{1-\xi Q}$ converges as $\varepsilon \to 0$ (in probability with respect to an appropriate topology) to a random metric space on S^2. Moreover, in the case $\gamma = \sqrt{8/3}$, it coincides [96] up to a global rescaling with the metric constructed from ϕ via Quantum Loewner Evolution [88-90], which in turn has the same law as the Brownian sphere from section "Definition of the Brownian Sphere" [89,106]. An even more precise link between the Brownian sphere and Liouville quantum gravity has been obtained in [107] by establishing scaling limits of both the measure and

the metric space with respect to a certain discrete conformal embedding of uniform random triangulations in the Euclidean plane, which forms a discrete counterpart of the uniformization (58).

已有研究证明 [95, 96, 105] ，经过适当归一化后，$D_\phi^\varepsilon(\cdot,\cdot)/a_\varepsilon$ 会随着 $\varepsilon \to 0$ (在对应合适拓扑依概率收敛) 收敛到 S^2 上的随机度量空间 $a_\varepsilon \approx \varepsilon^{1-\xi Q}$ 。此外，在 $\gamma = \sqrt{8/3}$ 的情形下，它与通过量子洛厄纳演化从 ϕ 构造出的度量仅相差全局缩放 [96]，而该度量和“布朗球的定义”一节中的布朗球服从相同的分布 [89,106]。文献 [107] 通过建立欧氏平面中一致随机三角剖分在特定离散共形嵌入下测度与度量空间的标度极限，得到了布朗球与刘维尔量子引力之间更精确的关联，该标度极限正是一致化 (58) 的离散对应物。

Local Limits

局部极限

Before moving on to the complementary method of peeling explorations, this is a good moment to introduce a framework in which we can deal with infinite random maps via local limits. In a sense, this is a problem analogous to that of defining statistical systems, like the Ising model, on a fixed infinite lattice, where Gibbs measures [108, 109] play an important role. Just like Ising configurations on an infinite lattice, there are uncountably many infinite maps, so we need to start by introducing a convenient topology.

在介绍补充方法剥皮探索之前，我们正好借此机会引入一个框架，通过局部极限来处理无限随机地图。从某种意义上说，这个问题类似于在固定无限格上定义统计系统 (比如伊辛模型) 的问题，其中吉布斯测度 [108, 109] 发挥着重要作用。和无限格上的伊辛构型一样，不可数无穷多的无限地图存在，因此我们首先需要引入一个方便的拓扑。

Following the foundational work of Benjamini and Schramm [110], let us introduce the local topology, in which, informally, two rooted maps are close to each other if they are identical in a large neighborhood of the root. More precisely, if $\mathfrak{m}$ is a rooted map, we let the ball $B_r(\mathfrak{m})$ of radius r be the subset of $\mathfrak{m}$ consisting of all vertices at graph distance at most r from the start of the root edge and all edges that have at least one of their endpoints at distance smaller than r . Then the local distance between two maps $\mathfrak{m}$ and $\mathfrak{m}'$ is defined to be

遵循 Benjamini 和 Schramm 的基础性工作 [110]，我们引入局部拓扑: 通俗来说，若两个带根地图在根的大邻域内完全一致，它们就彼此接近。更准确地说，若 $\mathfrak{m}$ 是一个带根地图，我们定义半径 r 的球 $B_r(\mathfrak{m})$ 为 $\mathfrak{m}$ 的子集，它包含所有与根边起点的图距离不超过 r 的顶点，以及所有至少有一个端点距离小于 r 的边。那么两个地图 $\mathfrak{m}$ 和 $\mathfrak{m}'$ 之间的局部距离定义为

$$d_{\mathrm{Loc}}(\mathfrak{m},\mathfrak{m}') = \frac{1}{1+\sup\{r\geq 0 : B_r(\mathfrak{m}) = B_r(\mathfrak{m}')\}}. \tag{68}$$

Any other strictly decreasing function approaching zero instead of the reciprocal could have been used, the point being that d_{Loc} satisfies the triangle inequality and $d_{\mathrm{Loc}}(\mathfrak{m},\mathfrak{m}') = 0$ if and only if $\mathfrak{m} = \mathfrak{m}'$ and therefore defines a metric on the space of all finite rooted planar maps $\mathcal{M}$. It is not a complete metric (some Cauchy sequences do not have a limit) but becomes one when we add infinite rooted planar maps $\overline{\mathcal{M}} = \mathcal{M} \cup \mathcal{M}_\infty$. Here we could define an infinite map $\mathfrak{m} \in \mathcal{M}_\infty$ as a sequence of finite maps $\mathfrak{m}_0, \mathfrak{m}_1, \mathfrak{m}_2, \ldots \in \mathcal{M}$

representing the balls of increasing radius in $\mathfrak{m}$, meaning that $B_r(\mathfrak{m}_j) = \mathfrak{m}_r$ for all $j \geq r \geq 0$. With this definition, all vertices of $\mathfrak{m}$ must have finite degree, but $\mathfrak{m}$ can have faces of infinite degree. The simplest example of this is the map which has an infinite sequence of edges heading away from the root edge (top of Fig. 10), which has a single face of infinite degree. It is an example of a one-ended infinite planar map, which is a planar map for which the removal of any finite subset of edges results in connected components of which exactly one is infinite. Another example of a one-ended infinite planar map is the square grid with vertex set $\mathbb{Z}^2 \subset \mathbb{R}^2$ (bottom of Fig. 10). Just like a (finite) planar map can be viewed as a graph that is properly embedded in the sphere, a one-ended infinite planar map is an infinite graph that is properly embedded in the plane, in a locally finite fashion with its end at infinity [50, section 2.1].

我们也可以使用其他任意趋近于零的严格递减函数代替倒数，核心在于 d_{Loc} 满足三角不等式，且 $d_{\mathrm{Loc}}(\mathfrak{m}, \mathfrak{m}') = 0$ 当且仅当 $\mathfrak{m} = \mathfrak{m}'$，因此它在所有有限带根平面地图 $\mathcal{M}$ 的空间上定义了一个度量。这个度量不是完备的 (部分柯西序列不存在极限)，但当我们加入无限带根平面地图 $\overline{\mathcal{M}} = \mathcal{M} \cup \mathcal{M}_\infty$ 后，它就成为了完备度量。这里我们可以将无限地图 $\mathfrak{m} \in \mathcal{M}_\infty$ 定义为有限地图 $\mathfrak{m}_0, \mathfrak{m}_1, \mathfrak{m}_2, \ldots \in \mathcal{M}$ 构成的序列，代表 $\mathfrak{m}$ 中半径递增的球，即对所有 $j \geq r \geq 0$ 都满足 $B_r(\mathfrak{m}_j) = \mathfrak{m}_r$。根据这个定义，$\mathfrak{m}$ 的所有顶点都必须具有有限度数，但 $\mathfrak{m}$ 可以存在无限度数的面。最简单的例子是从根边向外延伸出无限边序列的地图 (图 10 顶部)，它仅有一个无限度数的面。这是单端无限平面地图的一个例子: 这类平面地图满足，移除任意有限边子集后，恰好有一个连通分支是无限的。另一个单端无限平面地图的例子是顶点集为 $\mathbb{Z}^2 \subset \mathbb{R}^2$ 的正方形网格 (图 10 底部)。正如 (有限) 平面地图可以被视为正确嵌入球面的图，单端无限平面地图是以局部有限方式正确嵌入平面、端点在无穷远的无限图 [50, 第 2.1 节]。

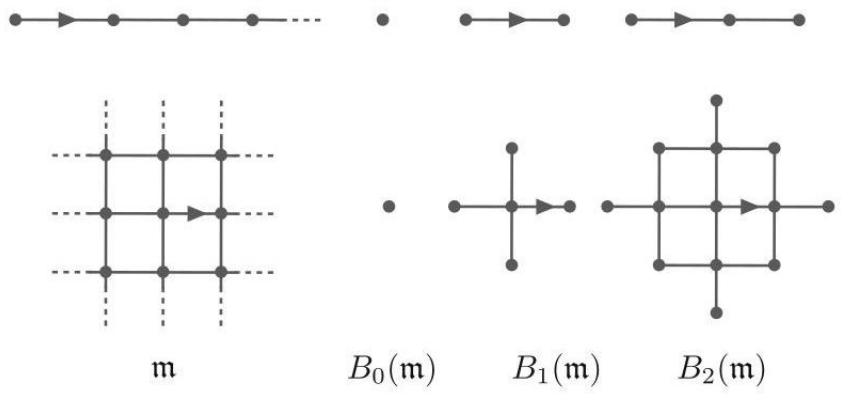

Fig. 10 Two examples of one-ended infinite planar maps $\mathfrak{m}$ together with their balls $B_r(\mathfrak{m})$ of increasing radius with respect to the graph distance

图 10 两个单端无限平面地图 $\mathfrak{m}$ 的示例，以及它们相对于图距离的半径递增的球 $B_r(\mathfrak{m})$

The local distance induces a topology on $\overline{\mathcal{M}}$ that provides a notion of local convergence (in distribution) of random planar maps to a random infinite map. Suppose $\mathfrak{m}^{(1)}, \mathfrak{m}^{(2)}, \ldots$ are random (finite or infinite) planar maps and $\mathfrak{m}$ is a random infinite planar map; then local convergence of $\mathfrak{m}^{(n)}$ to $\mathfrak{m}$ as $n \to \infty$ is equivalent to convergence in distribution of the balls of all radii, i.e., $B_r(\mathfrak{m}^{(n)}) \xrightarrow[n\to\infty]{\text{(d)}} B_r(\mathfrak{m})$ for all $r \geq 0$.

局部距离在 $\overline{\mathcal{M}}$ 上诱导出一个拓扑，该拓扑给出了随机平面地图依分布局部收敛到随机无限平面地图的概念。设 $\mathfrak{m}^{(1)}, \mathfrak{m}^{(2)}, \ldots$ 是随机 (有限或无限) 平面地图，$\mathfrak{m}$ 是随机无限平面地图；则当 $n \to \infty$ 时，$\mathfrak{m}^{(n)}$ 局部收敛到 $\mathfrak{m}$ 等价于所有半径的球依分布收敛，即对所有 $r \geq 0$ 成立 $B_r\left(\mathfrak{m}^{(n)}\right) \xrightarrow[n\to\infty]{(\mathrm{d})} B_r(\mathfrak{m})$。

Many models of random planar maps admit such a local convergence. The first result in this direction was the local convergence as $n \to \infty$ of the uniform planar triangulation with $2n$ triangles to the uniform infinite planar triangulation (UIPT) obtained by Angel and Schramm in [111]. Similarly, uniform quadrangulations were shown to converge to the uniform infinite planar quadrangulation (UIPQ) [112- 115]. This was extended to the case of bipartite Boltzmann maps conditioned on the number of edge n by Björnberg and Stefánsson in [116] (and later to general Boltzmann maps by Stephenson in [117]). To be precise, if $\mathbf{q}$ is a critical weight sequence and $\mathfrak{m}^{(n)}$ is a (rooted) $\mathbf{q}$ -Boltzmann planar map conditioned to have n edges, then $\mathfrak{m}^{(n)}$ converges locally to a unique one-ended random infinite map $\mathfrak{m}$ called the infinite Boltzmann planar map (q-IBPM) (Fig. 11).

许多随机平面地图模型都满足这类局部收敛性。该方向的第一个结果是 Angel 和 Schramm 在文献 [111] 中得到的: 含 $2n$ 个三角形的均匀平面三角剖分当 $n \to \infty$ 时局部收敛到均匀无限平面三角剖分 (UIPT)。类似地，人们证明了均匀四角化收敛到均匀无限平面四角化 (UIPQ)[112-115]。Björnberg 和 Stefánsson 在文献 [116] 中将该结论推广到了以边数 n 为条件的二分玻尔兹曼地图 (后续 Stephenson 在文献 [117] 中推广到了一般玻尔兹曼地图)。准确来说，若 $\mathbf{q}$ 是临界权序列，$\mathfrak{m}^{(n)}$ 是条件化为含 n 条边的 (带根) $\mathbf{q}$ -玻尔兹曼平面地图，则 $\mathfrak{m}^{(n)}$ 局部收敛到唯一的单端随机无限地图 $\mathfrak{m}$，即无限玻尔兹曼平面地图 (q-IBPM)(图 11)。

This local convergence can be understood from the point of view of the tree bijections of the previous section. Let us illustrate this in the case of the UIPQ following [115]. Recall the bijective encoding of rooted, pointed quadrangulations $\mathfrak{m}^{(n)}$ with n faces by labeled plane trees $\mathfrak{t}^{(n)}$ with n edges of section "Geodesic Distance Statistics" (and Fig. 5). One can imagine that a local neighborhood of the root in the quadrangulation $\mathfrak{m}^{(n)}$ is typically determined by a local neighborhood in the corresponding tree $t^{(n)}$, suggesting that one should consider the local limit of the random labeled tree first. The latter, when forgetting the labels for a moment, is an example of a Bienayme-Galton-Watson tree conditioned on its size, for which general local limits have been established by Kesten [118]. The limit corresponds to a one-ended infinite tree t consisting of a spine, i.e., an infinite line of vertices starting at the root vertex, with independent critical plane trees growing out on both sides (Fig. 12). The labels have independent increments along the edges that are uniform in $\{-1, 0, 1\}$ and such that the root vertex has label 0 . Since the labels along the spine describe a random walk with no drift, the range of the labels is almost surely the whole of $\mathbb{Z}$. Applying the rules described in section "From Trees to Planar Maps" to t, where we skip the first step (since there is no minimal label, we do not need to add a new vertex to become the origin), results in an infinite quadrangulation (Fig. 12). The result is one-ended and can be shown to be the local limit of $\mathfrak{m}^{(n)}$ and therefore to describe the UIPQ [115]. Note that the origin of $\mathfrak{m}^{(n)}$, the distinguished vertex used to construct the distance labeling, does not appear in the limiting UIPQ anymore: in a sense it has drifted away to infinity in the limit.

这种局部收敛可以从上一节的树双射角度来理解。我们按照文献 [115] 以 UIPQ 为例说明这一点。回顾“测地线距离统计”一节 (及图 5) 中，带根带点四边形 $\mathfrak{m}^{(n)}$ (含 n 个面) 可双射编码为带标记平面树 $\mathfrak{t}^{(n)}$ (含 n 条边)。不难发现，四边形 $\mathfrak{m}^{(n)}$ 中根顶点的局部邻域通常由对应树 $t^{(n)}$ 的局部邻域决定，这说明我们应当先考虑随机带标记树的局部极限。暂时忽略标记的话，该极限就是条件化于给定大小的比安梅-高尔顿-沃森树，Kesten 已经在文献 [118] 中给出了这类树的一般局部极限结论。极限是一棵单端无限树 t，它包含一条脊线——即从根顶点出发的无限顶点线，两侧都生长着独立的临界平面树 (图 12)。标记沿边的增量独立，均匀分布在 $\{-1,0,1\}$ 中，且根顶点的标记为 0。由于脊线上的标记对应零漂移随机游走，标记的范围几乎必然覆盖整个 $\mathbb{Z}$。将“从树到平面图”一节的规则应用到 t 上 (我们跳过第一步: 因为不存在最小标记，不需要额外添加顶点作为原点)，最终得到一个无限四边形 (图 12)。这个结果是单端的，可以证明它就是 $\mathfrak{m}^{(n)}$ 的局部极限，因此对应 UIPQ[115]。注意，$\mathfrak{m}^{(n)}$ 的原点——也就是构造距离标记时用到的特殊顶点，已经不在极限 UIPQ 中了: 从某种意义上说，它在极限中飘向了无穷远。

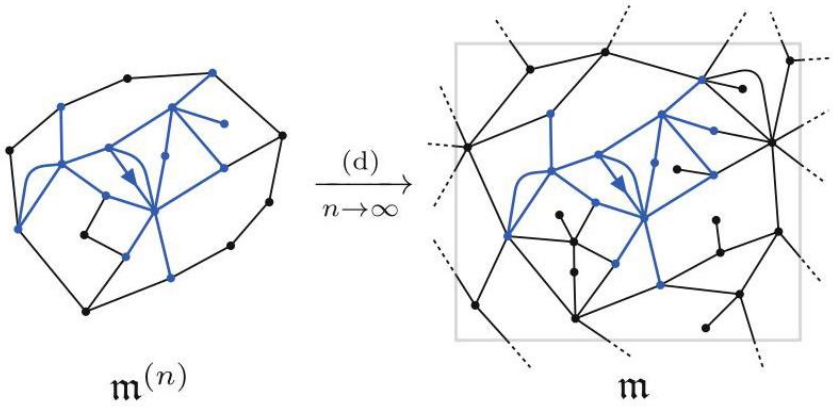

Fig. 11 Illustration of the local convergence of a $\mathbf{q}$ -Boltzmann planar map $\mathfrak{m}^{(n)}$ with n edges to the $\mathbf{q}$ -IBPM $\mathfrak{m}$. For this, it is necessary that for any fixed rooted map $\mathfrak{b}$, like the one indicated in thick blue, the probability of $\mathfrak{b}$ occurring as the ball of radius r converges as $n \to \infty$, i.e., $\lim_{n\to\infty} \mathbb{P}\left(B_r\left(\mathfrak{m}^{(n)}\right)=\mathfrak{b}\right) = \mathbb{P}\left(B_r\left(\mathfrak{m}\right)=\mathfrak{b}\right)$

图 11 $\mathbf{q}$ -玻尔兹曼平面图 $\mathfrak{m}^{(n)}$ (含 n 条边) 局部收敛到 $\mathbf{q}$ -IBPM $\mathfrak{m}$ 的示意图。对该收敛而言，对任意固定的带根地图 $\mathfrak{b}$ (例如粗蓝线标出的这个)，随着 $n \to \infty$ 趋向极限，$\mathfrak{b}$ 作为半径 r 球出现的概率收敛，即 $\lim_{n\to\infty} \mathbb{P}\left(B_r\left(\mathfrak{m}^{(n)}\right)=\mathfrak{b}\right) = \mathbb{P}\left(B_r\left(\mathfrak{m}\right)=\mathfrak{b}\right)$

As we will see in more detail in the next section, when discussing the peeling exploration, infinite random maps are particularly useful when discussing scaling properties. For instance, in the UIPQ the expected number of vertices at distance r grows like r^3 as $r \to \infty$ [113], nicely reflecting the Hausdorff dimension of 4 .

正如我们下一节讨论剥皮探索时会更详细说明的，讨论标度性质时，无限随机地图格外有用。例如，在 UIPQ 中，距离为 r 处的期望顶点数随 $r \to \infty$ 增长，渐近为 r^3 [113]，恰好对应豪斯多夫维数为 4。

Starting from random infinite maps, one can again consider continuum limits, the difference with before being that one does not have to worry about the size of the map and the scaling only has to be applied to the distances. A convergence of this type has been established for the UIPQ with respect to a local version of the Gromov-Hausdorff topology in [119], and the limit is called the Brownian plane because it has the topology

of $\mathbb{R}^2$. The Brownian plane is an example of a random metric space with exact scaling symmetry, in the sense that its distribution is unchanged when all distances are multiplied by a positive constant. It can also be obtained by considering the infinite-volume limit of the Brownian sphere [119].

从无限随机地图出发，我们仍然可以考虑连续极限，它和之前的区别在于无需再考虑地图的大小，只需要对距离做标度。文献 [119] 已经证明了 UIPQ 在局部版本的格罗莫夫-豪斯多夫拓扑下的这类收敛，该极限称为布朗平面，因为它具有 $\mathbb{R}^2$ 的拓扑。布朗平面是具有精确标度对称性的随机度量空间的例子: 也就是说，当所有距离乘以任意正常数，它的分布保持不变。它也可以通过布朗球面的无限体积极限得到 [119]。

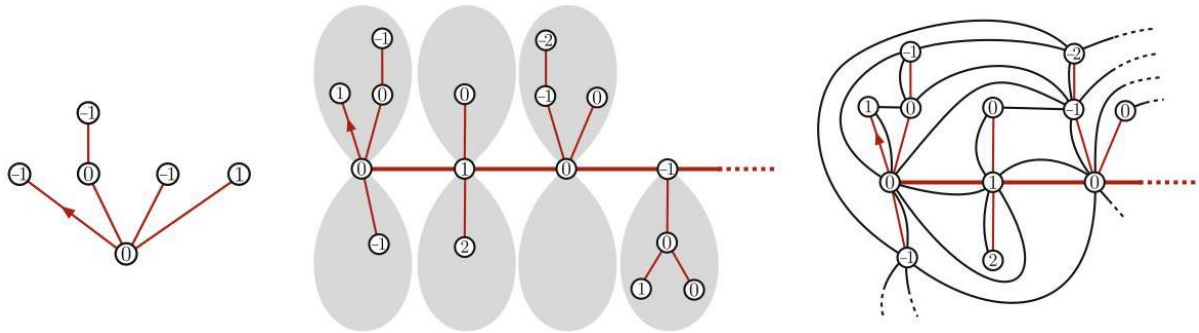

Fig. 12 The local limit of a uniform (labeled) plane tree with n edges (left) is an infinite tree consisting of a line with independent critical plane trees (shaded in gray) growing from both sides (middle). Applying the rules of the inverse Cori-Vauquelin-Schaeffer bijection to the infinite tree produces the UIPQ

图 12 含 n 条边的均匀 (带标记) 平面树的局部极限 (左) 是一棵无限树，由一条主干线两侧各生长出独立临界平面树 (灰色阴影区域) 构成 (中)。对这棵无限树应用逆科里-沃克兰-谢弗双射规则可得到 UIPQ

The Peeling Process

剥皮过程

We have seen that bijections with labeled trees provide an explanation for the universal properties of planar map enumeration, while providing an economical way to study statistics of geodesic distances. In this section we will discuss a complementary approach that displays the universality in a different way and gives access to other classes of statistics. This approach goes under the umbrella name of peeling, which amounts to analyzing an exploration process on a random map (see Fig. 13 for an illustration). Such a peeling process was first described by Watabiki [120] in the setting of the Euclidean dynamical triangulation approach to noncritical string theory. It formed the basis for the first calculation of the geodesic two-point function (49) by Ambjørn and Watabiki [58]. The first appearance of peeling in the mathematics literature was in the work of Angel [121] on percolation on the uniform infinite planar triangulation (see section "Local Limits"), which sparked many related investigations (for example [56, 122-124]). We will focus on a type of peeling process, going under the name of lazy peeling or edge peeling, that is particularly convenient for the study

of Boltzmann planar maps. It was formulated in [125] and has been used as a tool to investigate many types of statistics related to these maps (e.g., [53,126-128]). For an in-depth discussion and many applications, we direct the reader to the lecture notes on the topic by Curien [50].

我们已经看到，带标记树的双射解释了平面地图计数的普适性质，同时为研究测地线距离的统计量提供了简洁的方法。在本节中，我们将讨论一种互补方法，它以不同的方式展现普适性，并可用于获取其他类别的统计量。该方法统称为剥皮法，本质是分析随机地图上的探索过程 (示例见图 13)。这类剥皮过程最早由 Watabiki[120] 在欧几里得动力学三角化方法处理非临界弦理论的研究框架中提出，它是 Ambjørn 与 Watabiki[58] 首次计算测地线两点函数 (49) 的基础。剥皮法最早出现在数学文献中，是 Angel[121] 对均匀无限平面三角化上渗流的研究 (参见“局部极限”一节)，这项工作引发了诸多相关研究 (例如 [56, 122-124])。我们将聚焦于一类特别适合研究玻尔兹曼平面地图的剥皮过程，称为惰性剥皮或边剥皮。该方法在文献 [125] 中被提出，此后一直被用作研究这类平面地图多种统计量的工具 (例如 [53,126-128])。若想要了解该主题的深入讨论与更多应用，我们推荐读者阅读 Curien 的相关讲义 [50]。

Peeling Explorations

剥皮探索

Let $\mathfrak{m}$ be a (rooted) bipartite planar map. The intuitive idea of (lazy) peeling of $\mathfrak{m}$ is that we explore $\mathfrak{m}$ one edge at a time starting from the root face until we have seen the entire map. To formalize this we require a way to encode what part of $\mathfrak{m}$ has been explored at each step. To this end we introduce a planar map with holes to be a planar map $\mathfrak{e}$ (the ”explored” part) with a distinguished set of faces not including the root face, which we call the holes of $\mathfrak{e}$ (left side of Fig. 14). Each hole is required to be simple, meaning that its contour does not visit any vertex twice, and the holes are not allowed to touch each other. Given a hole h of degree $2k$ and a planar map $\mathfrak{u}$ (the ”unexplored” part) with root face of degree $2k$, we have a natural operation of gluing $\mathfrak{u}$ into the hole h of $\mathfrak{e}$, which is best explained in a picture (see Fig. 14). (Note that to make this operation unambiguous, one should fix an algorithm to select an edge in the contour of hole h to which the root edge of $\mathfrak{u}$ is to be glued. There are many choices for such an algorithm, but since it will not affect any of the further considerations, we will leave it unspecified.).

设 $\mathfrak{m}$ 是一个 (带根) 二部平面图。对 $\mathfrak{m}$ 进行 (迟缓) 剥皮的直观思路是: 从根面开始，每次探索 $\mathfrak{m}$ 的一条边，直至遍历整张图。为了将其形式化，我们需要一种方式编码在每一步中 $\mathfrak{m}$ 的哪一部分已被探索。为此我们引入带洞平面图的概念: 它是一张平面图 $\mathfrak{e}$ (即“已探索”部分)，其不含根面的一组特殊面被我们称为 $\mathfrak{e}$ 的洞 (图 14 左侧)。要求每个洞都是单洞，即它的轮廓不会经过任意顶点两次，且任意两个洞不能相交。给定一个次数为 $2k$ 的洞 h ，以及一张根面次数为 $2k$ 的平面图 $\mathfrak{u}$ (即“未探索”部分)，我们可以自然地将 $\mathfrak{u}$ 粘入 $\mathfrak{e}$ 的洞 h 中，这个操作最好用图示说明 (见图 14)。(请注意，为了让该操作明确无歧义，需要固定一个算法，在洞 h 的轮廓中选出一条边，将 $\mathfrak{u}$ 的根边粘到这条边上。这类算法有很多可选，但它不会影响后续任何推导，因此我们不做具体指定。)

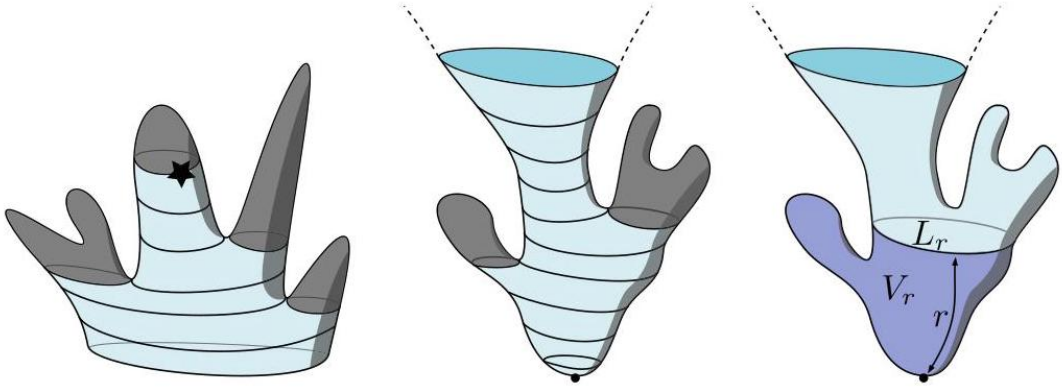

Fig. 13 An intuitive picture of the peeling exploration of a pointed map starting at the boundary (left) and of an infinite map starting at the root (middle). We will see how to use the exploration to track the boundary length L_r and area V_r of geodesic ball of radius r around the root (right)

图 13 起点在边界的带点图剥皮探索 (左)，以及起点在根的无限图剥皮探索 (中) 的直观示意图。我们后续会介绍如何利用该探索追踪根周围半径 r 的测地球的边界长度 L_r 和面积 V_r (右)

If $\mathfrak{e}$ is a planar map with $p \geq 0$ holes $h_1, \dots, h_p$, then $\mathfrak{e}$ is said to be a submap of $\mathfrak{m}$, denoted $\mathfrak{e} \subset \mathfrak{m}$, if planar maps $\mathfrak{u}_1, \dots, \mathfrak{u}_p$ exist such that the result of gluing $\mathfrak{u}_i$ into the hole h_i is $\mathfrak{m}$. More generally, if $\mathfrak{e}'$ is another planar map with holes, we can make sense of $\mathfrak{e}$ being a submap of $\mathfrak{e}'$, by allowing the maps $\mathfrak{u}_i$ to have holes themselves. Importantly, we may convince ourselves that as soon as $\mathfrak{e} \subset \mathfrak{e}'$, the maps $\mathfrak{u}_i$ that need to be glued in the holes of $\mathfrak{e}$ are uniquely determined. We will call the edges and vertices of $\mathfrak{e}$ that are adjacent to a hole active and the other ones explored.

若 $\mathfrak{e}$ 是一张带有 $p \geq 0$ 个洞 $h_1, \dots, h_p$ 的平面图，且存在平面图 $\mathfrak{u}_1, \dots, \mathfrak{u}_p$ ，使得将 $\mathfrak{u}_i$ 粘入 $\mathfrak{e}$ 的洞 h_i 后得到的图是 $\mathfrak{m}$ ，则称 $\mathfrak{e}$ 是 $\mathfrak{m}$ 的子图，记为 $\mathfrak{e} \subset \mathfrak{m}$ 。更一般地，若 $\mathfrak{e}'$ 是另一张带洞平面图，允许粘入的图 $\mathfrak{u}_i$ 本身也带洞，我们就可以定义 $\mathfrak{e}$ 是 $\mathfrak{e}'$ 的子图。重要的是，我们可以确认，只要满足 $\mathfrak{e} \subset \mathfrak{e}'$ ，需要粘入 $\mathfrak{e}$ 各个洞的图 $\mathfrak{u}_i$ 是唯一确定的。我们将 $\mathfrak{e}$ 中与洞相邻的边和顶点称为活跃边顶点，其余称为已探索边顶点。

A lazy peeling or edge peeling exploration of $\mathfrak{m}$ then is an increasing sequence of submaps

因此，对 $\mathfrak{m}$ 的迟缓剥皮或逐边剥皮探索就是一个递增的子图序列

$$\mathfrak{e}_0 \subset \mathfrak{e}_1 \subset \mathfrak{e}_2 \subset \cdots \subset \mathfrak{e}_{|\mathrm{E}(\mathfrak{m})|} = \mathfrak{m}, \tag{69}$$

where $\mathfrak{e}_i$ has precisely i internal edges. In particular, the initial submap $\mathfrak{e}_0 \subset \mathfrak{m}$ has just two faces, the root face and a hole of the same degree. (See Fig. 15 for an example.) This definition is a bit abstract but should become more clear if we analyze the possible transitions $\mathfrak{e}_i \subset \mathfrak{e}_{i+1}$. This transition is a result of the operation of peeling an edge e where e is an active edge of $\mathfrak{e}_i$ (indicated by orange shading in Fig. 15). Note that e corresponds to a unique (side of an) edge in m , and let f be the face of $\mathfrak{m}$ that sits on the other side of this edge. Then we distinguish two types of events depending on whether f is new to $\mathfrak{e}_i$ or not:

其中 $\mathfrak{e}_i$ 恰好有 i 条内部边。特别地，初始子图 $\mathfrak{e}_0 \subset \mathfrak{m}$ 只有两个面: 根面和度数相同的洞。(示例参见图 15) 该定义略显抽象，但在分析可能的转移 $\mathfrak{e}_i \subset \mathfrak{e}_{i+1}$ 后会变得更清晰。这种转移是剥离边 e 操作的结果，其中 e 是 $\mathfrak{e}_i$ 的一条活动边 (图 15 中以橙色阴影标出)。注意 e 对应 $\mathfrak{m}$ 中唯一的一条 (边的) 侧边，设 f 是 $\mathfrak{m}$ 中位于这条边另一侧的面。接下来我们根据 f 对 $\mathfrak{e}_i$ 而言是否为新面区分两类事件:

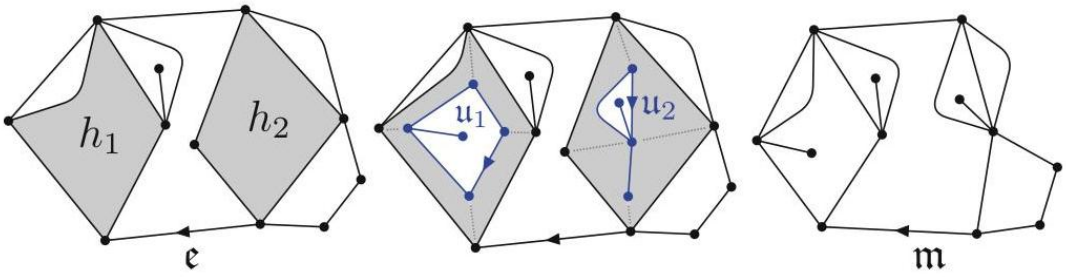

Fig. 14 The planar map $\mathfrak{e}$ with two holes h_1 and h_2 is a submap of $\mathfrak{m}$, because gluing $\mathfrak{u}_1$ and $\mathfrak{u}_2$ into the holes yields $\mathfrak{m}$

图 14 含两个洞 h_1 和 h_2 的平面地图 $\mathfrak{e}$ 是 $\mathfrak{m}$ 的子图，因为将 $\mathfrak{u}_1$ 和 $\mathfrak{u}_2$ 粘入洞后得到 $\mathfrak{m}$

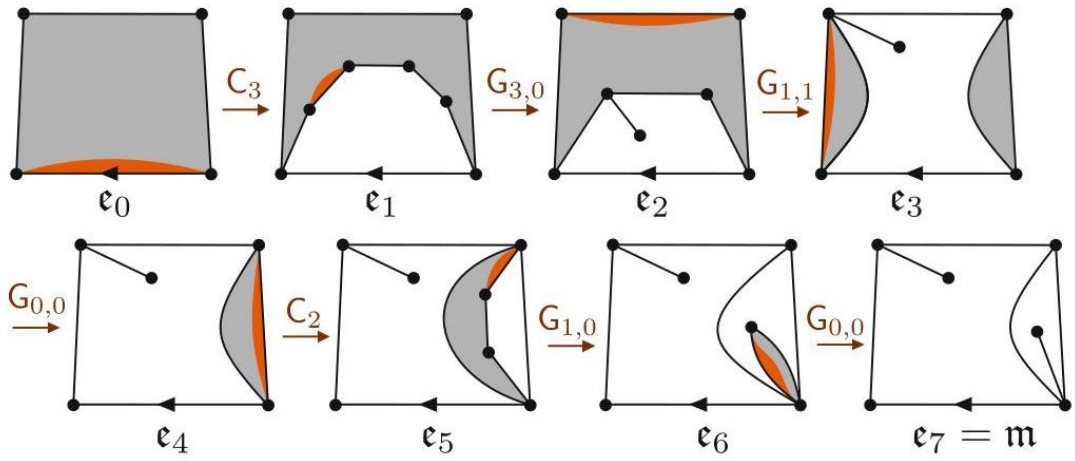

Fig. 15 Example of a peeling exploration of a map $\mathfrak{m}$ with 7 edges. The peel edge selected by the (unspecified) algorithm $\mathcal{A}$ is shown with orange shading, and the peeling transitions $\mathbf{C}_k$ or $\mathbf{G}_{k_1,k_2}$ are indicated

图 15 含 7 条边的地图 $\mathfrak{m}$ 的剥离探索示例。(未指定的) 算法 $\mathcal{A}$ 选中的待剥离边以橙色阴影标出，并标出了剥离转移 $\mathbf{C}_k$ 和 $\mathbf{G}_{k_1,k_2}$

- Event $\mathbf{C}_k$, when f was not already in $\mathfrak{e}_i$ and its degree is $2k$. Then $\mathfrak{e}_{i+1}$ is obtained from $\mathfrak{e}_i$ by attaching a $2k$ -gon to e inside the hole.

  - 事件 $\mathbf{C}_k$ ，此时 f 不在 $\mathfrak{e}_i$ 中，且它的度数为 $2k$ 。此时 $\mathfrak{e}_{i+1}$ 由 $\mathfrak{e}_i$ 在洞内的 e 处拼接一个 $2k$ 边形得到。

- Event $\mathbf{G}_{k_1,k_2}$, when f was already present in $\mathfrak{e}_i$. In this case $\mathfrak{e}_{i+1}$ is obtained from $\mathfrak{e}_i$ by gluing e to another edge e' in the contour of the same hole, splitting the hole into two holes of degrees $2k_1 \geq 0$ and $2k_2 \geq 0$ (the first on the right of e , the second on the left). We can have $k_1 = 0$ or $k_2 = 0$ when e and e' are adjacent, in which case the corresponding hole is not really a hole but a single vertex.

- 事件 $\mathbf{G}_{k_1,k_2}$ ， 此时 f 已存在于 $\mathfrak{e}_i$ 中。这种情况下 $\mathfrak{e}_{i+1}$ 由 $\mathfrak{e}_i$ 将 e 粘到同一个洞轮廓上的另一条边 e' 得到，原洞会被分割为两个度数分别为 $2k_1 \geq 0$ 和 $2k_2 \geq 0$ 的洞 ($2k_1 \geq 0$ 在 e 右侧，$2k_2 \geq 0$ 在左侧)。当 e 与 e' 相邻时， 会出现 $k_1 = 0$ 或 $k_2 = 0$ ， 此时对应的区域其实不是洞，而是一个单点顶点。

In particular, given $\mathfrak{e}_i \subset \mathfrak{m}$, the edge e uniquely determines the result $\mathfrak{e}_{i+1}$. So if we choose a peeling algorithm $\mathcal{A}$ that chooses from any planar map with holes an active edge $e = \mathcal{A}(\mathfrak{e})$ to peel, then $\mathcal{A}$ and $\mathfrak{m}$ together uniquely specify the exploration (69). The versatility of the peeling approach lies in the freedom one has in specifying the algorithm $\mathcal{A}$, while the results that follow are independent of this choice.

特别地，给定 $\mathfrak{e}_i \subset \mathfrak{m}$ ， 边 e 可以唯一确定结果 $\mathfrak{e}_{i+1}$ 。因此，如果我们选定一个剥离算法 $\mathcal{A}$ ， 由它从任意带洞的平面地图中选出一条待剥离的活动边 $e = \mathcal{A}(\mathfrak{e})$ ， 那么 $\mathcal{A}$ 和 $\mathfrak{m}$ 就能共同唯一确定探索过程 (69)。剥离方法的多功能性来源于指定算法 $\mathcal{A}$ 时的自由度，而后续得到的结论与算法的选择无关。

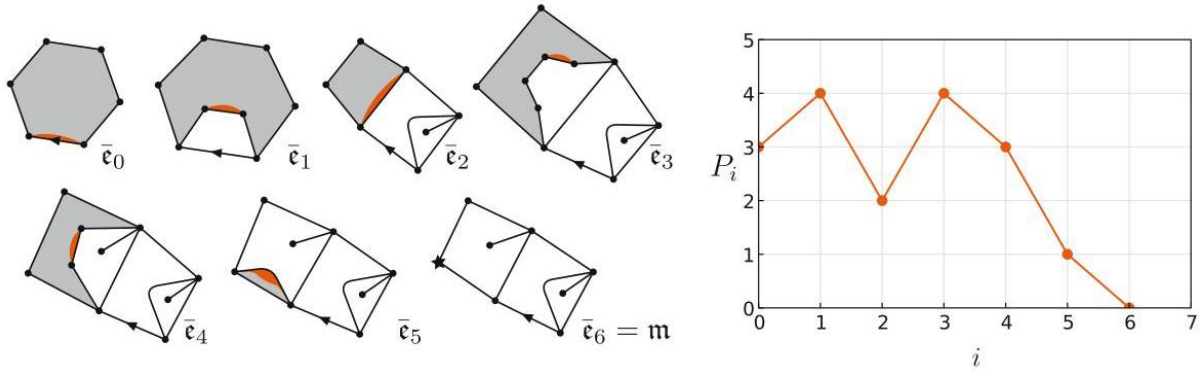

Fig. 16 Example of a targeted peeling exploration of a pointed map $\mathfrak{m}$ together with the corresponding perimeter process $(P_i)_{i\geq 0}$. The peel edge selected by the (unspecified) algorithm $\mathcal{A}$ is indicated with the orange shading

图 16 带标记地图的目标剥离探索示例 $\mathfrak{m}$ ， 以及对应的周长过程 $(P_i)_{i\geq 0}$ 。(未指定) 算法 $\mathcal{A}$ 选定的剥离边由橙色阴影标出

Targeted Peeling of a Pointed or Infinite Planar Map

带根点或无限平面地图的目标剥皮法

It is often useful to consider a targeted version of the peeling exploration. The target, depicted by a star $\star$, can be the distinguished vertex in a pointed map or the boundary at infinity in a one-ended infinite map.

In the former case, the exploration process stops when the target is explored, while evidently in the latter case, the exploration continues indefinitely. Either way, it makes sense to speed up the exploration process, by filling in a newly produced hole h with its corresponding unexplored region $\mathfrak{u}$ of $\mathfrak{m}$ whenever $\mathfrak{u}$ does not contain the target. In this way, the peeling exploration becomes a sequence of submaps

研究目标版剥皮探索通常很有意义。目标用星形标记 $\star$ 表示，它可以是带根点地图中的特殊顶点，也可以是单端无限地图的无穷远边界。在前一种情况中，探索过程会在目标被探索到时停止，而在后一种情况中，探索显然会无限进行下去。无论哪种情况，只要新生成的孔 h 对应的未探索区域 $\mathfrak{u}$ 不包含目标 $\mathfrak{m}$，我们就可以填充该孔来加速探索过程。这样一来，剥皮探索就变成了一系列子映射

$$\bar{\mathfrak{e}}_0 \subset \bar{\mathfrak{e}}_1 \subset \cdots \subset \mathfrak{m}, \tag{70}$$

where $\bar{\mathfrak{e}}_0 = \mathfrak{e}_0$ as before and each of the submaps $\bar{\mathfrak{e}}_0, \dots, \bar{\mathfrak{e}}_{n-1}$ has a single hole. The transitions can be deduced from those of the untargeted peeling. In the event of $\mathbf{C}_k$, no hole needs to be filled in. In the case of $\mathbf{G}_{k_1,k_2}$, there are two possibilities: either the hole of degree $2k_1$ is filled in, an event that we denote by $\mathbf{G}_{k_1,\star}$, or the hole of degree $2k_2$ is filled in, denoted by $\mathrm{G}_{\star,k_2}$. Note that the final step $\bar{\mathfrak{e}}_{n-1} \subset \bar{\mathfrak{e}}_n = \mathfrak{m}$ in the pointed case necessarily corresponds to an event $\mathrm{G}_{\star,p-1}$ or $\mathrm{G}_{p-1,\star}$ where $2p$ is the degree of the hole of $\bar{\mathfrak{e}}_{n-1}$, because only when the two active edges adjacent to the target are glued, the target is explored (Fig. 16).

其中 $\bar{\mathfrak{e}}_0 = \mathfrak{e}_0$ 与之前一致，每个子映射 $\bar{\mathfrak{e}}_0, \dots, \bar{\mathfrak{e}}_{n-1}$ 都仅有一个孔。转移可以从非目标剥皮的转移推导得到。在 $\mathbf{C}_k$ 的情况下，不需要填充任何孔。在 $\mathbf{G}_{k_1,k_2}$ 的情况下，存在两种可能性: 要么度数为 $2k_1$ 的孔被填充，我们将该事件记为 $\mathbf{G}_{k_1,\star}$，要么度数为 $2k_2$ 的孔被填充，记为 $\mathrm{G}_{\star,k_2}$。注意，带根点情形的最后一步 $\bar{\mathfrak{e}}_{n-1} \subset \bar{\mathfrak{e}}_n = \mathfrak{m}$ 必然对应事件 $\mathrm{G}_{\star,p-1}$ 或 $\mathrm{G}_{p-1,\star}$，其中 $2p$ 是 $\bar{\mathfrak{e}}_{n-1}$ 的孔的度数，因为只有当目标相邻的两条活性边粘合后，目标才会被探索 (图 16)。

To a targeted peeling exploration, one may naturally associate the sequence $(P_i)_{i\geq 0}$ of integers, called the perimeter process, by setting P_i to be half the degree of the hole of $\mathfrak{e}_i$. Then P_0 is equal to half the perimeter of $\mathfrak{m}$, and $P_i > 0$ for all $i > 0$ in case $\mathfrak{m}$ is an infinite map, while $P_i > 0$ for $i < n$ and $P_n = 0$ for a pointed map $\mathfrak{m} = \bar{\mathfrak{e}}_n$. The increments $P_{i+1} - P_i$ are determined by the peeling event leading from $\bar{\mathfrak{e}}_i$ to $\bar{\mathfrak{e}}_{i+1}$. Indeed, we see that

对于目标剥皮探索，我们可以自然关联出整数序列 $(P_i)_{i\geq 0}$，称之为周长过程: 将 P_i 设为 $\mathfrak{e}_i$ 的孔的度数的一半。那么 P_0 等于 $\mathfrak{m}$ 周长的一半，若 $\mathfrak{m}$ 是无限地图，则对所有 $i > 0$ 都有 $P_i > 0$；而对于带根点地图 $\mathfrak{m} = \bar{\mathfrak{e}}_n$，则满足 $P_i > 0$ 对 $i < n$ 成立，$P_n = 0$ 成立。增量 $P_{i+1} - P_i$ 由从 $\bar{\mathfrak{e}}_i$ 到 $\bar{\mathfrak{e}}_{i+1}$ 的剥皮事件决定，我们可以得到:

$$P_{i+1} - P_i = \begin{cases} k-1 & \text{in the event } \mathbf{C}_k, \\ -k-1 & \text{in the event } \mathbf{G}_{\star,k} \text{ or } G_{k,\star}. \end{cases} \tag{71}$$

Peeling Pointed Boltzmann Planar Maps

剥离带点玻尔兹曼平面地图

Now suppose $\mathbf{q}$ is admissible and $\mathfrak{m}$ is a pointed $\mathbf{q}$ -Boltzmann planar map with specified root face degree 2ℓ . In other words, we consider the probability distribution

现在假设 $\mathbf{q}$ 是可容许的，且 $\mathfrak{m}$ 是一个根面度指定为 2ℓ 的带点 $\mathbf{q}$ -玻尔兹曼平面地图。换言之，我们考虑如下概率分布

$$\mathbb{P}_\bullet^{(2\ell)}(\mathfrak{m}) := \frac{w_{\mathbf{q}}(\mathfrak{m})}{W_\bullet^{(2\ell)}}, \tag{72}$$

with the weight $w_{\mathbf{q}}(\mathfrak{m})$ as in (10). If we fix a peeling algorithm $\mathcal{A}$, then $\mathfrak{m}$ determines a random peeling exploration $\bar{\mathfrak{e}}_0 \subset \bar{\mathfrak{e}}_1 \subset \cdots \subset \mathfrak{m}$, which has a simple description. The reason for the simplicity is the following domain Markov property following from the factorized form the distribution (72): for any i , conditionally on $\mathfrak{e}_i$, the unexplored region $\mathfrak{u}$ corresponding to the hole of degree $2p$ of $\mathfrak{e}_i$ has distribution $\mathbb{P}_\bullet^{(2p)}$. From this we deduce that the event $\mathbf{C}_k$ occurs with probability

其中权重 $w_{\mathbf{q}}(\mathfrak{m})$ 如式 (10) 所示。若固定一个剥离算法 $\mathcal{A}$ ，则 $\mathfrak{m}$ 确定了一个随机剥离探索 $\bar{\mathfrak{e}}_0 \subset \bar{\mathfrak{e}}_1 \subset \cdots \subset \mathfrak{m}$ ，它具有简洁的描述。这种简洁性来源于分布 (72) 的因式分解形式带来的如下区域马尔可夫性: 对任意 i ，在给定 $\mathfrak{e}_i$ 的条件下，对应于 $\mathfrak{e}_i$ 中度为 $2p$ 的洞的未探索区域 $\mathfrak{u}$ 服从分布 $\mathbb{P}_\bullet^{(2p)}$ 。由此我们推得事件 $\mathbf{C}_k$ 发生的概率为

$$\frac{q_{2k} W_\bullet^{(2p+2k-2)}}{W_\bullet^{(2p)}} \tag{73}$$

and the events $\mathrm{G}_{\star,k}$ and $\mathrm{G}_{k,\star}$ each with probability

事件 $\mathrm{G}_{\star,k}$ 和事件 $\mathrm{G}_{k,\star}$ 各自发生的概率为

$$\frac{W_\bullet^{(2p-2k-2)} W^{(2k)}}{W_\bullet^{(2p)}} . \tag{74}$$

That these probabilities add up to one, can be checked from taking a t -derivative of the Tutte equation (11) and using $W_\bullet^{(2\ell)} = \frac{\partial}{\partial t} W^{(2\ell)}$ before setting $t = 1$.

这些概率之和为 1，可以通过对塔特方程 (11) 求 t 导数，并在设定 $t = 1$ 之前利用 $W_\bullet^{(2\ell)} = \frac{\partial}{\partial t} W^{(2\ell)}$ 验证。

It follows from (71) that the perimeter process $(P_i)_{i=0}^n$ becomes a Markov process on the non-negative integers with transition probabilities

由式 (71) 可知，周过程 $(P_i)_{i=0}^n$ 是定义在非负整数上、具有如下转移概率的马尔可夫过程

$$\mathbb{P}_\bullet^{(2\ell)}(P_{i+1} = p + k \mid P_i = p) = \frac{W_\bullet^{(2p+2k)}}{W_\bullet^{(2p)}} \begin{cases} q_{2k+2} & \text{if } k \geq 0 \\ 2W^{(-2k-2)} & \text{if } -p \leq k \leq -1, \end{cases}$$

(75)

where the process stops at the first time i for which $P_i = 0$, i.e., when $\bar{\mathfrak{e}}_i = \mathfrak{m}$. Recalling the universal form (28) of the pointed disk function and introducing the notation

过程会在首次满足 i 使 $P_i = 0$ 时停止，也就是当 $\bar{\mathfrak{e}}_i = \mathfrak{m}$ 时停止。回顾带点圆盘函数的通用形式 (28)，并引入记号

$$h^{\downarrow}(\ell) = 4^{-\ell}\binom{2\ell}{\ell}\mathbf{1}_{\{\ell\geq 0\}},\ \upsilon_{\mathbf{q}}(k) = \begin{cases} q_{2k+2}(4R)^k & \text{if } k \geq 0 \\ 2W^{(-2k-2)}(4R)^k & \text{if } k \leq -1, \end{cases} \tag{76}$$

the transition probabilities can be summarized as

转移概率可以总结为

$$\mathbb{P}_{\bullet}^{(2\ell)}(P_{i+1} = p + k \mid P_i = p) = \frac{h^{\downarrow}(p+k)}{h^{\downarrow}(p)}\upsilon_{\mathbf{q}}(k). \tag{77}$$

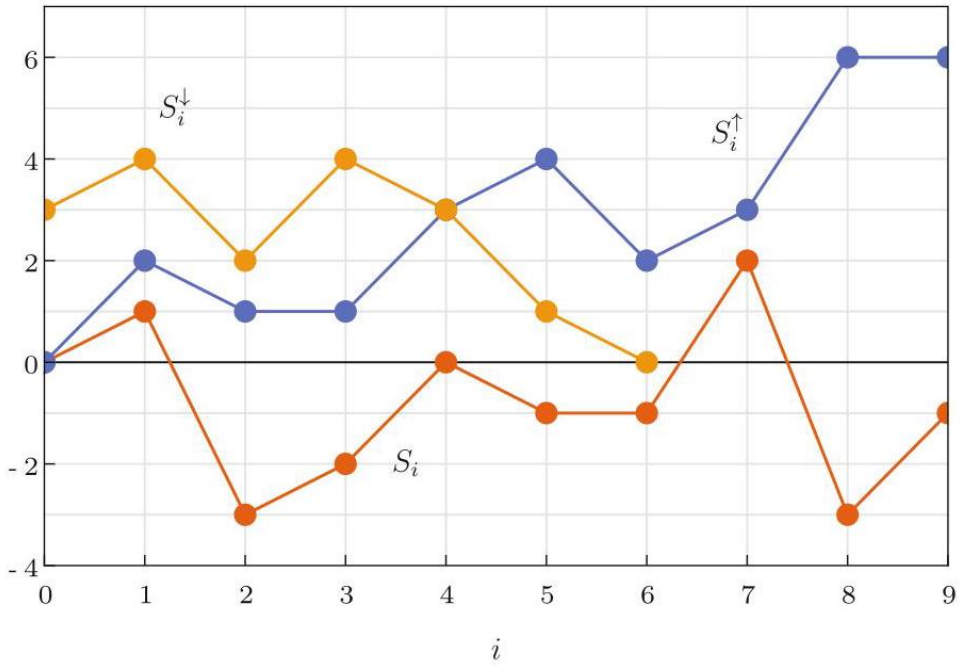

Fig. 17 Illustration of the random walk $(S_i)_{i\geq 0}$ with increments distributed as $\upsilon_{\mathbf{q}}$, and its conditioned counterparts $\left(S_i^{\downarrow}\right)_{i\geq 0}$ and $\left(S_i^{\uparrow}\right)_{i\geq 0}$

图 17 增量服从 $\upsilon_{\mathbf{q}}$ 分布的随机游走 $(S_i)_{i\geq 0}$ 及其条件对应物 $\left(S_i^{\downarrow}\right)_{i\geq 0}$ 和 $\left(S_i^{\uparrow}\right)_{i\geq 0}$ 的示意图

Using (12) and (16), we may check that

利用式 (12) 和 (16)，我们可以验证得到

$$\sum_{k=-\infty}^{\infty}\upsilon_{\mathbf{q}}(k) \overset{(12)}{=} 1 - \frac{V'\left(\sqrt{4R}\right)}{\sqrt{4R}} + 2\frac{W\left(\sqrt{4R}\right)}{\sqrt{4R}} \overset{(16)}{=} 1. \tag{78}$$

Therefore, $\upsilon_{\mathbf{q}}$ determines a probability measure on $\mathbb{Z}$, corresponding to the distribution of increments of the perimeter process in the large-perimeter limit, i.e., the large- p limit of (77).

因此，$\upsilon_{\mathbf{q}}$ 在 $\mathbb{Z}$ 上确定了一个概率测度，对应大周极限下 (即式 (77) 的大 p 极限) 周过程增量的分布。

Let us consider a random walk $(S_n)_{n\geq 0}$ with independent increments of law $\upsilon_{\mathbf{q}}$ (Fig. 17). One may show [50, 125] that this random walk cannot have a positive drift. (In case $\upsilon_{\mathbf{q}}$ has a finite first moment, a positive drift means $\mathbb{E}[S_{i+1}-S_i]=\sum_{k=-\infty}^{\infty} k\upsilon_{\mathbf{q}}(k)>0$. More generally, a random walk has a positive drift if it has a nonzero probability of never visiting the negative integers.) By summing the probabilities (77) over k, we deduce that $h^{\downarrow}$ is harmonic on the positive integers with respect to $\upsilon_{\mathbf{q}}$, i.e.,

我们来考虑一个具有独立增量、服从分布 $\upsilon_{\mathbf{q}}$ 的随机游走 $(S_n)_{n\geq 0}$ (图 17)。可以证明 [50, 125] 该随机游走不可能具有正漂移。(若 $\upsilon_{\mathbf{q}}$ 一阶矩有限，正漂移的含义是 $\mathbb{E}[S_{i+1}-S_i]=\sum_{k=-\infty}^{\infty} k\upsilon_{\mathbf{q}}(k)>0$。更一般地说，若随机游走永不访问负整数的概率非零，则它具有正漂移。) 对 k 求和所有概率 (77)，我们可推得 $h^{\downarrow}$ 在正整数上关于 $\upsilon_{\mathbf{q}}$ 是调和的，即:

$$\sum_{k=-\infty}^{\infty} h^{\downarrow}(p+k)\,\upsilon_{\mathbf{q}}(k)=h^{\downarrow}(p) \quad \text{for } p\geq 1. \tag{79}$$

Since $h^{\downarrow}(p)\leq h^{\downarrow}(0)=1$, the function $h^{\downarrow}$ acquires a simple probabilistic interpretation: when the random walk $(S_n)_{n\geq 0}$ is started at $p\geq 0$ and we consider the first time it visits the non-positive integers $\mathbb{Z}_{\leq 0}$, then $h^{\downarrow}(p)$ is the probability that it does so at 0. In the theory of random walks, $h^{\downarrow}$ is said to be the pre-renewal function of the random walk. The transition probabilities (77) then allow us to interpret the perimeter process $(P_i)_{i\geq 0}$ as having the law of the random walk $(S_n)_{n\geq 0}$ when conditioned on hitting $\mathbb{Z}_{\leq 0}$ at 0 and killing it at that instance, which we denote by $\left(S_n^{\downarrow}\right)_{n\geq 0}$. This conditioning with the help of a harmonic function is an example of a transformation of Markov chains known as Doob's h-transform [129].

由于 $h^{\downarrow}(p)\leq h^{\downarrow}(0)=1$，函数 $h^{\downarrow}$ 有一个简洁的概率解释: 当随机游走 $(S_n)_{n\geq 0}$ 从 $p\geq 0$ 出发，我们考虑它首次访问非正整数 $\mathbb{Z}_{\leq 0}$ 的时刻，则 $h^{\downarrow}(p)$ 就是该首次访问发生在 0 点的概率。在随机游走理论中，$h^{\downarrow}$ 被称为该随机游走的更新前函数。借助转移概率 (77)，我们可以将周长过程 $(P_i)_{i\geq 0}$ 解释为: 服从随机游走 $(S_n)_{n\geq 0}$ 在击中 0 点的 $\mathbb{Z}_{\leq 0}$ 处被杀死的条件分布，我们将其记为 $\left(S_n^{\downarrow}\right)_{n\geq 0}$。这种借助调和函数的条件化是马尔可夫链变换的一个实例，即著名的杜布 h 变换 [129]。

In fact, the relation between admissible weight sequences and probability measures on $\mathbb{Z}$ is bijective [125], in the sense that any random walk on $\mathbb{Z}$ that has $h^{\downarrow}$ as its pre-renewal function has increments with law $\upsilon_{\mathbf{q}}$ for some admissible weight sequence $\mathbf{q}$. This provides a different explanation for the universality observed in $\mathbf{q}$-Boltzmann maps and makes the measure $\upsilon_{\mathbf{q}}$ an economical alternative for $\mathbf{q}$ to specify a Boltzmann map model. (This could be made more explicit as follows [130]. The Tutte equation (11) is equivalent to $\upsilon_{\mathbf{q}}(-\ell-1)=\frac{1}{2}\sum_{p=-\infty}^{\infty}\upsilon_{\mathbf{q}}(p)\,\upsilon_{\mathbf{q}}(-p-k-1)$, which can be shown to imply that the law of the successive minima of $(S_i)_{i\geq 0}$ is universal, i.e., independent of $\mathbf{q}$. This in turn implies the universality of the probabilities $h^{\downarrow}(p)$ and thus of $W_{\bullet}^{(2\ell)}$.)

事实上，容许权重序列与 $\mathbb{Z}$ 上的概率测度是双射关系 [125]，也就是说，以 $h^{\downarrow}$ 为更新前函数的 $\mathbb{Z}$ 上任意随机游走，其增量分布对某个容许权重序列 $\mathbf{q}$ 而言即为 $\upsilon_{\mathbf{q}}$ 。这为 $\mathbf{q}$ -玻尔兹曼映射中观察到的普适性提供了另一种解释，并且对于指定玻尔兹曼映射模型，测度 $\upsilon_{\mathbf{q}}$ 是比 $\mathbf{q}$ 更简洁的替代方案。(文献 [130] 给出了更明确的阐释: 图特方程 (11) 等价于 $\upsilon_{\mathbf{q}}(-\ell-1)=\frac{1}{2}\sum_{p=-\infty}^{\infty}\upsilon_{\mathbf{q}}(p)\,\upsilon_{\mathbf{q}}(-p-k-1)$ ，由此可推出 $(S_i)_{i\geq 0}$ 逐次极小值的分布具有普适性，即与 $\mathbf{q}$ 无关。这反过来又推出概率 $h^{\downarrow}(p)$ 进而 $W_{\bullet}^{(2\ell)}$ 的普适性。)

Peeling Infinite Boltzmann Planar Maps

剥离无限玻尔兹曼平面地图

Note that (79) for $p=1$ is nothing but a disguised version of the admissibility criterion $g_{\mathbf{q}}(R)=1$ that we found in section "Admissibility and Criticality," because

注意，针对 $p=1$ 的式 (79) 不过是我们在“容许性与临界性”一节中得到的容许性判据 $g_{\mathbf{q}}(R)=1$ 的变形，因为

$$g_{\mathbf{q}}(R)-1\overset{(76)}{=}2R\left(h^{\downarrow}(1)-\sum_{k=-1}^{\infty}h^{\downarrow}(k+1)\,\upsilon_{\mathbf{q}}(k)\right). \tag{80}$$

How about the criticality of $\mathbf{q}$? We claim that $\mathbf{q}$ is critical if the random walk $(S_n)_{n\geq 0}$ has no drift and thus is subcritical when it has negative drift. (More accurate terminology for "no drift" is that the random walk oscillates, meaning that almost surely the range of the walk is unbounded above and below. In the case of finite first moments, this is equivalent to zero expectation value for the increments, $\sum_{k=-\infty}^{\infty}k\upsilon_{\mathbf{q}}(k)=0$. However, the latter criterion is not very useful here, because in the next section, we will see that for $\mathbf{q}$ subcritical $\upsilon_{\mathbf{q}}$ never has finite first moments.). To see this, we note that the criterion $g'_{\mathbf{q}}(R)=0$ for criticality from section "Admissibility and Criticality" translates into

那么 $\mathbf{q}$ 的临界性如何呢？我们认为 $\mathbf{q}$ 在随机游走 $(S_n)_{n\geq 0}$ 无漂移时是临界的，因此当随机游走有负漂移时 $\mathbf{q}$ 是次临界的。“无漂移”更准确的表述是随机游走振荡，即几乎必然游走的值域无上界也无下界。在一阶矩有限的情况下，这等价于增量的期望为零，即 $\sum_{k=-\infty}^{\infty}k\upsilon_{\mathbf{q}}(k)=0$ 。但这个判据在此处用处不大，因为在下一节中我们会看到，对于次临界的 $\mathbf{q}$ ，$\upsilon_{\mathbf{q}}$ 的一阶矩永远有限。) 要说明这一点，我们注意到“容许性与临界性”一节中给出的临界性判据 $g'_{\mathbf{q}}(R)=0$ 可转化为

$$0=g'_{\mathbf{q}}(R)=h^{\uparrow}(1)-\sum_{k=0}^{\infty}h^{\uparrow}(k+1)\,\upsilon_{\mathbf{q}}(k). \tag{81}$$

where we have introduced the renewal function (see [131, Ch. XII] or [50, App. A] for background on renewal theory of random walks)

其中我们引入了更新函数 (随机游走更新理论的背景知识参见 [131, 第十二章] 或 [50, 附录 A])

$$h^{\uparrow}(\ell) := \sum_{p=0}^{\ell-1} h^{\downarrow}(p) = 2\ell h^{\downarrow}(\ell). \tag{82}$$

Knowing that $h^{\downarrow}$ is harmonic on $\mathbb{Z}_{>0}$, the condition (81) and therefore criticality of $\mathbf{q}$ is seen to be equivalent to $h^{\uparrow}$ being harmonic on $\mathbb{Z}_{>0}$ as well, meaning that it satisfies the same equation (79) with $h^{\downarrow}$ replaced by $h^{\uparrow}$. But the renewal function of a random walk is harmonic if and only if it does not have negative drift [132]. Since we already know that it cannot have positive drift, this verifies our claim.

已知 $h^{\downarrow}$ 在 $\mathbb{Z}_{>0}$ 上是调和的，可知条件 (81)，也就是 $\mathbf{q}$ 的临界性，等价于 $h^{\uparrow}$ 也在 $\mathbb{Z}_{>0}$ 上调和，即它满足同一个方程 (79)，仅将 $h^{\downarrow}$ 替换为 $h^{\uparrow}$。而随机游走的更新函数调和当且仅当随机游走没有负漂移 [132]。结合我们已经已知它不可能有正漂移，这就验证了我们的结论。

Since $h^{\uparrow}$ is harmonic on the positive integers when $\mathbf{q}$ is critical, one may consider the $h^{\uparrow}$-transform of the random walk $(S_n)_{n\geq 0}$ resulting in the Markov chain $\left(S_i^{\uparrow}\right)_{i\geq 0}$ with transition probabilities

由于当 $\mathbf{q}$ 临界时，$h^{\uparrow}$ 在正整数集上是调和的，我们可以考虑随机游走 $(S_n)_{n\geq 0}$ 的 $h^{\uparrow}$ 变换，得到马尔可夫链 $\left(S_i^{\uparrow}\right)_{i\geq 0}$，其转移概率为

$$\mathbb{P}\left(S_{i+1}^{\uparrow} = p + k \mid S_i^{\uparrow} = p\right) = \frac{h^{\uparrow}(p+k)}{h^{\uparrow}(p)} \upsilon_{\mathbf{q}}(k). \tag{83}$$

Since $h^{\uparrow}(\ell) = 0$ for $\ell \leq 0$, the Markov chain $\left(S_n^{\uparrow}\right)_{n\geq 0}$ will never hit $\mathbb{Z}_{\leq 0}$ and can thus be interpreted as the random walk $(S_n)_{n\geq 0}$ conditioned to stay positive forever [132]. Perhaps not surprisingly, this is exactly the law of the perimeter process of the infinite q-Boltzmann planar map [125]. In other words, the targeted peeling explorations of a (critical) pointed q-Boltzmann map and the exploration of its local limit are related by conditioning the perimeter process of the former to stay positive, by the transformation

由于对应 $\ell \leq 0$ 的 $h^{\uparrow}(\ell) = 0$ 满足条件，马尔可夫链 $\left(S_n^{\uparrow}\right)_{n\geq 0}$ 永远不会到达 $\mathbb{Z}_{\leq 0}$，因此它可以被解释为始终保持为正的条件随机游走 $(S_n)_{n\geq 0}$ [132]。这恰好就是无限 q-玻尔兹曼平面地图周长过程的分布规律 [125]，或许并不出人意料。换言之，(临界) 带点 q-玻尔兹曼地图的目标剥离探测，与其局部极限的探测之间的关系，可通过将前者的周长过程条件化始终保持为正得到，变换关系为

$$\mathbb{P}_{\infty}^{(2\ell)}(P_{i+1} = m \mid P_i = p) = \frac{m}{p}\mathbb{P}_{\bullet}^{(2\ell)}(P_{i+1} = m \mid P_i = p). \tag{84}$$

Let's try to understand why this is the case and at the same time construct the q-IBPM as the limit of a Boltzmann planar map conditioned to have a large number n of vertices. From the definition in section "Local Limits," we deduce that a necessary condition for local convergence is that for every map $\mathfrak{e}$ with a single hole, we have the limit

我们来尝试理解为什么会这样，同时将 q-IBPM 构造为顶点数 n 很大的条件玻尔兹曼平面地图的极限。根据“局部极限”一节中的定义，我们可以推出，局部收敛的一个必要条件是: 对任意带有单洞的地图 $\mathfrak{e}$，极限存在

$$\lim_{n\to\infty} \mathbb{P}_{\bullet}^{(2\ell)}(\mathfrak{e} \subset \mathfrak{m} \,||\mathrm{V}(\mathfrak{m})| = n|) = \mathbb{P}_{\infty}^{(2\ell)}(\mathfrak{e} \subset \mathfrak{m}). \tag{85}$$

If $|\mathrm{V}(\mathfrak{e})| = k$ and the hole of $\mathfrak{e}$ has degree $2p$, then the probability on the left-hand side is given explicitly by

若 $|\mathrm{V}(\mathfrak{e})| = k$ 成立，且 $\mathfrak{e}$ 的洞的度数为 $2p$，则左侧概率可显式写为

$$\mathbb{P}_{\bullet}^{(2\ell)}(\mathfrak{e} \subset \mathfrak{m} \,||\, \mathrm{V}(\mathfrak{m})| = n) = w_{\mathbf{q}}(\mathfrak{e}) \frac{[t^{n-k}]\, W_{\bullet}^{(2p)}(t, \mathbf{q})}{[t^n]\, W_{\bullet}^{(2\ell)}(t, \mathbf{q})} \tag{86}$$

$$= w_{\mathbf{q}}(\mathfrak{e}) \frac{h^{\downarrow}(p)}{h^{\downarrow}(\ell)} 4^{p-\ell} \frac{[t^{n-k}]\, R(t, \mathbf{q})^p}{[t^n]\, R(t, \mathbf{q})^{\ell}}. \tag{87}$$

The asymptotics for $R(t, \mathbf{q})$ derived in section "Admissibility and Criticality" imply that the latter ratio approaches $\frac{p}{\ell} R^{p-\ell}$ as $n \to \infty$. Hence,(85) holds if and only if

在“可容许性与临界性”一节中推导得到的 $R(t, \mathbf{q})$ 渐近性质表明，当 $n \to \infty$ 时，后一比值趋近于 $\frac{p}{\ell} R^{p-\ell}$。因此，当且仅当以下条件成立时，式 (85) 成立

$$\mathbb{P}_{\infty}^{(2\ell)}(\mathfrak{e} \subset \mathfrak{m}) = w_{\mathbf{q}}(\mathfrak{e}) (4R)^{p-\ell} \frac{h^{\uparrow}(p)}{h^{\uparrow}(\ell)} = \frac{p}{\ell} \mathbb{P}_{\bullet}^{(2\ell)}(\mathfrak{e} \subset \mathfrak{m}). \tag{88}$$

Specializing to the targeted peeling exploration, this in turn implies that the perimeter processes satisfy (84).

专门针对目标剥离探索而言，这反过来又表明周长过程满足式 (84)。

In fact, these arguments give a convenient way of proving the local limit by an explicit construction of the $\mathbf{q}$ -IBPM. If we know the perimeter process $(P_i)_{i \geq 0}$, we can deduce from (71) the sequence of events $\mathrm{C}_k, \mathrm{G}_{\star,k}, \mathrm{G}_{k,\star}$, flipping a coin to choose between the latter two, and construct the q-IBPM by performing the peeling operations and filling in any holes with independent q-Boltzmann maps. The resulting infinite map is one-ended by construction and indeed satisfies (88) (see [50, Chapter VII] for details).

事实上，这些论证为通过显式构造 $\mathbf{q}$ -IBPM 证明局部极限提供了一种便捷方法。若我们已知周长过程 $(P_i)_{i \geq 0}$，就可以从式 (71) 推导出事件序列 $\mathrm{C}_k, \mathrm{G}_{\star,k}, \mathrm{G}_{k,\star}$，掷硬币在后两种情况中做选择，再通过执行剥离操作、用独立 q-Boltzmann 地图填充所有孔洞来构造 q-IBPM。通过构造得到的无限地图是单端的，且确实满足式 (88)(详见文献 [50，第七章])。

Scaling Limit of the Perimeter Process

周长过程的标度极限

Having related the perimeter process of the pointed and infinite Boltzmann planar maps to conditioned random walks, we are in a good position to discuss scaling limits. We first focus on the unconditioned random walk $(S_i)_{i \geq 0}$, because the conditioning of the walk via the h -transform should transfer to a similar conditioning of the continuous stochastic process in the limit. Contrary to the random walks we encountered in sections "Continuum Random Tree" and "Definition of the Brownian Sphere," the scaling limit will not be Brownian motion, because the probability measure $\upsilon_{\mathbf{q}}$ necessarily has infinite variance.

在将带点无限博尔茨曼平面地图的周长过程与条件随机游联系起来后，我们已经具备了很好的基础来讨论标度极限。我们首先聚焦于无条件随机游走 $(S_i)_{i\geq 0}$，因为通过 h 变换对游走施加的条件应当会在极限中转移到连续随机过程的类似条件上。和我们在“连续统随机树”与“布朗球面的定义”两节中遇到的随机游走不同，这里的标度极限不会是布朗运动，因为概率测度 $\upsilon_{\mathbf{q}}$ 必然具有无限方差。

To see this, we need a better handle on the disk function $W^{(2\ell)}$, because it enters the negative half of the probability measure $\upsilon_{\mathbf{q}}$. One way is to use (37) in combination with (28), which leads to the explicit expression

为了说明这一点，我们需要更好地处理圆盘函数 $W^{(2\ell)}$，因为它会进入概率测度 $\upsilon_{\mathbf{q}}$ 的负半部分。一种方法是将 (37) 与 (28) 结合使用，由此可以得到显式表达式

$$W^{(2\ell)} = \int_0^1 \mathrm{d}t W_\bullet^{(2\ell)}(t,\mathbf{q}) = \binom{2\ell}{\ell} \int_0^1 \mathrm{d}t R(t,\mathbf{q})^\ell = \binom{2\ell}{\ell} \int_0^R \mathrm{d}r g'_{\mathbf{q}}(r)\, r^\ell.$$

(89)

When $\mathbf{q}$ is subcritical, $g'_{\mathbf{q}}(R) > 0$, we read off that as $\ell \to \infty$ we have the asymptotics

当 $\mathbf{q}$ 处于次临界状态 $g'_{\mathbf{q}}(R) > 0$ 时，我们可以直接读出当 $\ell \to \infty$ 时的渐近行为

$$W^{(2\ell)} \sim \binom{2\ell}{\ell} g'_{\mathbf{q}}(R)\, \frac{R^{\ell+1}}{\ell+1} \sim \frac{\mathrm{p}_{\mathbf{q}}}{2} (4R)^{\ell+1} \ell^{-3/2},\ \mathrm{p}_{\mathbf{q}} = \frac{g'_{\mathbf{q}}(R)}{2\sqrt{\pi}}, \tag{90}$$

while in the generic critical $\left(a = \frac{5}{2}\right)$ and non-generic critical case $\left(\frac{3}{2} < a < \frac{5}{2}\right)$ with expansion $g_{\mathbf{q}}(r) = 1 - C(R-r)^{a-1/2} + o\left((R-r)^{a-\frac{1}{2}}\right)$, we deduce that

而在一般临界 $\left(a = \frac{5}{2}\right)$ 和带有展开式 $g_{\mathbf{q}}(r) = 1 - C(R-r)^{a-1/2} + o\left((R-r)^{a-\frac{1}{2}}\right)$ 的非一般临界情形 $\left(\frac{3}{2} < a < \frac{5}{2}\right)$ 下，我们可以推导出

$$W^{(2\ell)} \sim \binom{2\ell}{\ell} C R^{\ell+a-\frac{1}{2}} \ell^{\frac{1}{2}-a} \Gamma\left(a+\frac{1}{2}\right) \sim \frac{\mathrm{p}_{\mathbf{q}}}{2} (4R)^{\ell+1} \ell^{-a}, \mathrm{p}_{\mathbf{q}} = \frac{C\Gamma\left(a+\frac{1}{2}\right) R^{a-\frac{3}{2}}}{4\sqrt{\pi}}.$$

(91)

Hence, if we set $a = 3/2$ in the subcritical case, then we can summarize the negative tail behaviour as $\upsilon(-k) \sim \mathrm{p}_{\mathbf{q}} k^{-a}$. The positive tail can be shown [50, 53, 55, 125] to be negligible in the subcritical and generic critical case, while in the non-generic critical case, it is asymptotically smaller by a factor of $\cos a\pi$, as summarized in Table 1.

因此，如果我们在次临界情形下设置 $a = 3/2$，就可以将负尾行为总结为 $\upsilon(-k) \sim \mathrm{p}_{\mathbf{q}} k^{-a}$。可以证明 [50, 53, 55, 125]，在次临界和一般临界情形下正尾可以忽略，而在非一般临界情形下，正尾的渐近量级比负尾小 $\cos a\pi$ 倍，总结见表 1。

Based on the tails of the distribution, we should be looking at convergence of $(S_i)_{i\geq 0}$ to a Lévy stable process $(\mathrm{Y}(t))_{t\geq 0}$ with no drift or Brownian component but with Lévy measure

根据分布的尾部性质，我们应当研究 $(S_i)_{i\geq 0}$ 到 Lévy 稳定过程 $(\mathrm{Y}(t))_{t\geq 0}$ 的收敛性，该过程没有漂移项和布朗分量，但具有 Lévy 测度

$$\frac{\mathrm{d}x}{|x|^{a}}\mathbf{1}_{\{x<0\}}+\cos a\pi\frac{\mathrm{d}x}{|x|^{a}}\mathbf{1}_{\{x>0\}}, \tag{92}$$

which informally expresses the exponential rate at which the process performs jumps of size $x\in\mathbb{R}$. (See Fig. 18 for a simulations.) Like Brownian motion, its increments are independent and stationary (meaning that for any $s>0$, the increments $\mathrm{Y}(is)-\mathrm{Y}((i-1)s), i=1,2,\ldots$, are independent and identically distributed), but the sample paths are not continuous, and it satisfies a scaling relation with an exponent $a-1\neq 2$,

它非形式化地表示了过程发生幅度为 $x\in\mathbb{R}$ 的跳跃的指数速率。(模拟结果见图 18) 和布朗运动一样，它的增量是独立平稳的 (即对任意 $s>0$ ，增量 $\mathrm{Y}(is)-\mathrm{Y}((i-1)s), i=1,2,\ldots$ 独立同分布)，但样本轨道不连续，且满足指数为 $a-1\neq 2$ 的标度关系，

$$\left(\lambda^{-1}\mathrm{Y}\left(\lambda^{a-1}t\right)\right)_{t\geq 0}\overset{(\mathrm{d})}{=}(\mathrm{Y}(t))_{t\geq 0},\ \lambda>0. \tag{93}$$

According to the generalized central limit theorem [133], the sum S_n of n random integers with distribution $\upsilon_{\mathbf{q}}$ converges to the stable random variable

根据广义中心极限定理 [133]，服从分布 $\upsilon_{\mathbf{q}}$ 的 n 个随机整数的和 S_n 收敛到稳定随机变量

$$\frac{S_n}{n^{1/(a-1)}}\xrightarrow[n\to\infty]{(\mathrm{d})}\mathrm{Y}_a\left(\mathrm{p}_{\mathbf{q}}\right). \tag{94}$$

(Once the tails of $\upsilon_{\mathbf{q}}$ are known, the only nontrivial check to perform is that no centering of the sequence $n^{-1/(a-1)}S_n$ by an n -dependent shift is required for convergence. For $a\neq 2$ this is straightforward, while the case $a=2$ requires some care [134].). With an appropriate choice of topology on non-continuous sample paths (named after Skorokhod), this convergence extends to the full process [135],

(一旦知道 $\upsilon_{\mathbf{q}}$ 的尾部，唯一需要验证的非平凡结论是: 序列 $n^{-1/(a-1)}S_n$ 不需要通过依赖于 n 的平移进行中心化来实现收敛。对于 $a\neq 2$ 这很容易验证，而 $a=2$ 的情形则需要额外小心处理 [134]。) 在以 Skorokhod 命名的非连续样本轨道的合适拓扑下，这种收敛可以推广到整个过程 [135],

$$\left(\frac{S_{\lfloor \lambda t/p_{\mathbf{q}}\rfloor}}{\lambda^{1/(a-1)}}\right)_{t\geq 0}\xrightarrow[\lambda\to\infty]{(\mathrm{d})}(\mathrm{Y}(t))_{t\geq 0}. \tag{95}$$

Table 1 Scaling properties of the random walk $(S_i)_{i\geq 0}$ depending on type of weight sequence

表 1 随机游走 $(S_i)_{i\geq 0}$ 的标度性质，依权重序列的类型分类

Type	Subcritical	Generic critical	Non-generic critical $\left(\frac{3}{2} < a < \frac{5}{2}\right)$
Definition	$g'(R) > 0$	$g'(R) = 0$, $\lvert g''(R)\rvert < \infty$	$1 - g(r) \overset{r \to R}{\sim} C(R-r)^{a-\frac{1}{2}}$
Drift of $(S_n)_{n>0}$	Negative	No drift	No drift
$\upsilon_{\mathbf{q}}(-k)$	$k \to \infty \mathrm{p}_{\mathbf{q}} k^{-\frac{3}{2}}$	$k \to \infty \mathrm{p}_{\mathbf{q}} k^{-\frac{5}{2}}$	$k \to \infty \mathrm{p}_{\mathbf{q}} k^{-a}$
$\lim_{k\to\infty} \frac{\sum_{\ell=k}^{\infty} \upsilon_{\mathbf{q}}(\ell)}{\sum_{\ell=k}^{\infty} \upsilon_{\mathbf{q}}(-\ell)}$	0	0	$\cos a\pi$

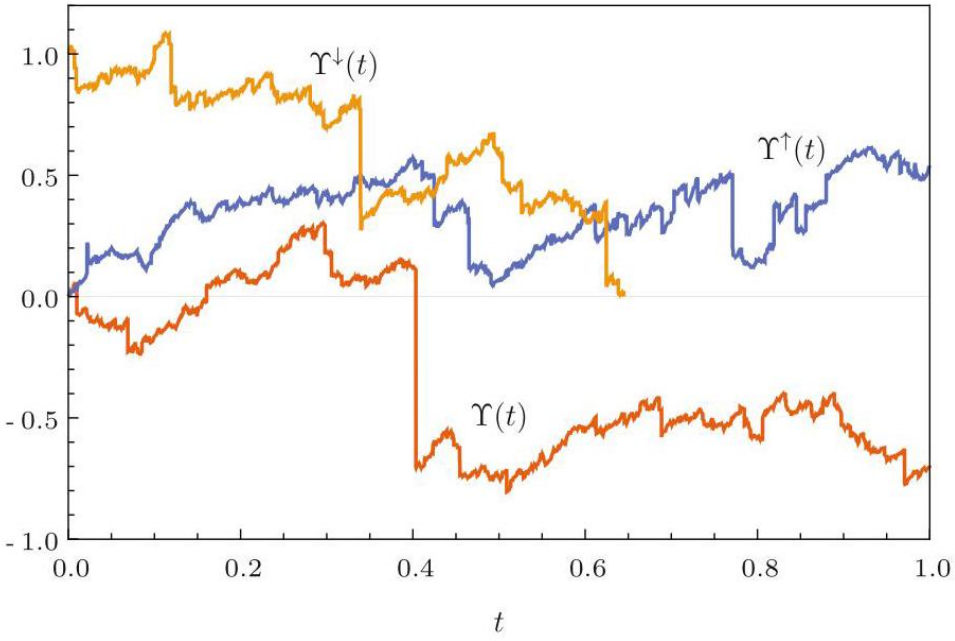

Fig. 18 Simulations of the self-similar processes $\mathrm{Y}(t), \mathrm{Y}^{\downarrow}(t)$, and $\mathrm{Y}^{\uparrow}(t)$ started at $\mathrm{Y}(0) = \mathrm{Y}^{\uparrow}(0) = 0$ and $\mathrm{Y}^{\downarrow}(0) = 1$ in the case $a = 2.4$. They correspond to a Lévy stable process with Lévy measure (92) and its counterparts that are conditioned to die continuously at 0, respectively, stay positive forever

图 18 自相似过程 $\mathrm{Y}(t), \mathrm{Y}^{\downarrow}(t)$ 与 $\mathrm{Y}^{\uparrow}(t)$ 在 $a = 2.4$ 情形下从 $\mathrm{Y}(0) = \mathrm{Y}^{\uparrow}(0) = 0$ 和 $\mathrm{Y}^{\downarrow}(0) = 1$ 出发的模拟。它们分别对应具有 Lévy 测度 (92) 的 Lévy 稳定过程，以及对应的被条件化后持续在 0 消亡、始终保持为正的过程

Due to an invariance principle of [136], one obtains a similar convergence of the random walk $\left(S_i^{\uparrow}\right)_{i\geq 0}$ conditioned to stay positive and therefore of the perimeter process $(P_i)_{i\geq 0}$ of the $\mathbf{q}$ -IBMP, which has the same law,

根据文献 [136] 的不变原理，我们可得条件化保持为正的随机游走 $\left(S_i^{\uparrow}\right)_{i\geq 0}$ 的类似收敛性，因此服从同一分布的 $\mathbf{q}$ -IBMP 的周长过程 $(P_i)_{i\geq 0}$ 也有类似收敛性，

$$\left(\frac{P_{\lfloor \lambda t/\mathrm{p}_{\mathrm{q}} \rfloor}}{\lambda^{1/(a-1)}}\right)_{t\geq 0} \xrightarrow[\lambda\to\infty]{\text{(d)}} \left(\mathrm{Y}^{\uparrow}(t)\right)_{t\geq 0}. \tag{96}$$

Here $\mathrm{Y}^{\uparrow}(t)$ is the stable process started at 0 and conditioned to stay positive for all $t > 0$. Note that in both convergences, the starting point, S_0, respectively P_0, is kept fixed.

此处 $\mathrm{Y}^{\uparrow}(t)$ 是从 0 出发、条件化对所有 $t>0$ 保持为正的稳定过程。注意在两种收敛中，起点 S_0 (对应 P_0) 都保持固定。

In the case of the conditioned random walk $\left(S_n^{\downarrow}\right)_{n\geq 0}$ started at $S_0=\ell$, one should instead consider the limit $\ell\to\infty$ and rescale time accordingly. So for the pointed $\mathbf{q}$ -Boltzmann planar map with perimeter 2ℓ we have, with the help of another invariance principle of [136], the convergence

在条件化随机游走 $\left(S_n^{\downarrow}\right)_{n\geq 0}$ 从 $S_0=\ell$ 出发的情形，我们应当转而考虑极限 $\ell\to\infty$ 并对时间做相应重缩放。因此对带有周长 2ℓ 的带点 $\mathbf{q}$ -Boltzmann 平面地图，借助文献 [136] 的另一不变原理，我们可得收敛性

$$\left(\frac{P_{\lfloor \ell^{a-1}t/\mathrm{p_q}\rfloor}}{\ell}\right)_{t\geq 0}\xrightarrow[\ell\to\infty]{\text{(d)}}\left(\mathrm{Y}^{\downarrow}(t)\right)_{t\geq 0}, \tag{97}$$

where $\mathrm{Y}^{\downarrow}(t)$ is the stable process $\mathrm{Y}(t)$ conditioned to die continuously at 0, meaning that it is killed at time $\tau=\inf\{t:\mathrm{Y}(t)\leq 0\}$ and conditioned to do so continuously, $\lim_{t\nearrow\tau}\mathrm{Y}(t)=0$. The processes $\mathrm{Y}^{\uparrow}(t)$ and $\mathrm{Y}^{\downarrow}(t)$ are examples of (positive) self-similar Markov processes (see, e.g., [137]), meaning that, even though the increments are no longer independent or stationary, they satisfy the same scaling relation (93), with the understanding that if the process $\mathrm{Y}^{\downarrow}$ on the left-hand side starts at $\mathrm{Y}^{\downarrow}(0)=x$ then the one on the right-hand side starts at $\mathrm{Y}^{\downarrow}(0)=x/\lambda$.

其中 $\mathrm{Y}^{\downarrow}(t)$ 是稳定过程 $\mathrm{Y}(t)$ 条件化后在 0 持续消亡的结果，也就是说它在时刻 $\tau=\inf\{t:\mathrm{Y}(t)\leq 0\}$ 被杀灭，且条件化要求该过程是连续发生的，即 $\lim_{t\nearrow\tau}\mathrm{Y}(t)=0$ 。过程 $\mathrm{Y}^{\uparrow}(t)$ 和 $\mathrm{Y}^{\downarrow}(t)$ 是 (正) 自相似马尔可夫过程的例子 (参见例如文献 [137])，这意味着即使增量不再独立或平稳，它们仍满足相同的标度关系 (93)，此处应当理解为: 若左侧过程 $\mathrm{Y}^{\downarrow}$ 从 $\mathrm{Y}^{\downarrow}(0)=x$ 出发，则右侧过程从 $\mathrm{Y}^{\downarrow}(0)=x/\lambda$ 出发。

A consequence of (97) is that in the large- ℓ limit it takes the targeted peeling exploration on the order of ℓ^{a-1} steps to find the target. This is much smaller than the total number of faces and vertices in the map, which is of order $\ell^{a-1/2}$. Indeed, it is straightforward to compute the expected number of vertices in a (unpointed) q-Boltzmann planar map with root face degree 2ℓ since it is given by the ratio of the pointed and unpointed disk function,

(97) 的一个推论是，在大 ℓ 极限下，目标剥皮探索找到目标大约需要 ℓ^{a-1} 步，远小于地图中总面数和顶点数——后者的量级为 $\ell^{a-1/2}$ 。事实上，计算根面度为 2ℓ 的 (无点)q-Boltzmann 平面地图的期望顶点数是很直接的，因为该期望由有点圆盘函数与无点圆盘函数的比值给出，

$$\mathbb{E}_{\mathbf{q}}\left[|\mathrm{V}(\mathfrak{m})|\right]=\frac{W_{\bullet}^{(2\ell)}}{W^{(2\ell)}}=\frac{h^{\downarrow}(\ell)}{4Rv_{\mathbf{q}}(-\ell-1)}\sim \mathrm{b}_{\mathbf{q}}\ell^{a-\frac{1}{2}},\quad \mathrm{b}_{\mathbf{q}}=\frac{1}{2R\mathrm{p}_{\mathbf{q}}\sqrt{\pi}}. \tag{98}$$

More precisely, based on singularity analysis of $W^{(2\ell)}$ in (89), one may verify that there exists a real random variable ξ of mean 1 such that [53]

更准确地说，基于 (89) 中 $W^{(2\ell)}$ 的奇点分析，可以验证存在一个均值为 1 的实随机变量 ξ ，使得文献 [53] 中得到:

$$\frac{|\mathrm{V}(\mathfrak{m})|}{\mathrm{b}_{\mathbf{q}}\ell^{a-\frac{1}{2}}} \underset{\ell\to\infty}{\to} \xi,\ \mathbb{E}\left[\xi e^{-\lambda\xi}\right] = \exp\left(-\left[\Gamma\left(a+\frac{1}{2}\right)\lambda\right]^{\frac{1}{a-1/2}}\right). \tag{99}$$

Letting $|\mathrm{V}(\overline{\mathrm{e}}_i)|$ be the number of explored vertices after i steps in the targeted peeling exploration, then $|\mathrm{V}(\overline{\mathrm{e}}_{i+1})| - |\mathrm{V}(\overline{\mathrm{e}}_i)|$ is nonzero only in the gluing event $\mathrm{G}_{\star,k}$ or $\mathrm{G}_{k,\star}$. In this case it is the number of vertices of an independent $\mathbf{q}$ -Boltzmann map with root face degree $2k$. It should therefore not come as a surprise that $|\mathrm{V}(\overline{\mathrm{e}}_i)|$ possesses a scaling limit that jumps whenever $S^{\uparrow}$ makes a negative jump [53, 138] ,

设 $|\mathrm{V}(\overline{\mathrm{e}}_i)|$ 为目标剥皮探索中经过 i 步后已探测顶点数，则 $|\mathrm{V}(\overline{\mathrm{e}}_{i+1})| - |\mathrm{V}(\overline{\mathrm{e}}_i)|$ 仅在粘合事件 $\mathrm{G}_{\star,k}$ 或 $\mathrm{G}_{k,\star}$ 中不为零。此时 $|\mathrm{V}(\overline{\mathrm{e}}_{i+1})| - |\mathrm{V}(\overline{\mathrm{e}}_i)|$ 是根面度为 $2k$ 的独立 $\mathbf{q}$ -玻尔兹曼映射的顶点数，因此 $|\mathrm{V}(\overline{\mathrm{e}}_i)|$ 具有尺度极限，且会在 $S^{\uparrow}$ 发生负跳 [53, 138] 时跳转，这一点不足为奇，

$$\left(\frac{P_{\lfloor \lambda t/\mathbf{p}_{\mathbf{q}}\rfloor}}{\lambda^{1/(a-1)}}, \frac{\left|\mathcal{V}\left(\overline{\mathbf{e}}_{\lfloor \lambda t/\mathbf{p}_{\mathbf{q}}\rfloor}\right)\right|}{\mathbf{b}_{\mathbf{q}}\lambda^{\frac{a-1/2}{a-1}}}\right) \xrightarrow[\ell\to\infty]{\text{(d)}} \left(\mathrm{Y}^{\uparrow}(t), \mathcal{V}(t)\right)_{t\geq 0}. \tag{100}$$

Here $\mathcal{V}(t)$ is the increasing stochastic process defined as follows. Since the jumps of $\mathrm{Y}^{\uparrow}$ are countable, we can list the times of negative jumps as $t_1, t_2, \ldots$ and denote their magnitudes by $\Delta_i = \lim_{\varepsilon\nearrow 0} \mathrm{Y}^{\uparrow}(t_i-\varepsilon) - \mathrm{Y}^{\uparrow}(t_i+\varepsilon)$. If $\xi_1, \xi_2, \ldots$ are independent random variables with the distribution of ξ then $\mathcal{V}(t)$ is given by

此处 $\mathcal{V}(t)$ 是按如下方式定义的增随机过程: 由于 $\mathrm{Y}^{\uparrow}$ 的负跳可数，我们可以将负跳时刻列为 $t_1, t_2, \ldots$ ，并用 $\Delta_i = \lim_{\varepsilon\nearrow 0} \mathrm{Y}^{\uparrow}(t_i-\varepsilon) - \mathrm{Y}^{\uparrow}(t_i+\varepsilon)$ 记它们的跳幅。若 $\xi_1, \xi_2, \ldots$ 是服从 ξ 分布的独立随机变量，则 $\mathcal{V}(t)$ 可表示为

$$\mathcal{V}(t) = \sum_{i=1}^{\infty} \xi_i \Delta_i^{a-\frac{1}{2}} \mathbf{1}_{\{t_i<t\}}. \tag{101}$$

Observe that $\left(\mathrm{Y}^{\uparrow}(t), \mathcal{V}(t)\right)_{t\geq 0}$ is exactly self-similar again, in the sense that

注意到 $\left(\mathrm{Y}^{\uparrow}(t), \mathcal{V}(t)\right)_{t\geq 0}$ 仍然是严格自相似的，其意义为

$$\left(\lambda^{-1}\mathrm{Y}^{\uparrow}\left(\lambda^{a-1}t\right), \lambda^{a-1/2}\mathcal{V}\left(\lambda^{a-1}t\right)\right)_{t\geq 0} \overset{\text{(d)}}{=} \left(\mathrm{Y}^{\uparrow}(t), \mathcal{V}(t)\right)_{t\geq 0}. \tag{102}$$

Geometry

几何性质

So far we have not specified a peeling algorithm $\mathcal{A}$, since the law of the perimeter process and the collection of Boltzmann maps that fill in the holes were independent of this choice. We may thus design the algorithm to suit whatever application we have in mind. To connect with the study or the distances discussed in previous sections, we will focus on explorations in infinite q-Boltzmann planar maps that correspond to balls of growing radius around the root. Contrary to the tree bijections that rely on the graph distance on the map, the peeling exploration is most naturally formulated in terms of distances on its dual.

到目前为止我们还没有指定具体的剥皮算法 $\mathcal{A}$，因为周长过程的规律以及填充孔洞的玻尔兹曼映射集合都和算法选择无关。因此我们可以根据具体应用需求设计算法。为了对接之前章节讨论的距离研究，我们将重点关注无限 q-玻尔兹曼平面映射中，对应根周围半径递增球的探索过程。和依赖映射图距离的树对合不同，剥皮探索最自然的表述是基于其对偶距离建立的。

To be precise, the dual graph distance $d^\dagger(f, f')$ between faces f and f' of a map $\mathfrak{m}$ is given by fewest number of hops between adjacent faces necessary to get from f to f'. We then let the dual ball of radius r in $\mathfrak{m}$ be the submap $\mathrm{Ball}_r^\dagger(\mathfrak{m}) \subset \mathfrak{m}$ given by keeping all faces of $\mathfrak{m}$ that are at dual graph distance at most r from the root face, but cutting open every edge shared by two faces at distance exactly r. In addition, we consider its hull $\overline{\mathrm{Ball}}_r^\dagger(\mathfrak{m}) \subset \mathfrak{m}$ to be the ball $\mathrm{Ball}_r^\dagger(\mathfrak{m}) \subset \mathfrak{m}$ with all finite holes filled in. (See Fig. 19 for some simulations of hulls $\overline{\mathrm{Ball}}_r^\dagger(\mathfrak{m})$ and Fig. 20 for an illustration.)

准确地说，地图 $\mathfrak{m}$ 的面 f 和 f' 之间的对偶图距离 $d^\dagger(f, f')$ 由从 f 到 f' 所需经过相邻面的最少跳数给出。然后，我们将 $\mathfrak{m}$ 中半径为 r 的对偶球定义为子图 $\mathrm{Ball}_r^\dagger(\mathfrak{m}) \subset \mathfrak{m}$，其通过保留 $\mathfrak{m}$ 中所有与根面的对偶图距离至多为 r 的面，并切断所有由两个距离恰好为 r 的面共享的边得到。此外，我们将其外壳 $\overline{\mathrm{Ball}}_r^\dagger(\mathfrak{m}) \subset \mathfrak{m}$ 视为填充了所有有限孔洞的球 $\mathrm{Ball}_r^\dagger(\mathfrak{m}) \subset \mathfrak{m}$。(有关外壳 $\overline{\mathrm{Ball}}_r^\dagger(\mathfrak{m})$ 的一些模拟请参见图 19，示例请参见图 20。)

The reason for these particular definitions is that we can choose the peeling algorithm $\mathcal{A}$ in such a way that all hulls $\overrightarrow{\mathrm{Ball}}_r^\dagger(\mathfrak{m}), r \geq 0$, occur in the targeted peeling exploration,

这些特定定义的原因在于，我们可以选择剥皮算法 $\mathcal{A}$，使得所有包壳 $\overrightarrow{\mathrm{Ball}}_r^\dagger(\mathfrak{m}), r \geq 0$ 都能出现在目标剥皮探索中，

$$\bar{\mathfrak{e}}_{\theta_r} = \overline{\mathrm{Ball}}_r^\dagger(\mathfrak{m}) \tag{103}$$

for some increasing sequence of indices $0 = \theta_0 < \theta_1 < \theta_2 < \cdots$.

对应某个递增的索引序列 $0 = \theta_0 < \theta_1 < \theta_2 < \cdots$。

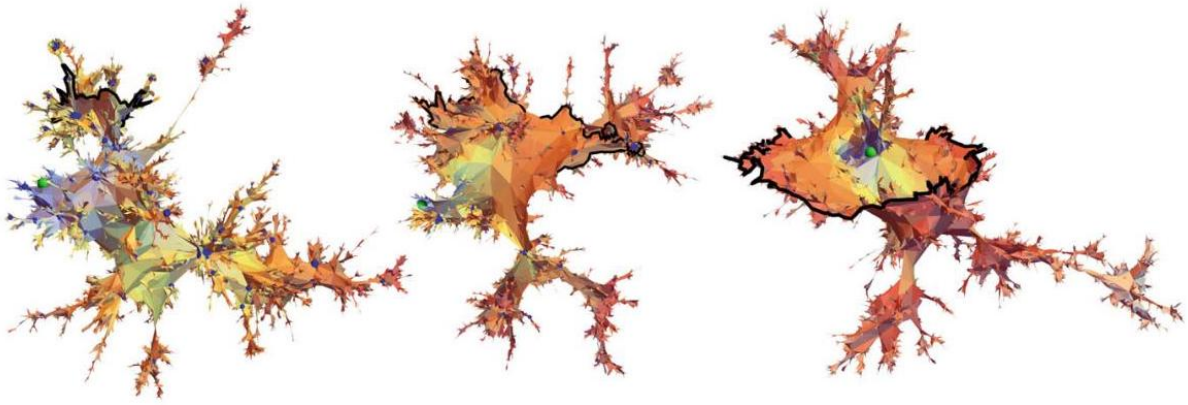

Fig. 19 Simulations of the hull $\overline{\mathrm{Ball}}_r^\dagger(\mathfrak{m})$ of radius $r \approx 20$ in infinite $\mathbf{q}$-Boltzmann maps of type $a = 2.1, 2.25, 2.5$ (left to right). The boundary of the hull (of length L_r) is drawn in black and the root as a green sphere. Blue spheres indicate faces of $\mathfrak{m}$ of high degree

图 19 无限 $\mathbf{q}$ -玻尔兹曼映射中类型为 $a = 2.1, 2.25, 2.5$ 、半径为 $r \approx 20$ 的包壳 $\overline{\mathrm{Ball}}_r^{\dagger}(\mathfrak{m})$ 模拟 (从左到右排列)。包壳的边界 (长度为 L_r) 用黑色绘制，根用绿色球体标注。蓝色球体表示 $\mathfrak{m}$ 中高度数的面

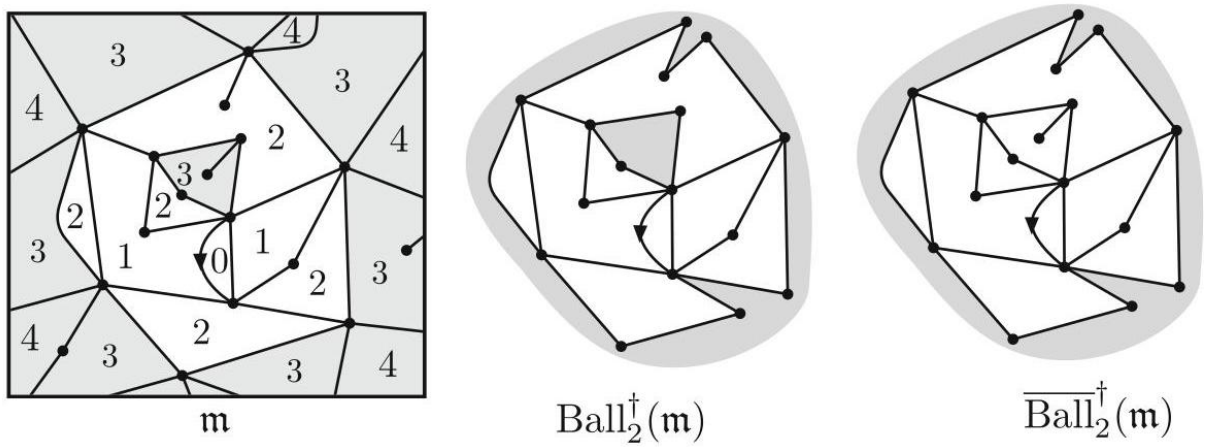

Fig. 20 A portion of an infinite map $\mathfrak{m}$ is shown with its faces labeled by dual graph distance to the root face (the face to the left of the root edge). The submaps corresponding to the dual ball of radius 2 and its hull are shown on the right

图 20 无限映射 $\mathfrak{m}$ 的一部分，各个面按其到根面 (根边左侧的面) 的对偶图距离标注。右侧给出了半径为 2 的对偶球及其包壳对应的子映射

This is achieved by taking $\mathcal{A}\left(\bar{\mathbf{e}}_i\right)$ to return an active edge of minimal height [53], where we define the height of an active edge e to be the dual graph distance between the root face and the face of $\bar{e}_i$ that is adjacent to e . We denote this minimal height by H_i . One may verify inductively that at any time in such an exploration all active edges in $\bar{e}_i$ are adjacent to a face at distance H_i or $H_i + 1$ and that (103) holds for

只需令 $\mathcal{A}\left(\bar{\mathbf{e}}_i\right)$ 返回最小高度的活跃边即可实现这一点 [53]，其中我们将活跃边 e 的高度定义为根面与相邻于 e 的 $\bar{e}_i$ 中那个面之间的对偶图距离。我们将这个最小高度记为 H_i 。可以通过归纳验证，在这类探索的任意时刻，$\bar{e}_i$ 中所有活跃边都相邻于距离为 H_i 或 $H_i + 1$ 的面，且 (103) 式对成立

$$\theta_r = \inf\{i : H_i \geq r\} \tag{104}$$

To specify $\mathcal{A}$ more precisely, one could choose to explore layer by layer in a clockwise fashion, meaning that one takes $\mathcal{A}\left(\bar{\mathbf{e}}_i\right)$ to be the active edge at height H_i that sits just to the right of one at height $H_i + 1$ (if it exists). This ensures that the active edges at height H_i always make up a connected portion of the boundary.

为了更精确地指定 $\mathcal{A}$ ，可以选择按顺时针方向逐层探索，也就是说将 $\mathcal{A}\left(\bar{\mathbf{e}}_i\right)$ 取为高度 H_i 处、恰好位于高度 $H_i + 1$ 处那条边右侧的活动边 (若该边存在)。这能保证高度 H_i 处的活动边始终构成边界的一个连通部分。

We can now apply the scaling limit results of section "Scaling Limit of the Perimeter Process" to analyze the growth of the boundary length and volume of the geodesic ball around the root of increasing radius (as illustated in Fig. 13). To be precise, we set L_r to be half of the degree of the hole of the dual ball hull $\overline{\mathrm{Ball}}_r^{\dagger}(\mathfrak{m})$

and V_r its number of vertices. By our previous considerations, L_r and V_r are related to the perimeter process $(P_i)_{i\geq 0}$ via

我们现在可以运用“周长过程的标度极限”一节的标度极限结论，分析半径递增的根周围测地球的边界长度和体积增长 (如图 13 所示)。准确来说，我们令 L_r 为对偶球包 $\overline{\mathrm{Ball}}_r^{\dagger}(\mathfrak{m})$ 的孔洞度数的一半，令 V_r 为其顶点数。根据我们之前的讨论，L_r 和 V_r 通过以下关系与周长过程 $(P_i)_{i\geq 0}$ 关联

$$L_r = P_{\theta_r},\ V_r = \left|\mathrm{V}\left(\bar{\mathfrak{e}}_{\theta_r}\right)\right|, \tag{105}$$

so we need to get a handle on θ_r , in particular on the number of peeling steps $\Delta\theta_r = \theta_{r+1} - \theta_r$ required to explore all faces at dual graph distance $r+1$.

因此我们需要掌握 θ_r 的性质，尤其是探索完对偶图距离为 $r+1$ 的所有面所需的剥皮步数 $\Delta\theta_r = \theta_{r+1} - \theta_r$ 。

At time θ_r there are precisely $2p = 2P_{\theta_r}$ active edges at height r , so our first guess would be that $\Delta\theta_r \approx 2p$. This would be the exact answer if each of the peeling steps would uncover a new face (event C_k), necessarily at dual graph distance $r+1$. However, this is accelerated by gluing events $\mathrm{G}_{\star,k}$ that will typically swallow k additional active edges at height r . The probability of $\mathrm{G}_{\star,k}$ in the large- p limit is $\frac{1}{2}\upsilon_{\mathbf{q}}(-k-1) \sim \mathrm{p}_{\mathbf{q}} k^{-a}$, so whether this acceleration changes the scaling depends on the type a [53, 134] . If $a > 2$ then each step swallows on average a finite number of edges, so $\Delta\theta_r$ is still proportional to the perimeter $2p$; if $a \leq 2$ then edges are swallowed fast enough that the scaling changes and $\Delta\theta_r$ becomes of the order $p/\log p$ for $a = 2$ and p^{a-1} for $a < 2$. In terms of the height H_n after n steps, this translates into the approximate growth

在时刻 θ_r ，高度 r 处恰好有 $2p = 2P_{\theta_r}$ 条活动边，因此我们首先猜测 $\Delta\theta_r \approx 2p$ 。如果每一步剥皮都能揭示一个新面 (事件 C_k)，且这个新面必然位于对偶图距离 $r+1$ 处，那么上述猜测就是准确答案。但粘合事件 $\mathrm{G}_{\star,k}$ 会加快这个过程，这类事件通常会吞噬高度 r 处额外的 k 条活动边。在大 p 极限下，$\mathrm{G}_{\star,k}$ 发生的概率为 $\frac{1}{2}\upsilon_{\mathbf{q}}(-k-1) \sim \mathrm{p}_{\mathbf{q}} k^{-a}$ ，因此这种加速是否会改变标度取决于类型 a [53, 134] 。若满足 $a > 2$ ，则每一步平均吞噬有限条边，因此 $\Delta\theta_r$ 仍与周长 $2p$ 成正比；若满足 $a \leq 2$ ，则边被吞噬的速度足够快，标度会发生改变，$\Delta\theta_r$ 的阶对 $a = 2$ 为 $p/\log p$ ，对 $a < 2$ 为 p^{a-1} 。对应 n 步后的高度 H_n ，这可以转化为近似增长关系

$$H_n \approx \begin{cases} \sum_{i=1}^{n} \frac{1}{P_i} \approx n^{\frac{a-2}{a-1}} & \text{for } a \in \left(2, \frac{5}{2}\right], \\ \sum_{i=1}^{n} \frac{\log P_i}{P_i} \approx \log^2 n & \text{for } a = 2, \\ \sum_{i=1}^{n} P_i^{1-a} \approx \log n & \text{for } a \in \left(\frac{3}{2}, 2\right), \end{cases} \tag{106}$$

where we used that $P_n \approx n^{\frac{1}{a-1}}$ as $n \to \infty$.

其中我们利用了当 $n \to \infty$ 时 $P_n \approx n^{\frac{1}{a-1}}$ 成立。

For $a \leq 2$ we conclude that θ_r grows faster than any power law in r , and the same therefore holds for L_r and V_r . In fact, one may show [53, 134] rigorously that as $r \to \infty$ we have the convergence in probability

对于 $a \leq 2$，我们推导出 θ_r 的增长速度快于 r 中的任意幂律，因此 L_r 和 V_r 也满足同样的结论。事实上，我们可以严格证明 [53, 134]，当 $r \to \infty$ 时，依概率收敛成立

$$\log L_r \sim \pi\sqrt{2r},\ \log V_r \sim \pi\frac{3\pi}{\sqrt{2}}\sqrt{r} \ \text{ for } a = 2 \tag{107}$$

$$\log L_r \sim cr,\ \log V_r \sim \left(a - \frac{1}{2}\right)cr \ \text{ for } a \in \left(\frac{3}{2}, 2\right). \tag{108}$$

This implies that the random metric spaces obtained from the dual graph distance on the vertex set of (pointed or infinite) $\mathbf{q}$ -Boltzmann maps that are non-generic critical of type $a \leq 2$ do not possess scaling limits. Informally, one could say that they correspond to a pathological situation of infinite Hausdorff dimension.

这意味着，由 (带点或无穷) $\mathbf{q}$ -玻尔兹曼映射顶点集上的对偶图距离得到的随机度量空间，若属于类型 $a \leq 2$ 的非一般临界，不存在标度极限。通俗来说，它们对应于无穷豪斯多夫维数的极端情形。

In the generic critical case $a = \frac{5}{2}$ or the non-generic critical case $a \in \left(2, \frac{5}{2}\right)$, we see that $\theta_r \approx n^{\frac{a-1}{a-2}}$ and therefore $L_r = P_{\theta_r} \approx r^{\frac{1}{a-2}}$. The estimate (106) can be justified and turned into a scaling limit jointly with that of the perimeter process [53]: there exists a $c > 0$ such that

在一般临界情形 $a = \frac{5}{2}$ 或非一般临界情形 $a \in \left(2, \frac{5}{2}\right)$ 中，我们可知 $\theta_r \approx n^{\frac{a-1}{a-2}}$，因此有 $L_r = P_{\theta_r} \approx r^{\frac{1}{a-2}}$。估计式 (106) 可被严格证明，并可与周长过程的标度极限一起得到 [53]: 存在 $c > 0$ 使得

$$\left(c\lambda^{\frac{a-1}{a-2}} H_{\lfloor \lambda t \rfloor}\right)_{t \geq 0} \xrightarrow[\lambda \to \infty]{\text{(d)}} \left(\int_0^t \frac{\mathrm{d}u}{\mathrm{Y}^{\uparrow}(u)}\right)_{t \geq 0}, \tag{109}$$

and the right-hand side can be shown to be finite almost surely. Combining with (100) and (105), this implies that L_r and V_r scale toward a reparametrized version of the Markov process $\left(\mathrm{Y}^{\uparrow}(t), \mathcal{V}(t)\right)$,

且可证其右端几乎处处有限。结合 (100) 与 (105)，可得 L_r 和 V_r 经重参数化后标度收敛于马尔可夫过程 $\left(\mathrm{Y}^{\uparrow}(t), \mathcal{V}(t)\right)$,

$$\left(\frac{L_{\lfloor \lambda x/(cp_{\mathbf{q}}) \rfloor}}{\lambda^{\frac{1}{a-2}}}, \frac{V_{\lfloor \lambda x/(cp_{\mathbf{q}}) \rfloor}}{b_{\mathbf{q}}\lambda^{\frac{a-1/2}{a-2}}}\right)_{x \geq 0} \xrightarrow[\lambda \to \infty]{(d)} \left(\mathrm{Y}^{\uparrow}(\vartheta(x)), \mathcal{V}(\vartheta(x))\right)_{x \geq 0}, \tag{110}$$

$$\vartheta(x) := \inf\left\{t : \int_0^t \frac{\mathrm{d}u}{\mathrm{Y}^{\uparrow}(u)} \geq x\right\}. \tag{111}$$

Although the limit may not feel like a very tangible stochastic process, it is universal in the sense that its distribution only depends on the type a. In the generic case $a = \frac{5}{2}$, it corresponds to the boundary length and area of hulls of geodesic radius x in the Brownian plane [139], and explicit formulae for the distribution of $\mathrm{Y}^{\uparrow}(\vartheta(x))$ and $\mathcal{V}(\vartheta_x)$ can be derived using various approaches [138-141].

尽管该极限可能并非一个非常直观的随机过程，但它具有普适性，其分布仅依赖于类型 a。在一般情形 $a = \frac{5}{2}$ 中，它对应布朗平面 [139] 中测地半径为 x 的包的边界长度与面积，且可通过多种方法推导得到 $\mathrm{Y}^{\uparrow}(\vartheta(x))$ 和 $\mathcal{V}(\vartheta_x)$ 分布的显式公式 [138-141]。

In general, it follows from the self-similarity relation

一般而言，由自相似关系可得

$$\left(\lambda^{-\frac{1}{a-2}}\mathrm{Y}^{\uparrow}\left(\vartheta\left(\lambda x\right),\lambda^{-\frac{a-1/2}{a-2}}\mathcal{V}\left(\vartheta\left(\lambda x\right)\right)\right)\right)_{x\geq 0}\overset{(\mathrm{d})}{=}\left(\mathrm{Y}^{\uparrow}\left(\vartheta\left(x\right)\right),\mathcal{V}\left(\vartheta\left(x\right)\right)\right)_{x\geq 0}, \tag{112}$$

that a potential scaling limit in the Gromov-Hausdorff sense must have a Hausdorff dimension

Gromov-Hausdorff 意义下潜在的标度极限的豪斯多夫维数必为

$$d_{\mathrm{H}}=\frac{a-\frac{1}{2}}{a-2} \tag{113}$$

In the generic critical case $a=5/2$, this reproduces the Hausdorff dimension $d_{\mathrm{H}}=4$ from the construction of the Brownian sphere in section "Definition of the Brownian Sphere." For $a\in\left(2,\frac{5}{2}\right)$, it is conjectured that the scaling limits correspond to a new family of universality classes of random metrics on the 2-sphere, tentatively referred to as the stable spheres, but a full construction of these random metrics is still out of reach [53, 126].

在一般临界情形 $a=5/2$ 下，这与“布朗球面的定义”一节中构造布朗球面得到的豪斯多夫维数 $d_{\mathrm{H}}=4$ 一致。对于 $a\in\left(2,\frac{5}{2}\right)$，目前猜想其标度极限对应二维球面上随机度量的一族新普适类，暂称为稳定球面，但这类随机度量的完整构造仍未解决 [53, 126]。

These metric spaces are quite different from the ones obtained by examining the normal graph distance in non-generic critical maps of type $a\in\left(\frac{3}{2},\frac{5}{2}\right)$. Gromov-Hausdorff limits (at least along subsequences) of the latter have been obtained in [52] and are referred to as stable maps. They have Hausdorff dimension $d_{\mathrm{H}}=2a-1$ and do not have the topology of the 2-sphere but contain macroscopic holes (arising from faces of macroscopic degree in the limit).

这些度量空间与通过检验 $a\in\left(\frac{3}{2},\frac{5}{2}\right)$ 类非一般临界映射中的常规图距离得到的度量空间完全不同。后者的格罗莫夫-豪斯多夫极限 (至少沿子序列) 已在文献 [52] 中得到，被称为稳定映射。它们的豪斯多夫维数为 $d_{\mathrm{H}}=2a-1$ ，不具备二维球面拓扑，且包含宏观孔洞 (由极限中宏观度的面产生)。

Cross-References

交叉引用

From Trees to Gravity

从树到引力

The Causality Road from Dynamical Triangulations to Quantum Gravity That Describes Our Universe

从动力学三角剖分到描述我们宇宙的量子引力的因果之路

Acknowledgments This work is supported by the START-UP 2018 program with project number 740.018.017 and the VIDI program with project number VI.Vidi.193.048, which are financed by the Dutch Research Council (NWO).

致谢本工作得到 2018 年 START-UP 项目 (项目编号 740.018.017) 与 VIDI 项目 (项目编号 VI.Vidi.193.048) 的支持，两个项目均由荷兰研究理事会 (NWO) 资助。

References

参考文献

1. G. Gibbons, S. Hawking, Action integrals and partition functions in quantum gravity. Phys. Rev. D 15(10), 2752-2756 (1977)

2. G.W. Gibbons, S.W. Hawking, Euclidean Quantum Gravity (World Scientific, Singapore, 1993)

3. G. Gibbons, S. Hawking, M. Perry, Path integrals and the indefiniteness of the gravitational action. Nucl. Phys. B 138(1), 141-150 (1978)

4. P.O. Mazur, E. Mottola, The path integral measure, conformal factor problem and stability of the ground state of quantum gravity. Nucl. Phys. B 341(1), 187-212 (1990)

5. M. Reuter, Nonperturbative evolution equation for quantum gravity. Phys. Rev. D 57(2), 971 (1998)

6. D. Dou, R. Percacci, The running gravitational couplings. Class. Quant. Grav. 15(11), 3449 (1998)

7. M. Reuter, F. Saueressig, Renormalization group flow of quantum gravity in the Einstein-Hilbert truncation. Phys. Rev. D 65, 065016 (2002)

8. M. Reuter, F. Saueressig, Quantum Gravity and The Functional Renormalization Group: The Road Towards Asymptotic Safety (Cambridge University Press, Cambridge, 2019)

9. S. Weinberg, Ultraviolet divergences in quantum theories of gravitation. In: SW. Hawking, W. Israel, (eds.) General Relativity: An Einstein Centenary Survey, pp. 790-831 (Cambridge University Press, Cambridge, 1979)

10. D. Boulatov, A. Krzywicki, On the phase diagram of three-dimensional simplicial quantum gravity. Mod. Phys. Lett. A 6(32), 3005-3014 (1991)

11. J. Ambjørn, J. Jurkiewicz, Four-dimensional simplicial quantum gravity. Phys. Lett. B 278(1), 42-50 (1992)

12. J. Ambjørn, D. Boulatov, A. Krzywicki, S. Varsted, The vacuum in three-dimensional simplicial quantum gravity. Phys. Lett. B 276(4), 432-436 (1992)

13. M. Agishtein, A.A. Migdal, Three-dimensional quantum gravity as dynamical triangulation. Mod. Phys. Lett. A 6(20), 1863-1884 (1991)

14. J. Ambjørn, A. Görlich, J. Jurkiewicz, R. Loll, Nonperturbative quantum gravity. Phys. Rep. 519(4), 127-210 (2012).

15. R. Loll, Quantum gravity from causal dynamical triangulations: a review. Class. Quant. Grav. 37(1), 013002 (2019)

16. F. David, Planar diagrams, two-dimensional lattice gravity and surface models. Nucl. Phys. B 257, 45-58 (1985)

17. J. Ambjørn, B. Durhuus, J. Fröhlich, Diseases of triangulated random surface models, and possible cures. Nucl. Phys. B 257, 433-449 (1985)

18. V.A. Kazakov, I. Kostov, A. Migdal, Critical properties of randomly triangulated planar random surfaces. Phys. Lett. B 157(4), 295-300 (1985)

19. J. Ambjørn, J. Jurkiewicz, Y. Makeenko, Multiloop correlators for two-dimensional quantum gravity. Phys. Lett. B 251(4), 517-524 (1990)

20. J. Ambjørn, B. Durhuus, T. Jonsson, Quantum Geometry: A Statistical Field Theory Approach. Cambridge Monographs on Mathematical Physics (Cambridge University Press, Cambridge, 1997)

21. G. 't Hooft, A Planar Diagram Theory for Strong Interactions, in The Large N Expansion In Quantum Field Theory And Statistical Physics: From Spin Systems to 2-Dimensional Gravity (World Scientific, Singapore, 1993), pp. 80-92

22. E. Brézin, C. Itzykson, G. Parisi, J.-B. Zuber, Planar diagrams. Commun. Math. Phys. 59(1), 35-51 (1978)

23. P. Di Francesco, P. Ginsparg, J. Zinn-Justin, 2d gravity and random matrices. Phys. Rep. 254(1-2), 1-133 (1995)

24. A.M. Polyakov, Quantum geometry of bosonic strings. Phys. Lett. B 103(3), 207-210 (1981)

25. V. Knizhnik, A. Polyakov, A. Zamolodchikov, Fractal structure of 2d-quantum gravity. Mod. Phys. Lett. A 03(08), 819-826 (1988)

26. E. David, Conformal field theories coupled to 2-d gravity in the conformal gauge. Mod. Phys. Lett. A 3(17), 1651-1656 (1988)

27. J. Distler, H. Kawai, Conformal field theory and 2D quantum gravity. Nucl. Phys. B 321(2), 509-527 (1989)

28. P. Di Francesco, C. Itzykson, A generating function for fatgraphs. Ann. Inst. H. Poincaré Phys. Théor. 59(2), 117-139 (1993)

29. V.A. Kazakov, M. Staudacher, T. Wynter, Character expansion methods for matrix models of dually weighted graphs. Comm. Math. Phys. 177(2), 451-468 (1996)

30. V.A. Kazakov, M. Staudacher, T. Wynter, Exact solution of discrete two-dimensional R^2 gravity. Nucl. Phys. B 471(1), 309-333 (1996)

31. V. Kazakov, F. Levkovich-Maslyuk, Disc partition function of 2 dR^2 gravity from DWG matrix model. J. High Energy Phys. 2022(1), 1-41 (2022)

32. W.T. Tutte, A census of planar triangulations. Can. J. Math. 14, 21-38 (1962)

33. W.T. Tutte, A census of planar maps. Can. J. Math. 15, 249-271 (1963)

34. W.T. Tutte, On the enumeration of planar maps. Bull. Am. Math. Soc. 74, 64-74 (1968)

35. B. Eynard, Counting Surfaces, in Progress in Mathematical Physics, vol. 70 (Birkhäuser/Springer, Basel, Switzerland, 2016). CRM Aisenstadt chair lectures

36. J. Ambjorn, Elementary Introduction to Quantum Geometry, 1st edn. (CRC Press, Milton Park, Abingdon, Oxfordshire, 2022)

37. W.G. Brown, On the existence of square roots in certain rings of power series. Math. Ann. 158, 82-89 (1965)

38. B. Eynard, Topological expansion for the 1-hermitian matrix model correlation functions. J. High Energy Phys. 2004(11), 031 (2005)

39. B. Eynard, N. Orantin, Invariants of algebraic curves and topological expansion. Commun. Number Theory Phys. 1(2), 347-452 (2007)

40. J. Ambjørn, Y.M. Makeenko, Properties of loop equations for the hermitian matrix model and for two-dimensional quantum gravity. Mod. Phys. Lett. A 5(22), 1753-1763 (1990)

41. P. Flajolet, R. Sedgewick, Analytic Combinatorics (cambridge University press, Cambridge, 2009)

42. R. Cori, B. Vauquelin, Planar maps are well labeled trees. Can. J. Math. 33(5), 1023-1042 (1981)

43. G. Schaeffer, Bijective census and random generation of Eulerian planar maps with prescribed vertex degrees. Electron. J. Combin. 4(1), 14 (1997). Research Paper 20

44. G. Schaeffer, Conjugaison d'arbres et cartes combinatoires aléatoires, Ph.D. thesis, Université de Bordeaux, 1998

45. J. Bouttier, P. Di Francesco, E. Guitter, Planar maps as labeled mobiles. Electron. J. Combin. 11(1), 27 (2004). Research Paper 69, (electronic)

46. D. Poulalhon, G. Schaeffer, Optimal coding and sampling of triangulations. Algorithmica 46(3-4), 505-527 (2006)

47. O. Bernardi, E. Fusy, Unified bijections for maps with prescribed degrees and girth. J. Combin. Theory Ser. A 119(6), 1351-1387 (2012)

48. J.-F. Le Gall, The topological structure of scaling limits of large planar maps. Invent. Math. 169(3), 621-670 (2007)

49. O. Bernardi, N. Curien, G. Miermont, A Boltzmann approach to percolation on random triangulations. Can. J. Math. 71(1), 1-43 (2019)

50. N. Curien, Peeling random planar maps. Saint-Flour course (2019). https://www.imo.universite-paris-saclay.fr/~curien/enseignement.html

51. J.-F. Marckert, G. Miermont, Invariance principles for random bipartite planar maps. Ann. Prob. 35(5), 1642-1705 (2007)

52. J.-F. Le Gall, G. Miermont, Scaling limits of random planar maps with large faces. Ann. Prob. 39(1), 1-69 (2011)

53. T. Budd, N. Curien, Geometry of infinite planar maps with high degrees. Electron. J. Probab. 22, 37 (2017). Paper No. 35

54. J. Ambjørn, T. Budd, Y. Makeenko, Generalized multicritical one-matrix models. Nucl. Phys. B 913, 357-380 (2016)

55. G. Borot, J. Bouttier, E. Guitter, A recursive approach to the $O(n)$ model on random maps via nested loops. J. Phys. A 45(4), 04500238 (2012)

56. J. Ambjørn, T.G. Budd, Multi-point functions of weighted cubic maps. Ann. Inst. Henri Poincaré Comb. Phys. Interact. 3(1), 1-44 (2016)

57. J. Bouttier, P. Di Francesco, E. Guitter, Geodesic distance in planar graphs. Nucl. Phys. B 663(3), 535-567 (2003)

58. J. Ambjorn, Y. Watabiki, Scaling in quantum gravity. Nucl. Phys. B 445(1), 129-142 (1995)

59. A. Carrance, Convergence of Eulerian triangulations. Electron. J. Probab. 26, 48 (2021). Paper No. 18

60. D. Burago, Y. Burago, S. Ivanov, A Course in Metric Geometry, in Graduate Studies in Mathematics, vol. 33 (American Mathematical Society, Providence, RI, 2001)

61. J.-F. Le Gall, Uniqueness and universality of the Brownian map. Ann. Probab. 41(4), 2880- 2960 (2013)

62. G. Miermont, The Brownian map is the scaling limit of uniform random plane quadrangula-tions. Acta Math. 210(2), 319-401 (2013)

63. C. Marzouk, Scaling limits of random bipartite planar maps with a prescribed degree sequence. Random Struct. Algorithms 53(3), 448-503 (2018)

64. J. Bettinelli, E. Jacob, G. Miermont, The scaling limit of uniform random plane maps, via the Ambjørn-Budd bijection. Electron. J. Probab. 19(74), 16 (2014)

65. L. Addario-Berry, M. Albenque, The scaling limit of random simple triangulations and random simple quadrangulations. Ann. Probab. 45(5), 2767-2825 (2017)

66. L. Addario-Berry, M. Albenque, Convergence of non-bipartite maps via symmetrization of labeled trees. Ann. H. Lebesgue 4, 653-683 (2021)

67. M. Albenque, É. Fusy, T. Lehéricy, Random cubic planar graphs converge to the brownian sphere. arXiv preprint arXiv:2203.17245

68. N. Curien, J.-F. Le Gall, First-passage percolation and local modifications of distances in random triangulations. Ann. Sci. Éc. Norm. Sup. 52(3), 631-701 (2019)

69. D. Aldous, The continuum random tree. I. Ann. Prob. 19(1), 1-28 (1991)

70. D. Revuz, M. Yor, Continuous Martingales and Brownian Motion, in Grundlehren der math-ematischen Wissenschaften [Fundamental Principles of Mathematical Sciences], vol. 293 (Springer, Berlin, 1991)

71. J.-F. Le Gall, Random trees and applications. Prob. Surv. 2, (2005)

72. P.-G. De Gennes, Scaling Concepts in Polymer Physics, (Cornell university press, Ithaca, 1979)

73. M. Cates, The fractal dimension and connectivity of random surfaces. Phys. Lett. B 161(4-6), 363-367 (1985)

74. J. Ambjørn, B. Durhuus, J. Fröhlich, P. Orland, The appearance of critical dimensions in regulated string theories. Nucl. Phys. B 270, 457-482 (1986)

75. J.-F. Le Gall, Spatial Branching Processes, Random Snakes and Partial Differential Equations. Lectures in Mathematics ETH Zürich. (Birkhäuser, Basel, 1999)

76. J.-F. Marckert, A. Mokkadem, Limit of normalized quadrangulations: the Brownian map. Ann. Prob. 34(6), 2144-2202 (2006)

77. J.-F. Le Gall, F. Paulin, Scaling limits of bipartite planar maps are homeomorphic to the 2- sphere. Geom. Funct. Anal. 18(3), 893-918 (2008)

78. J.-F. Le Gall, Brownian disks and the Brownian snake. Ann. Inst. Henri Poincaré Probab. Stat. 55(1), 237-313 (2019)

79. C. Marzouk, On scaling limits of random trees and maps with a prescribed degree sequence. Ann. H. Lebesgue 5, 317-386 (2022)

80. J.-F. Le Gall, The volume measure of the Brownian sphere is a Hausdorff measure. Electron. J. Prob. 27, 28 (2022). Paper No. 113

81. J. Bouttier, E. Guitter, Confluence of geodesic paths and separating loops in large planar quadrangulations. J. Stat. Mech. Theory Exp. 44(3), P03001 (2009)

82. J.-F. Le Gall, Geodesics in large planar maps and in the Brownian map. Acta Math. 205(2), 287-360 (2010)

83. O. Angel, B. Kolesnik, G. Miermont, Stability of geodesics in the Brownian map. Ann. Probab. 45(5), 3451-3479 (2017)

84. J. Miller, W. Qian, Geodesics in the brownian map: strong confluence and geometric structure. (2020). arXiv preprint arXiv:2008.02242

85. J.-F. Le Gall, Geodesic stars in random geometry. Ann. Probab. 50(3), 1013-1058 (2022)

86. B. Duplantier, S. Sheffield, Liouville quantum gravity and KPZ. Invent. Math. 185(2), 333- 393 (2011)

87. S. Sheffield, Conformal weldings of random surfaces: SLE and the quantum gravity zipper. Ann. Probab. 44(5), 3474-3545 (2016)

88. J. Miller, S. Sheffield, Liouville quantum gravity and the Brownian map I: the QLE(8/3, 0) metric. Invent. Math. 219(1), 75-152 (2020)

89. J. Miller, S. Sheffield, Liouville quantum gravity and the Brownian map II: geodesics and continuity of the embedding. Ann. Prob. 49(6), 2732-2829 (2021)

90. J. Miller, S. Sheffield, Liouville quantum gravity and the Brownian map III: the conformal structure is determined. Prob. Theory Related Fields 179(3-4), 1183-1211 (2021)

91. B. Duplantier, J. Miller, S. Sheffield, Liouville quantum gravity as a mating of trees. Astérisque 427, viii+258 (2021)

92. F. David, A. Kupiainen, R. Rhodes, V. Vargas, Liouville quantum gravity on the Riemann sphere. Comm. Math. Phys. 342(3), 869-907 (2016)

93. E. Gwynne, N. Holden, X. Sun, A distance exponent for Liouville quantum gravity. Prob. Theory Related Fields 173(3), 931-997 (2019)

94. J. Ding, E. Gwynne, The fractal dimension of Liouville quantum gravity: universality, monotonicity, and bounds. Commun. Math. Phys. 374(3), 1877-1934 (2019)

95. J. Ding, J. Dubédat, A. Dunlap, H. Falconet, Tightness of Liouville first passage percolation for $\gamma \in (0, 2)$. Publ. Math. Inst. Hautes Études Sci. 132,353-403 (2020)

96. E. Gwynne, J. Miller, Existence and uniqueness of the Liouville quantum gravity metric for $\gamma \in (0, 2)$. Invent. Math. 223(1), 213-333 (2021)

97. E. Gwynne, N. Holden, X. Sun, Mating of trees for random planar maps and Liouville quantum gravity: a survey (2019). arXiv preprint arXiv:1910.04713

98. J. Ding, J. Dubedat, E. Gwynne, Introduction to the liouville quantum gravity metric (2021). arXiv preprint arXiv:2109.01252

99. S. Sheffield, What is a random surface?, in Proceedings of the ICM Contribution for 2022. (2022). arXiv preprint arXiv:2203.02470

100. J.-P. Kahane, Sur le chaos multiplicatif. Ann. Sci. Math. Québec 9(2), 105-150 (1985)

101. R. Rhodes, V. Vargas, Gaussian multiplicative chaos and applications: a review. Probab. Surv. 11, 315-392 (2014)

102. N. Berestycki, An elementary approach to Gaussian multiplicative chaos. Electr. Commun. Prob. 22, 1-12 (2017)

103. J. Aru, Y. Huang, X. Sun, Two perspectives of the 2D unit area quantum sphere and their equivalence. Comm. Math. Phys. 356(1), 261-283 (2017)

104. J. Ding, A. Dunlap, Liouville first-passage percolation: subsequential scaling limits at high temperature. Ann. Probab. 47(2), 690-742 (2019)

105. J. Dubédat, H. Falconet, E. Gwynne, J. Pfeffer, X. Sun, Weak LQG metrics and Liouville first passage percolation. Probab. Theory Related Fields 178(1-2), 369-436 (2020)

106. J. Miller, S. Sheffield, An axiomatic characterization of the Brownian map. J. Éc. Polytech. Math. 8, 609-731 (2021)

107. N. Holden, X. Sun, Convergence of uniform triangulations under the cardy embedding. Acta Math. (2019). To appear, arXiv preprint arXiv:1905.13207

108. P.L. Dobruschin, The description of a random field by means of conditional probabilities and conditions of its regularity. Theory Prob. Appl. 13(2), 197-224 (1968)

109. O.E. Lanford III, D. Ruelle, Observables at infinity and states with short range correlations in statistical mechanics. Comm. Math. Phys. 13, 194-215 (1969)

110. I. Benjamini, O. Schramm, Recurrence of distributional limits of finite planar graphs. Electron. J. Probab. 6(23), 13 (2001). (electronic)

111. O. Angel, O. Schramm, Uniform infinite planar triangulation. Comm. Math. Phys. 241(2-3), 191-213 (2003)

112. M. Krikun, Local structure of random quadrangulations (2006). arXiv preprint arXiv:math/0512304

113. P. Chassaing, B. Durhuus, Local limit of labeled trees and expected volume growth in a random quadrangulation. Ann. Prob. 34(3), 879-917 (2006)

114. L. Ménard, The two uniform infinite quadrangulations of the plane have the same law. Ann. Inst. H. Poincaré Probab. Statist. 46(1), 190-208 (2010)

115. N. Curien, L. Ménard, G. Miermont, A view from infinity of the uniform infinite planar quadrangulation. Lat. Am. J. Probab. Math. Stat. 10(1), 45-88 (2013)

116. J.E. Björnberg, S.O. Stefansson, Recurrence of bipartite planar maps. Electron. J. Probab. 19(31), 1-40 (2014)

117. R. Stephenson, Local convergence of large critical multi-type Galton-Watson trees and applications to random maps. J. Theor. Probab. 31(1), 159-205 (2018)

118. H. Kesten, Subdiffusive behavior of random walk on a random cluster. Ann. Inst. H. Poincaré Prob. Statist. 22(4), 425-487 (1986)

119. N. Curien, J.-F. Le Gall, The Brownian plane. J. Theoret. Probab. 27(4), 1249-1291 (2014)

120. Y. Watabiki, Construction of non-critical string field theory by transfer matrix formalism in dynamical triangulation. Nucl. Phys. B 441(1), 119-163 (1995)

121. O. Angel, Growth and percolation on the uniform infinite planar triangulation. Geom. Funct. Anal. 13(5), 935-974 (2003)

122. I. Benjamini, N. Curien, Simple random walk on the uniform infinite planar quadrangulation: subdiffusivity via pioneer points. Geom. Funct. Anal. 23(2), 501-531 (2013)

123. O. Angel, N. Curien, Percolations on infinite random maps, half-plane models. Ann. Inst. H. Poincaré Prob. Statist. 51(2), 405-431 (2014)

124. L. Richier, Universal aspects of critical percolation on random half-planar maps. Electr. J. Prob. 20, 1-45 (2015)

125. T. Budd, The peeling process of infinite Boltzmann planar maps. Electr. J. Combinatorics 23(1), 1-28 (2016)

126. J. Bertoin, T. Budd, N. Curien, I. Kortchemski, Martingales in self-similar growth-fragmentations and their connections with random planar maps. Prob. Theory Relative Fields 172, 1-62 (2017)

127. N. Curien, C. Marzouk, Infinite stable Boltzmann planar maps are subdiffusive. Prob. Math. Phys. 2(1), 1-26 (2021)

128. T. Budzinski, B. Louf, Local limits of bipartite maps with prescribed face degrees in high genus. Ann. Probab. 50(3), 1059-1126 (2022)

129. J.L. Doob, Conditional Brownian motion and the boundary limits of harmonic functions. Bull. Soc. Math. France 85, 431-458 (1957)

130. T. Budd, Peeling of random planar maps. Lecture notes for Mini-School on Random Maps and the Gaussian Free Field (2017). https://hef.ru.nl/~tbudd/docs/mappeeling.pdf

131. W. Feller, An Introduction to Probability Theory and its Applications. vol. II, 2nd edn. (John Wiley & Sons, Inc., New York-London-Sydney, 1971)

132. J. Bertoin, R.A. Doney, On conditioning a random walk to stay nonnegative. Ann. Prob. 22(4), 2152-2167 (1994)

133. B.V. Gnedenko, A.N. Kolmogorov, Limit Distributions for Sums of Independent Random Variables (Addison-Wesley Publishing Co., Inc., Cambridge, Mass, 1954). Translated and annotated by K. L. Chung. With an Appendix by J.L. Doob

134. T. Budd, N. Curien, C. Marzouk, Infinite random planar maps related to Cauchy processes. J. Éc. Polytech. Math. 5, 749-791 (2018)

135. J. Jacod, A.N. Shiryaev, Limit Theorems for Stochastic Processes, in Grundlehren der Mathe-matischen Wissenschaften [Fundamental Principles of Mathematical Sciences], vol. 288, 2nd edn. (Springer, Berlin, 2003)

136. F. Caravenna, L. Chaumont, Invariance principles for random walks conditioned to stay positive. Ann. Inst. Henri Poincaré Probab. Stat. 44(1), 170-190 (2008)

137. A.E. Kyprianou, Fluctuations of Lévy Processes with Applications: Introductory Lectures (Springer Science & Business Media, Heidelberg, 2014)

138. N. Curien, J.-F. Le Gall, Scaling limits for the peeling process on random maps. Ann. Inst. Henri Poincaré Prob. Stat. 53(1), 322-357 (2017)

139. N. Curien, J.-F. Le Gall, The hull process of the Brownian plane Prob. Theory Related Fields 166(1-2), 187-231 (2016)

140. M.A. Krikun, Uniform infinite planar triangulation and related time-reversed critical branching process. J. Math. Sci. 131(2), 5520-5537 (2005)

141. L. Ménard, Volumes in the uniform infinite planar triangulation: from skeletons to generating functions (2016). arXiv preprint arXiv:1604.00908